A STUDY OF ADVANCED CONTROL CHARTS FOR COMPLEX TIME-BETWEEN-EVENTS DATA

XIE YUJUAN

NATIONAL UNIVERSITY OF SINGAPORE

2012

A STUDY OF ADVANCED CONTROL CHARTS FOR COMPLEX TIME-BETWEEN-EVENTS DATA

XIE YUJUAN

(*B.Eng, University of Science and Technology of China*)

A THESIS SUBMITTED

FOR THE DEGREE OF DOCTOR OF PHILOSOPHY
DEPARTMENT OF INDUSTRIAL AND SYSTEMS ENGINEERING
NATIONAL UNIVERSITY OF SINGAPORE
2012

DECLARATION

I hereby declare that the thesis is my original work and it has been written by me in its entirety. I have duly acknowledged all the sources of information which have been used in the thesis.

This thesis has also not been submitted for any degree in any university previously.

Signature: Xie Yujuan Date: 24 May 2012

ACKNOWLEDGEMENTS

The 4-year PHD study in National University of Singapore is an unforgettable journey for me. During this period, I have been fully trained as a research student, leant lots of academic knowledge and also met lots of friends. At the end of my PHD study, I would like give my regards to all the peoples that cared about me and supported me.

First I would like to express my profound gratitude to my supervisor Prof. Xie Min for his guidance, assistance and support during my whole PHD candidature. Not only he guided me all the way through my research life, but also taught me lots of things that benefit my entire life. I am also deeply indebted to my co-supervisor Prof. Goh Thong Ngee for his invaluable suggestions and warmhearted advices. Without their great help, this dissertation is impossible.

Besides, I would like to thank National University of Singapore for giving me the Scholarship and Department of Industrial and Systems Engineering for its nice facilities. I would also like to thank all the faculty members and staff at the Department for their supports. My thanks extend to all my friends Wei Wei, Peng Rui, Wu Jun, Li Xiang, Zhang Haiyun, Xiong Chengjie, Jiang Hong, Wu Yanping, Long Quan, Deng Peipei, Jiang Yixing, Ye Zhisheng, Jiang Jun for their help.

Last but not least, I present my full regards to my parents, my aunt and my whole family for their love, support and encouragement in this endeavor.

TABLE OF CONTENTS

SUMMARY

The time-between-events (TBE) control charts have shown to be very effective in monitoring high quality manufacturing process. This thesis aims to develop more advanced univariate control charts for more generalized TBE dada, propose effective control charts for multivariate TBE data and study the optimal statistical design issue of the proposed control charts.

Chapters 1 provides an introduction of the principle of the control charts technique, the statistical design of the control charts and the TBE control charts. Chapter 2 reviews the current research trend of TBE control charts and the multivariate control charts technique.

In Chapter 3, an exponential weighted moving average (EWMA) chart for Weibull-distributed time between events data is developed with the help of the Box-Cox transformation method. The statistical design of the proposed chart is investigated based on the consideration of average run length (ARL) property.

Charter 4 proposed two multivariate exponential weighted moving average (MEWMA) control charts for the Gumbel's bivariate exponential (GBE) distributed data, one based on the raw GBE data , the other on the transformed data. The performance of the two control charts are compared to other three control charts schemes for monitoring simulated GBE data.

Chapter 5 and Chapter 6 concern the statistical designs of the two MEWMA charts separately. Chapter 5 studies the optimal design for the MEWMA charts on raw

GBE data and Charter 6 studies the optimal design for the MEWMA charts on transformed GBE data. The robustness of the two control charts to the estimation errors of the dependence parameter is also examined.

Chapter 7 concludes the whole thesis and presents some possible future research topics that are suggested by the author.

This thesis reviews the current trend in the area of TBE control charts, develops an advanced control chart for the more generalized Weibull-distributed TBE data, and further more extends the univariate TBE control chart research topic to the multivariate cases. The studies show that the proposed approaches do generalize the applications of TBE control charts for complex TBE data, improve the effectiveness of the TBE control charts and extend the current univariate TBE chart research topic to the multivariate control chart technique area.

LIST OF TABLES

LIST OF FIGURES

LIST OF SYMBOLS

SQC	Statistical quality control
SPC	Statistical process control
DOE	Design of experiment
UCL	Upper control limit
CL	Central control limit
LCL	Lower control limit
ARL	Average run length
ARL_0	Average run length when the process is in-control
ARL_1	Average run length when the process is out-of-control
ATS	Average time to signal
ATS_0	Average time to signal when the process is in-control
ATS_1	Average time to signal when the process is out-of-control
CCC	Cumulative count of conforming
CQC	Cumulative quantity of conforming
CUSUM	Cumulative sum
EWMA	Exponentially weighted moving average
MCUSUM	Multivariate cumulative sum
EWMA	Multivariate exponentially weighted moving average
TBE	Time-between-events
SQRT	Square root transformation
η	Shape parameter of the Weibull distribution
β	Location parameter of the Weibull distribution
λ	Smoothing factor of the EWMA chart

L	Design parameter for the control limits of the EWMA chart
$\boldsymbol{\mu}$	Mean vector of the multivariate distribution
Σ	Variance-covariance matrix of the multivariate distribution
$\boldsymbol{\rho}$	Correlation coefficient matrix of the multivariate distribution
GBE	Gumbel's bivariate exponential
$MEWMA_{Raw}$	MEWMA chart based on the raw GBE data
$MEWMA_{Trans}$	MEWMA chart based on the transformed GBE data
r	Smoothing factor of the MEWMA charts
h	Control limits of the MEWMA charts
$\mathbf{z}_i$	The *i*th recursion statistics while setting up the MEWMA charts
E^2	The charting statistic of the MEWMA charts

CHAPTER 1 INTRODUCTION

Statistical process control (SPC) originated in the 1920's when Walter A. Shewhart developed control charts as a statistical approach to monitoring and control of manufacturing process variation. According to Montgomery (2005), SPC is a powerful collection of problem-solving tools useful in achieving process stability and improving capability through the reduction of variability. It is an important branch of Statistical Quality Control (SQC), which also included other statistical techniques, e.g. acceptance sampling, design of experiment (DOE), process capability analysis, and process improvement planning. Generally speaking, the purpose of implementing SPC is to monitor the process, eliminate variances induced by assignable causes, and at the end improve the process to meet its target value.

Technically, SPC can be applied to any process. The commonly known seven major tools of SPC include: histogram of stem-and-leaf plot, check sheet, Pareto chart, cause-and-effect diagram, defect concentration diagram, scatter diagram and control chart. Of these tools, control chart is the most technically sophisticated one and has drawn the most attention in the research area.

The organization of this chapter is as follows. Section 1.1 introduces the general concept of control chart. The TBE control charts and multivariate control charts

techniques are stated in Section 1.2 and Section 1.3 respectively. The research scope and organization dissertation are given in Section 1.4.

1.1 Control charts

The most commonly used SPC tool is the control chart, which is a graphical representation of certain descriptive statistics for specific quantitative measurements of the process. These descriptive statistics are displayed in a run chart together with their in-control sampling distributions so as to isolate the assignable cause from the natural variability.

Let w represent the quality characteristic of interest. The traditional control charts follow the underlying Shewhart model:

$$\begin{cases} UCL = \mu_w + L\sigma_w \\ CL = \mu_w \\ LCL = \mu_w - L\sigma_w \end{cases}, \tag{1-1}$$

where UCL is the upper control limit, LCL is the lower control limit, and L is the standard deviation distance of the control limits from the center line (CL). The in-control or target mean μ_w and the standard deviation σ_w of different charts differ according to the underlying distribution.

A lot of traditional control charts have been widely adopted in industries to help monitor, control and improve the process or product quality, including the Shewhart control charts for variables data (e.g. the X-bar and R chart, X-bar and S chart), the Shewhart control charts for attributes data (e.g. the *p* chart, *np* chart, *c* chart and *u* chart),

the Exponentially Weighted Moving Average (EWMA) chart, the Cumulative Sum (CUSUM) chart and so on. All of these control charts are originally developed under the normal assumption, i.e., it assumes that the sample statistics can be approximately modelled by a normal distribution. However, the rapid development of technology and increasing effort on process improvement have led to so called high-quality processes, e.g. Ye et al. 2012a,b. In high-quality process monitoring, the failure rate is so low that it is difficult to form rational samples that the sample statistics would approximate normal and the traditional control charts have encountered a lot of difficulties. In order to overcome difficulties of conventional control charts in detecting process shifts in high-quality processes, a new kind of control chart named time between events (TBE) control chart has been developed recently.

1.2 Time-between-events chart

The time-between-event (TBE) chart is an effective approach for process monitor, control and improve the process when the events occurrence rate is very low. Unlike the traditional control charts which monitor the number or the proportion of events occurring in a certain sampling interval, TBE charts monitor the time between successive occurrences of events. The word “events” and “time” may have different interpretations depending on particular applications. “Event” may refer to the occurrence of nonconforming items in manufacturing process, failures in reliability analysis, accidents in a traffic system, etc. And the word “time” is used to represent the attribute or variable data observed between consecutive events of concern.

The existing TBE control charts can be classified into two groups: attribute TBE control chart and variable TBE control chart. The attribute TBE chart include, but not limited to, the cumulative count of conforming (CCC) chart, the CCC-r chart and the geometric CUSUM chart. Most of the attribute TBE charts are based on the geometric distribution (e.g. the CCC chart) or negative binomial distribution (e.g. the CCC-r chart). One typical variable TBE chart is the cumulative quantity control (CQC) chart. Since the occurrence of the event follows a Poisson distribution, the cumulative quantity between two events follows an exponential distribution, so CQC chart can also be called exponential chart. A lot of TBE variable charts are set up based on the exponential distributed TBE data, e.g. the CQC chart, the exponential CUSUM chart and the exponential EWMA chart. However, the exponential assumption is true only when the events occurrence rate is constant. An extension is to use Weibull distribution to simulate various TBE situations (including exponential) with non-constant events occurrence rate by varying its scale and shape parameters (e.g. the t chart and t_r chart).

1.3 Multivariate control charts

Up to now, we have addressed control charts primarily from the univariate perspective; that is we have assumed that there is only one process output variable or quality characteristic of interest. In practice, however, there are many situations in which the simultaneous monitoring or control of two or more related quality-process characteristics is necessary. While monitoring several correlated variables, the results of using separate univariate charts can be very misleading, and does not account for correlation between

variables. The multivariate control charts which can simultaneous monitor or control two or more related quality-process characteristics are especially suitable for such problems.

Most commonly used multivariate control charts are the natural extension of the univariate charts, e.g. the Hotelling's T^2 charts (Hotelling 1947), multivariate exponential moving average (MEWMA) charts (Lowry 1992) and multivariate cumulative sum (MCUSUM) charts (Crosier 1988, Pignatiello and Runger 1990). These multivariate control charts are originally developed for multivariate normal distributed data. However, in high-quality process monitoring, the actually distribution is usually non-normal, or even highly skewed. Similar to the univariate case, the traditional multivariate charts also face a lot of practical difficulties for such scenarios, some of which even totally lost their efficiency in detecting process shift. As a result, there is a strong demand for the researchers to develop effective multivariate control charts for high-quality process.

1.4 Performance evaluation issue

There are several popular statistics for measuring and comparing the performance of control charts in literature.

The fisrt one is the average run lenth (ARL). The ARL is defined as the average number of points that must be plotted before the chart issues an out-of-control signal. ARL is a traditional performance measure for control chart design and comparison. Given Type I error (α) and Type II error (β) of the charting procedure, the in-control ARL (ARL_0) and the out-of-control ARL (ARL_1) can be calculated as $1/\alpha$ and $1/(1-\beta)$, respectively. In a statistical design, the control limits are generally adjusted to achieve certain ARL_0 for

the charts under comparison, and the one with the smallest ARL_0 is considered to be the best.

As the time spent on plotting each TBE point is usually different, a better alternative to measure TBE chart comparing to the ARL would be the average time to signal (ATS). ATS is usually defined as the average time taken for the chart to signal an out-of-control point. The decition criteria for statistical design based on ATS is similar to those on ARL.

Other measurements include the average number of observations to signal (ANOI), the avergae quantity of products inspected to signal (AQI), false detection rate (FDR), and succesive detection rate (SDR).

Another widely studied method for designing control charts is the economic design. An economic design is usually achieved based on an economic model of the process under consideration. Economic models are generally formulated using a total cost function which expressed the relationships between the control chart design parameters and the various types of costs involved. The performance of an economic design is assessed based on the specific economic objective. There is also the so-called economic-statistical design which imposes some constraints on the economic models to satisfy both statistical and economical objectives.

1.5 Research objective and scope

The purpose of this thesis is to develop advanced control charts for complex TBE data. The reminder of the thesis is organized as follows:

Chapter 2 reviews the current research trend of TBE control charts and the multivariate control charts technique.

In Chapter 3, an exponential weighted moving average (EWMA) chart is proposed for transformed Weibull-distributed TBE data. The statistical design of the proposed chart is investigated based on ARL criteria. Finally, the guidelines for optimal statistical design of the EWMA chart are given to promote the use of the chart in real applications.

Charter 4 proposes two multivariate exponential weighted moving average (MEWMA) control charts for the Gumbel's bivariate exponential (GBE) distributed data, one based on the raw GBE data , and the other on the transformed data. The performance of the two control charts are compared to three other control chart schemes for monitoring simulated GBE data. The comparison results show that the proposed MEWMA charts are superior to the other control chart schemes based on the consideration of ARL property.

Chapter 5 studies the optimal design of the MEWMA charts based on raw GBE data and Charter 6 studies the optimal design for the MEWMA charts based on transformed GBE data. The robustness of the two control charts to the estimation errors of the dependence parameter is also examined.

Chapter 7 makes conclusions and suggests some potential future works.

The structure of the thesis is demonstrated by Figure 1-1.

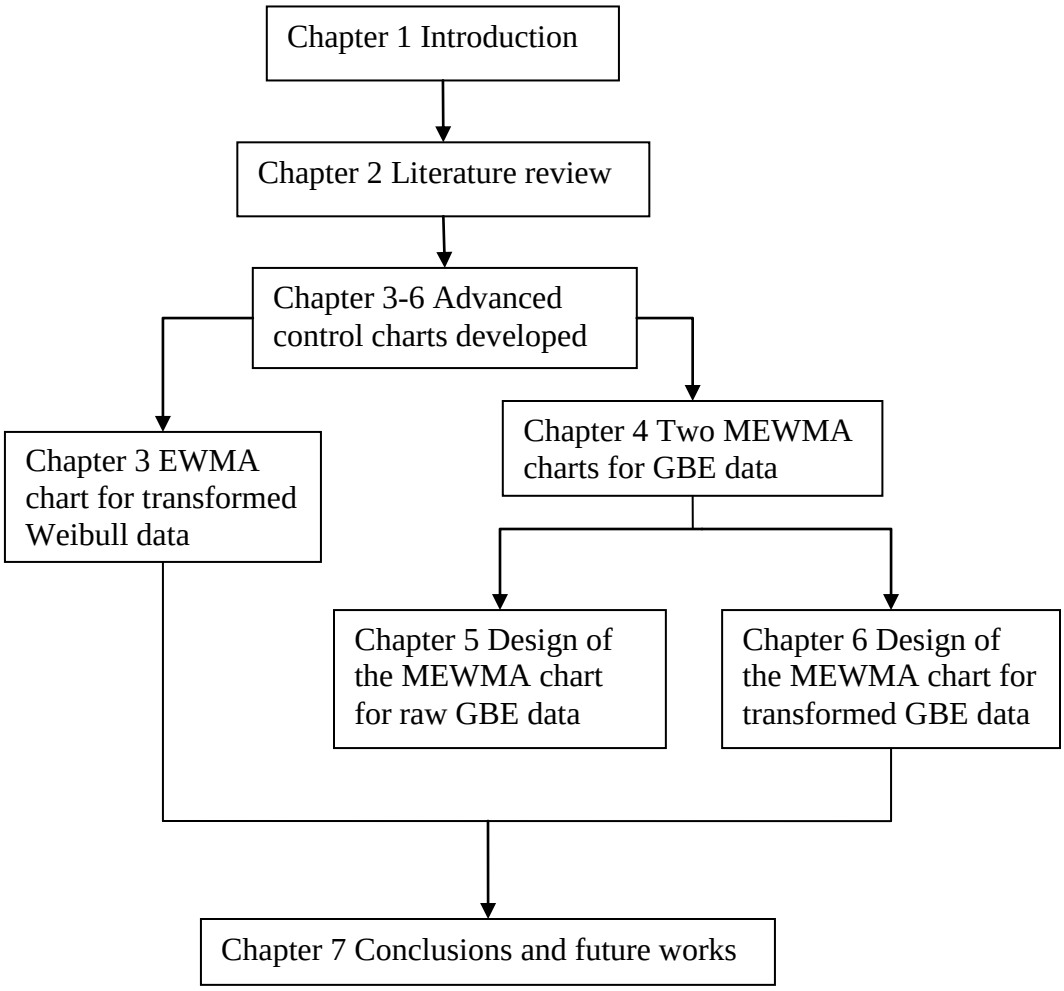

Figure 1-1 The structure of this thesis

This thesis reviews the current trend in the area of TBE control charts, develops an advanced control chart for the more generalized Weibull-distributed TBE data, and further more extends the univariate TBE control chart research topic to the multivariate case.

CHAPTER 2 LITERATURE REVIEW

This chapter reviews some important works related to TBE control charts and multivariate control charts.

2.1 Time-between-events control charts

2.1.1 Attribute TBE control charts

One typical attribute TBE control chart is the CCC chart (also called geometric chart or RL chart). The CCC chart, first proposed by Calvin (1983) and further developed by Goh (1987) and Bourke (1991), monitors the cumulative number of conforming items to obtain a nonconforming item with probability limits. Since the occurrence of the nonconforming item follows a binomial distribution, the cumulative counts of items inspected until a nonconforming item is observed follows a geometric distribution. Fixing the false alarm probability α at a desired level, the control limits *UCL*, *CL*, and *LCL* can be derived from the CDF of geometric distribution. The CCC chart has been further studied by many authors such as Kaminsky (1991), Xie and Goh (1997), and Xie et al. (1998). Xie et al. (2000) introduced the idea of transforming geometrical data into normal distribution so that the traditional run-rules and advanced process-monitoring techniques could also be used. Xie et al. (2001) constructed the economic model of CCC-chart based on LV model.

Zhang et al. (2004) proposed an improved design of CCC chart, which results in a nearly ARL-unbiased design. Liu et al. (2006) applied the idea of variable sampling intervals to the CCC-chart when 100% inspection is not available, which made the CCC-chart more flexible.

A natural extension of the CCC chart is the CCC-*r* chart, for which the sample statistic is the cumulative number of items inspected until the *r*-th nonconfromig item is encountered. Consequently, the sample statistic of the CCC-*r* chart follows a negative binomial distribution. Bourke (1991) and Xie et al. (1999) proposed the use of CCC-*r* chart and showed its sensitivity for detecting small process shifts. Wu et al. (2001) studied the sum-of-conforming-run-length (SCRL) chart which is similar to the CCC-*r* chart. Although plotting the cumulative count of conforming items until *r* nonconforming items happen increases the sensitivity of the chart to the shift, it needs to wait too long in order to see r nonconforming items. Chan (2003) introduced a two stage CCC-chart called CCC-1+r chart which is more flexible than the CCC-r chart.

Another useful attribute TBE chart is the geometric CUSUM chart. Xie et al. (1998) did a comparative study of CCC and CUSUM charts and suggested the usage of geometric CUSUM as it was shown to be more sensitive to high quality process shift. He also mentioned the idea that combining the CCC-chart and CUSUM-chart together in order to increase the sensitivity of the chart. Bourke (2001) further examined the properties of the geometric CUSUM chart under both 100% inspection and sampling inspection. Chang and Gan (2001) studied the sensitivities of the CUSUM charts based on geometric, Bernoulli,

and binomial data. Recommendations were given on how to choose the chart under different situations.

Some recent studies in the area of attribute TBE control charts are as follows. Albers (2010) developed a systematic approach for how to choose *r* in the CCC-r chart resulting a simple expression of the optimal *r* as a function of the desired false alarm rate and the supposed degree of increase of defect rate *p* compared to its value during in-control process. Later, Albert (2011) extended the CCC chart to the case of homogeneous health care data with large dispersion. Jae et al. (2011) proposed a G-EMWAG chart which combined a geometric chart and a EWMA chart for effectively detecting both small and large shifts on geometric distributed data. Liu et al. (2006) studied the performance of the CCC control charts with variable sampling intervals and Chen et al. (2011) extended Liu's work to the case of CCC control charts with variable sampling interval and variable control limits.

2.1.2 Exponential TBE control charts

A common assumption for variable TBE control chart is that the sample statistic follows an exponential distribution. Assume the event occurrence rate is constant and the occurrence of events can be modeled by a homogeneous Poisson process, therefore, the cumulative quantity before observing one event follows an exponential distribution. Until now, most of the studies on variable TBE monitoring charts are based on this assumption. The existing charts for exponential TBE data can be categorized into two types according to their methodology: TBE charts on raw data and TBE charts on transformed data.

"TBE charts on raw data" refers to the ones developed to directly monitor the exponentially distributed TBE data. Lucas (1985) and Vardeman and Ray (1985) were probably the first ones to study the exponentially distributed TBE data using CUSUM chart. Vardeman and Ray (1985) derived an exact method to obtain the ARL values for exponential CUSUM by solving Page's integral equation. Gan (1992) derived exact run length distribution for one-sided exponential CUSUM. Further, according to Gan (1994), the Poisson CUSUM and exponential CUSUM charts were found to have similar performances in detecting small and moderate changes in the Poisson rate. Borror et al. (2003) studied the robustness of the exponential CUSUM when the distribution deviated from exponential distribution. Control charting technique based on monitoring raw TBE data has been further extended to exponential EWMA by Gan (1998). Gan discussed the design of one-sided and two-sided EWMA chart, and provided a simple design procedure for determining the chart parameters of an optimal exponential EWMA chart. Gan and Chang (2000) presented the computer programs for computing ARL of exponential EWMA.

Chan et al. (2000) introduced a so called CQC chart for monitoring exponentially distributed quality characteristics based on probability limit method. The CQC chart is the counterpart part of the aforementioned CCC chart. This control chart is applicable to manufacturing process where the occurrence of defects can be modeled by a homogeneous Poisson process, whether the process is of high quality or not. Xie et al. (2002) investigated the use of CQC chart for monitoring the failure process of components or systems in reliability analysis. As the process goes on, the cumulative quantity between defects will gradually become large and eventually out of the control limits, so Chan et al.

(2002) proposed to plot the cumulative probability against the sample number in order to solve this problem.

Another approach of monitoring exponential TBE data is to first transform exponential distribution into normal distribution and then monitor normal distributed data. Nelson (1994) first proposed to transform the exponential data to normal data by using the power of 1/3.6. Kittlitz (1999) further demonstrated why the double square root (SQRT) transformation is recommended for transforming exponentially distributed data to normal for SPC applications like the I chart, EWMA and CUSUM charts. Kao et al. (2006) and Kao and Ho (2007) used the method of minimizing the sum of the squared difference to find the optimal value as the power for transforming the exponential distribution into normal distribution. Liu et al. (2006) used CUSUM and Liu et al. (2007) used EWMA to monitor the transformed exponential data and compared them with the X-MR chart, CQC chart and exponential CUSUM or EWMA chart.

All the papers cited in the above are focused on Phase II stage of the exponentially distributed TBE charts. Jones and Champ (2002) studied the Phase I stage of the exponentially distributed TBE when the parameters are known and unknown. Methods for computing the control limits were given. Zhang et al. (2006) revealed that the ARL of the exponential control charts designed in the traditional way may increase when the process deviates from the in-control state. In order to solve this problem, he proposed to an ARL-unbiased design using a sequential sampling scheme which showed to work very well.

2.1.3 Weibull TBE control charts

All of the variable TBE studies mentioned in the last section are based on the assumption that the TBE data follow an exponential distribution which is reasonable in manufacturing industry. However, under other circumstances, this assumption may not be true. For example, in reliability engineering, a Weibull distribution would be more suitable to describe the TBE data as it can take into consideration the increasing or decreasing as well as constant event occurrence rate.

Nelson (1979) designed a set of control charts for Weibull processes with standards given. He used the median chart, range chart, location chart and scale chart simultaneously to monitor Weibull processes. Bai and Choi (1995) proposed the design method of $\bar{X}$ and *R* chart for skewed population like exponential or Weibull distribution. Ramalhoto & Moriais (1999) studied the Shewhart control chart for monitoring scale parameter of a Weibull control variable with fixed and variable sampling intervals.

Xie et al. (2002) developed a charting method, named *t*-chart, for monitoring Weibull distributed time between failures based on probability limit method. Furthermore, a new procedure based on the monitoring of time between *r* failures, named, t_r-chart, was also proposed in order to improve the sensitivity to process shift. Here the Erlang distribution was used to model the time until the occurrence of *r* failures in a Poisson process.

Chang and Bai (2001) proposed a heuristic method of constructing $\bar{X}$, CUSUM, and EWMA chart for skewed populations with weighted standard deviation obtained by decomposing the standard deviation into upper and lower deviations adjusted in

accordance with the direction and degree of skewness. Chang (2007) further proposed a heuristic method of constructing multivariate CUSUM and EWMA control charts for skewed populations.

Hawkins and Olwell (1998) provided the optimal design of CUSUM for Weibull data with fixed shape parameter. Note that the proposed optimal design is limited to fixed shape parameter and can only detect the shifts in scale parameter. Borror et al. (2003) investigated the robustness of TBE CUSUM for Weibull-distributed. However, few methods have been proposed using EWMA chart to monitor Weibull TBE data. Zhang and Chen (2004) developed a lower-sided and upper sided EWMA chart for detecting mean shift of censored Weibull lifetimes with fixed censoring rate and shape parameter. Nichols and Padgett (2006) used a bootstrap method with pivotal quantities to monitor Weibull percentiles. Pascual and Zhang (2011) proposed control charts for monitoring the shape parameter of the Weibull distribution by first taking the natural logarithm of the Weibull distribution and then setting a control chart on the range value of random samples from the resulting smallest extreme population.

2.2 Multivariate control charts

2.2.1 Multivariate Shewhart control charts

Hotelling (1947) first applied multivariate process control methods to a bombsights problem based on the T^2 statistic. Mason and Young (2001) summarized the basic steps for the implementation of multivariate statistical process control using T^2 statistic. A detail

discussion of the practical development and application of control charts based on T^2 statistic can be found in Mason and Young (2002). The T^2 control charts were developed for detecting the shift (or shifts) in process mean vector assuming that the observation vector follows multivariate normal distribution and the process dispersion which is measured by the variance-covariance matrix Σ remains the same.

However, the process dispersion may also change in practice. Hence, it is necessary to develop control charts for monitoring process dispersion. Alt (1985) proposed a so-called W-chart for Phase II process dispersion monitoring which is a direct extension of the univariate s^2 control chart. He also gave a proper unbiased estimator for $|\Sigma|$, in order to define a Phase I control chart for process dispersion. Alt (1985), Alt and Smith (1988) and Aparisi et al. (1999, 2001) suggested a second chart based on the sample generalized variance-covariance $|S|$ which is the determinant of the sample covariance matrix.

In the literature, little work has been found dealing with multivariate attributes process, which are very important in practical production processes. Patel (1973) first proposed an X^2-chart for the multivariate binomial or multivariate Poisson population. Lu et al. (1998) studied a so-called MNO-chart which is a natural extension of the univariate *np*-chart. Recently, Skinner et al. (2003) have developed a procedure for monitoring discrete counts based on the likelihood ratio statistic for Poisson counts when input variables are measurable. Chiu and Kuo (2008) developed a so-called MP chart for monitoring the correlated multivariate Poisson count data. The control limits of the MP chart are developed by an exact probability method based on the sum of defects or non-conformities for each quality characteristics.

Multivariate Shewhart-type control charts use information only from the current sample and they are relatively insensitive to small and moderate shifts in the mean vector. MCUSUM and MEWMA control charts have been developed to overcome this problem.

2.2.2 MEWMA charts

Lowry et al. (1992) proposed a MEWMA control chart for monitoring the mean vector of the process as follows:

$$\mathbf{z}_i = \mathbf{R}(\boldsymbol{X}_i - \boldsymbol{\mu}_0) + (\mathbf{I} - \mathbf{R})\mathbf{z}_{i-1} \qquad (2\text{-}1)$$

where $\mathbf{R}$ = diag($r_1, r_2, \ldots, r_p$), $0 \le r_k \le 1$ for $k = 1,2,\ldots, p$, $\boldsymbol{z}_0 = 0$ and $\mathbf{I}$ is the identity matrix. The MEWMA chart gives an out-of-control signal if $\mathbf{z}_i^{\mathrm{t}}\boldsymbol{\Sigma}_{\mathbf{z}_i}^{-1}\mathbf{z}_i > h$, where $\boldsymbol{\Sigma}_{\mathbf{z}_i}$ is the variance-covariance matrix of $\mathbf{z}_i$. The value h is calculated by simulation to achieve a specified in-control ARL. Lowry pointed out that if the equality characteristics are equally weighted, the ARL performance only depends on the non-centrality parameter, using the proof of ARL performance of equal-weighted MCUSUM chart in Crosier (1988). They also provided some ARL profiles using simulation. Kramer and Schmid (1997) proposed a generalization of the MEWMA control scheme of Lowry et al. (1992) for multivariate time-dependent observations. Hawkins (2007) proposed a general MEWMA chart in which the smoothing matrix is full instead of one having only diagonal. The performance of this chart appears to be better than that of the MEWMA proposed by Lowry et al. (1992).

Rigdon (1995a, 1995b) gave an integral and a double-integral equation for the calculation of in-control and out-of-control ARLs, respectively. Molnau et al. (2001) presented a program that enables the calculation of the ARL for the MEWMA when the values of the shift in the mean vector, the control limit and the smoothing parameter are known. Several researchers have studied the statistical design of MEWMA charts using different measurements such as Runger and Prabhu (1996), Prabhu and Runger (1997) and Lee and Khoo (2006), and also the economic design under different cost model (e.g. Linderman and Love 2000 and Molnau et al. 2001).

The MEWMA chart has been promoted by various researchers for its effectiveness in monitoring non-normal populations. Stoumbos and Sullivan (2002) and Testik et al. (2003) independently investigated the robustness of the individuals MEWMA chart to non-normality. Following the univariate EWMA analyses of Borror et al. (1999), both studies considered the multivariate *t* distribution and the multivariate gamma distribution for comparisons with the multivariate normal distribution. Chang (2007) proposes a simple heuristic method of constructing MCUSUM and MEWMA control charts using the multivariate weighted standard deviation (WSD) method suggested by Chang and Bai (2004). The proposed charts adjust the charting statistics according to the degree and the direction of the skewness. The proposed charts are compared with the standard MCUSUM and MEWMA charts in terms of in-control and out-of-control ARLs for multivariate lognormal and Weibull distributions. Simulation studies indicate that considerable improvements over the standard method can be achieved by using the WSD method. For recent examples, see Hawkins and Maboudou-Tchao (2007), Zou and Tsung (2008), and Reynolds and Stoumbos (2008).

2.2.3 MCUSUM charts

We then present MCUSUM control charts, for which we assume that the direction of the shift (or shifts) is known. Healy (1987) used the fact that CUSUM charts can be viewed as a series of sequential probability ratio tests and developed MCUSUM charts for shift (or shifts) in mean vector and variance-covariance matrix. Hawkins (1991) introduced CUSUMs and MCUSUMs for regression-adjusted variables based on the idea that the most common situation found in practice is departures from control having some known structure. We have been unable to find any proposal in literature for an analogous charting procedure in the case where the mean vector and the variance-covariance matrix have to be estimated.

On the other hand, Crosier (1988) and Pignatiello and Runger (1990) have established MCUSUM schemes for cases where the direction of the shift is considered to be unknown. Crosier (1988) proposed two new multivariate CUSUM schemes. The first scheme is based on the square root of Hotelling's T^2 statistic, while the second can be derived by replacing the scalar quantities of a univariate CUSUM scheme with vectors. Moreover, Pignatiello and Runger (1990) introduced two new MCUSUM schemes .They referred to these MCUSUM charts as MCUSUM #1 and MCUSUM #2.

A lot of authors have developed different MCUSUM-type control charts, such as Ngai and Zhang (2001), Chan and Zhang (2001), Qiu and Hawkins (2001, 2003). Runger and Testik (2004) provided a comparison of the advantages and disadvantages of MCUSUM schemes, as well as performance evaluations and a description of their interrelationships. Jamal et al. (2007) introduced an artificial neural network (ANN) based

model to construct residuals Multivariate CUSUM chart for multivariate Auto-Regressive processes and show that the proposed chart performs better than the auto-correlated data MCUSUM chart proposed by Healy (1987) and better than time series based residuals chart for small shift values. Ben and Limam (2008) proposed to apply support vector regression (SVR) method for construction of a residuals Multivariate Cumulative Sum (MCUSUM) control chart, for monitoring changes in the process mean vector.

2.2.4 Recent development of multivariate statistical process control

One popular application area of the multivariate control charts is spatiotemporal surveillance. Spatiotemporal surveillance is an important aspect of multivariate surveillance, since several locations and time points are involved (see Sonesson and Frisén 2005). Rogerson and Yamada (2004) considered the spatiotemporal aggregated case for which the counts in the sub-regions were correlated at each particular time. They compared the performance of the use of multiple CUSUM charts for each region, and a multivariate CUSUM method. Joner et al. (2008) showed that the use of a one-sided version of the multivariate EWMA chart was a better approach to use in this case. Jiang et al. (2011) proposed a set of MCUSUM methods based on likelihood ratio tests for detection of outbreaks in the presence of spatial correlations, and showed the superiority to the existing surveillance methods. Moreover, for infectious disease, standard application of multivariate control charts could be inefficient, due to the potentially large variation in the background multivariate time series.

Profile monitoring is another important and emerging area of multivariate statistical process control in the latest literature. In many industrial applications, the quality of a

process may be better characterized by the relationship between one or more response variables and the explanatory variables. Instead of monitoring the moments of a set of quality characteristics, profile monitoring focuses on the monitoring of relationships, assuming a univariate or multivariate multiple linear regression model. In profile monitoring, the collection of observed data for all the process variables is treated as a single profile sample, and thus the profile monitoring problem naturally corresponds to multivariate SPC problem. Most literatures in profile monitoring focus on linear profiles, e.g. Kang and Albin (2000), Kim et al. (2003), Mahmoud and Woodall (2004) and Mahmoud et al. (2007). Moreover, profile monitoring with polynomial regressions are discussed by Zou et al. (2007) and Kazemzadeh et al. (2009). Multivariate statistical process control techniques are also considered for more generalized regression models such as nonlinear parametric and nonparametric profiles in the following references: Ding et al. (2006), Williams et al. (2007), Qiu and Zou (2010) and Qiu et al. (2010).

Moreover, self-starting methodology has gained more and more attention in multivariate process control to solve the problem caused by inaccurate in-control parameter estimation in the multivariate settings. In self-starting charts, the incoming process observations are transformed into a stream of mutually independent identically distributed data with a known in-control distribution. Each successive observation is used to update the mean and standard deviation of the observations up to date. And the updated mean and standard deviation are then used in the transformation procedure of the next process observation. Early works of self-starting multivariate control charts include Schaffer (1998), Quesenberry (1997), Sullivan and Jones (2002). Hawkins and Maboudou-Tchao (2007) proposed a self-starting multivariate exponentially weighted

moving average (SSMEWMA) chart for controlling the mean of multivariate normal distribution. Later, Maboudou-Tchao and Hawkins (2011) extends the approach to a self-stating multivariate exponentially weighted moving average and moving covariance matrix (SSMEWMAC) chart for monitoring both the mean and covariance matrix. Capizzi and Masarotto (2010) presented a self-starting cumulative score (CUSCORE) control chart for monitoring both the mean and covariance matrix of the multivariate normal distribution.

CHAPTER 3 A STUDY ON EWMA TBE CHART ON TRANSFORMED WEIBULL DATA

The exponentially weighted moving average (EWMA) charts, first proposed by Roberts (1959), has shown to be very effective in detecting small process shift for exponential TBE data and other non-normal data. However, few methods have been proposed using EWMA chart to monitor Weibull distributed TBE data. This section proposed a EWMA chart with transformed Weibull TBE data. The recommended Box-Cox transformation method is employed to transform Weibull data to approximate normal distributed data. Then a EWMA chart is set up on the transformed Weibull data.

Our design of EWMA chart is based on the consideration of ARL property using Markov chain calculation. It is found that the in-control ARLs of the EWMA charts with transformed Weibull data only depend on the design parameters of the control charts and are irrelevant to the distribution parameters. This property prompted us to study the statistical design of the proposed chart for the purpose of guiding the practical applications. Note that formal studies have shown that the in-control ARLs or other commonly used statistical measurements like average time to signal (ATS) of EWMA charts constructed directly on the Weibull distributed TBE data depend not only on the design parameters of the control charts but also on the distribution parameters, and thus it is difficult for us to conduct statistical design for such control charts or provide any general design guidelines.

3.1 Transform the Weibull data into Normal data using Box-Cox transformation

Many transformation methods like the simple power transformation, exponential transformation and Box-Cox transformation for transforming Weibull data to approximately normal distributed data have been studied by different researchers. Among them, the Box-Cox transformation is highly recommended in literature; see Box and Cox (1964), Sakia (1992), Yang Z.L. et al. (2003). Pavel et al. (2006) investigated the usability of some general types of transformations for transforming data sets with four non-normal distributions (logarithmic-normal, exponential, gamma, and Weibull) to normally distributed data. They also suggested using Box-Cox transformation for transforming Weibull data. Following these authors' suggestion, we use Box-Cox transformation to transform Weibull data in our study.

The probability density function (PDF) of two-parameter Weibull distribution $W(\beta,\eta)$ can be written as:

$$f(x)=\frac{\eta}{\beta}\left(\frac{x}{\beta}\right)^{\eta-1}e^{-(x/\beta)^{\eta}},\ x>0,\beta>0 \tag{3-1}$$

where β is the scale parameter and η is the shape parameter. When η is equal to 1, the Weibull distribution reduces to the exponential distribution.

The Box-Cox transformation is described by the equation:

$$y = \begin{cases} \dfrac{x^r - 1}{r} & \text{for } r \neq 0 \\ \ln x & \text{for } r = 0 \end{cases} \tag{3-2}$$

Hernandez and Johnson (1980) showed that the best normalizing transformation for Weibull is $r = 0.2654\eta$. So we use the following transformation function to setup the EWMA chart:

$$y = \frac{x^{0.2654\eta} - 1}{0.2654\eta} \tag{3-3}$$

Note that a two parameter Weibull distribution $W(\beta, \eta)$ becomes a three parameter Weibull distribution $W(\frac{\eta}{r}, \frac{\beta^r}{r}, -\frac{1}{r})$ after the Box-Cox transformation with shape parameter $\frac{\eta}{r}$, scale parameter $\frac{\beta^r}{r}$ and location parameter $\frac{1}{r}$. The mean and standard deviation of the transformed Weibull data are as follows:

$$\hat{\mu} = E(Y) = (0.9034\beta^{0.2654\eta} - 1) / 0.2654\eta$$

$$\hat{\sigma} = \sqrt{D(Y)} = 1.008\beta^{0.2654\eta} / \eta \tag{3-4}$$

And the cumulative distribution function (CDF) changes to

$$F(y) = 1 - e^{-(\frac{0.2654y+1}{\beta^{0.2654\eta}})^{3.7679}}, \; y \geq -\frac{1}{0.2654\eta} \tag{3-5}$$

The EWMA chart to be introduced later would be conducted on the transformed Weibull data using Box-Cox transformation method.

3.2 Setting up EWMA chart with transformed Weibull data

The idea of proposed EWMA chart is to use Box-Cox transformation method to convert Weibull data to approximate normal data, and then apply conventional design methods of EWMA chart for normal data to monitor the process. The main procedure of setting up a EWMA chart with transformed Weibull data are as follows:

Step 1: Transform the Weibull data X_t to approximately normal distributed data Y_t. The Box-Cox transformation is applied in our study:

$$y = \frac{x^{0.2654\eta} - 1}{0.2654\eta} \tag{3-6}$$

Step 2: Set up the two-sided EWMA chart with the recursive statistics:

$$Z_t = (1-\lambda)Z_{t-1} + \lambda Y_t \tag{3-7}$$

where $0 < \lambda \leq 1$is the smoothing factor. The starting value is the in-control mean value μ_0, i.e. the mean of data after transformation.

Step 3: The centre line and control limits can be calculated by

$$\begin{aligned} UCL &= \mu_0 + L\sigma_0\sqrt{\frac{\lambda}{(2-\lambda)}\left[1-(1-\lambda)^{2t}\right]} \\ CL &= \mu_0 \\ LCL &= \mu_0 - L\sigma_0\sqrt{\frac{\lambda}{(2-\lambda)}\left[1-(1-\lambda)^{2t}\right]} \end{aligned} \tag{3-8}$$

where L is a design parameter.

Step 4: The process is considered to be out-of-control when Z_t exceeds either the UCL or LCL. The μ_0 and σ_0 can be estimated from the transformed data with

$$\hat{\mu}_0 = \bar{y} = \sum_{t=1}^{n} y_t \text{ , and } \hat{\sigma}_0 = \sqrt{\frac{1}{n-1}\left[\sum_{t=1}^{n}(y_t - \bar{y})^2\right]} \tag{3-9}$$

3.3 Design of EWMA chart with transformed Weibull data

The proposed design method for EWMA chart with transformed Weibull data is based on ARL consideration. An acceptable in-control ARL is specified at the beginning to determine the probability of false alarm, and the optimal design is to find the values of design parameters with the shortest out-of-control ARL.

3.3.1 Markov chain method for ARL calculation

The approximate method using Markov chain method for ARL calculation was first proposed by Brook and Evans (1972), where the properties of the continuous-state Markov chain can be approximately evaluated by discretizing the infinite-state transition probability matrix.

Consider a two-sided EWMA chart with transformed Weibull data with design parameters λ and L, the interval between the LCL and UCL is divided into m subintervals of width w. Since the control limits will change with time t, and will approach a constant when t is large, the asymptotic a control limits are used to calculate the ARL instead of the exact control limits. Let h_U and h_L be the asymptotic control limits that it satisfy

$$h_U = \mu_0 + L\sigma_0\sqrt{\frac{\lambda}{2-\lambda}}, h_L = \mu_0 - L\sigma_0\sqrt{\frac{\lambda}{2-\lambda}} \tag{3-10}$$

Using the asymptotic control limits, w can be expressed as:

$$w = \frac{h_U - h_L}{m} = \frac{2L\sigma}{m}\sqrt{\frac{\lambda}{2-\lambda}} \tag{3-11}$$

The EWMA control statistics Z_t is said to be in transient state (j) at time (t) if $h_L + jw \le Z_t < h_L + (j+1)w$ for $j = 1, \ldots, m-1$ The midpoint of subinterval corresponding to state (j) can be written as

$$m_j = h_L + (j + 0.5)w,\ j = 0,1,\ldots,m-1 \tag{3-12}$$

The control statistics Z_t is regarded as in the absorbing state m if the point goes outside the control limits, i.e. $Z_t \le h_l$ or $Z_t \ge h_u$.

Let p_{ij} represent the transition probability that the control statistics Z_i goes from state (i) to state (j) in one step. To approximate the probability, we assume that the control statistics Z_t is equal to m_i whenever it is in state (i). This approximation is accurate enough when the number of state m is large. Then p_{ij} is given by

$$\begin{aligned} p_{ij} &= \Pr\{h_L + jw \le Z_t < h_L + (j+1)w \mid Z_{t-1} = m_i\} \\ &= \Pr\{h_L + jw \le \lambda y_t + (1-\lambda)Z_{t-1} < h_L + (j+1)w \mid Z_{t-1} = m_i\} \\ &= \Pr\left\{\frac{h_L + jw - (1-\lambda)m_i}{\lambda} \le y_i < \frac{h_L + (j+1)w - (1-\lambda)m_i}{\lambda}\right\}, \\ &\quad i = 0,1,\ldots,m-1;\ j = 0,1,\ldots m-1 \end{aligned} \tag{3-13}$$

$$\begin{aligned} p_{im} &= \Pr\{Z_t < h_L \text{ or } Z_t \ge h_U \mid Z_{t-1} = m_i\} \\ &= \Pr\{\lambda y_t + (1-\lambda)Z_{t-1} < h_L \text{ or } \lambda y_t + (1-\lambda)Z_{t-1} \ge h_U \mid Z_{t-1} = m_i\} \\ &= \Pr\left\{y_t < \frac{h_L - (1-\lambda)m_i}{\lambda}\right\} + \Pr\left\{y_t \ge \frac{h_U - (1-\lambda)m_i}{\lambda}\right\}, i = 0,1,\ldots m-1 \end{aligned}$$

$$p_{mj} = 0,\ j = 0,1,\ldots,m-1$$

$$p_{mm} = 1$$

Based on the Markov chain theory, the expected first passage times from state (i) to the absorbing state are

$$\mu_i = 1 + \sum_{j=1}^{m-1} p_{ij}\mu_j,\ i = 0,1,\ldots,m-1 \tag{3-14}$$

μ_i is the ARL given that the process started in state (i). Let R be the matrix of transition probabilities obtained by deleting the last row and column of P . The vector of ARLs μ can be calculated with

$$\mu = (I - R)^{-1}1 \tag{3-15}$$

where 1 is an $m \times 1$ vector with all elements equal to 1, and I is an $m \times m$ identity matrix. The elements in the vector μ are the ARL's when the EWMA chart starts in various states. The first element in the vector μ gives the ARL for the EWMA chart starting from zero, and the ARL given that $z_0 = \mu_0$ is just the middle entry, that is the $((m+1)/2)$th element in the vector .

3.3.2 In-control ARL

The in-control ARL (ARL_0) values with different design parameters λ and L are calculated by the aforementioned Markov chain approach. It can easily be proved that the ARL_0 of a EWMA chart with transformed Weibull data depends on the value of λ and L, and it is independent of the parameters of Weibull distribution $W(\beta, \eta)$. The prove is as follows:

Let $C = L\sqrt{\frac{\lambda}{2-\lambda}}$, $\mu_0 = (0.9034\beta_0^{\,0.2654\eta_0} - 1)/0.2654\eta_0 = (C_1\beta_0^{C_2\eta_0} - 1)/C_2\eta_0$, $\sigma_0 = 1.008\beta_0^{0.2654\eta_0}/\eta_0 = C_3\beta_0^{\,C_2\eta_0}/\eta_0$, then the p_{ij} $(i = 0,1,\ldots m-1;\ j = 0,1,\ldots m-1)$ can be expressed as:

$$p_{ij} = \Pr\left\{\frac{h_L + jw - (1-\lambda)m_i}{\lambda} \le y_t < \frac{h_L + (j+1)w - (1-\lambda)m_i}{\lambda}\right\}$$

$$= F\left(\frac{h_L + (j+1)w - (1-\lambda)m_i}{\lambda}\right) - F\left(\frac{h_L + jw - (1-\lambda)m_i}{\lambda}\right)$$

$$= 1 - \exp\left[-\left(\frac{C_1\eta_1(h_L + (j+1)w - (1-\lambda)m_i) + \lambda}{\lambda \cdot \beta_1^{\,C_2\eta_1}}\right)^{3.7679}\right]$$

$$-\left\{1-\exp\left[-\left(\frac{C_1\eta_1(h_L+jw-(1-\lambda)m_i)+\lambda}{\lambda\cdot\beta_1^{C_2\eta_1}}\right)^{3.7679}\right]\right\} \tag{3-16}$$

$$=\exp\left\{-\left(\frac{C_2\beta_0^{C_2\eta_0}\frac{\eta_1}{\eta_0}\left(\lambda\left(\frac{C_1}{C_2}-CC_3\right)+j\cdot\frac{2CC_3}{m}-(1-\lambda)\cdot(i+0.5)\cdot\frac{2CC_3}{m}\right)+\lambda\left(1-\frac{\eta_1}{\eta_0}\right)}{\lambda\cdot\beta_1^{C_2\eta_1}}\right)^{3.7679}\right\}$$

$$-\exp\left\{-\left(\frac{C_2\beta_0^{C_2\eta_0}\frac{\eta_1}{\eta_0}\left(\lambda\left(\frac{C_1}{C_2}-CC_3\right)+(j+1)\cdot\frac{2CC_3}{m}-(1-\lambda)\cdot(i+0.5)\cdot\frac{2CC_3}{m}\right)+\lambda\left(1-\frac{\eta_1}{\eta_0}\right)}{\lambda\cdot\beta_1^{C_2\eta_1}}\right)^{3.7679}\right\}$$

We can see from the formula that when the process is in-control i.e. $\beta_0=\beta_1,\eta_0=\eta_1$, the value of p_{ij} only depends on the value of design parameters λ and L and calculation parameter m. On the other hand, when the process become out-of-control, the value of (β_0,η_0) and (β_1,η_1) would influence the ARL_1 values. After study the relationship of ARL_0 and calculation parameter m, we could see that the value of ARL_0 trends to be more and more stable as m becomes larger and larger. We choose $m=301$ in our study.

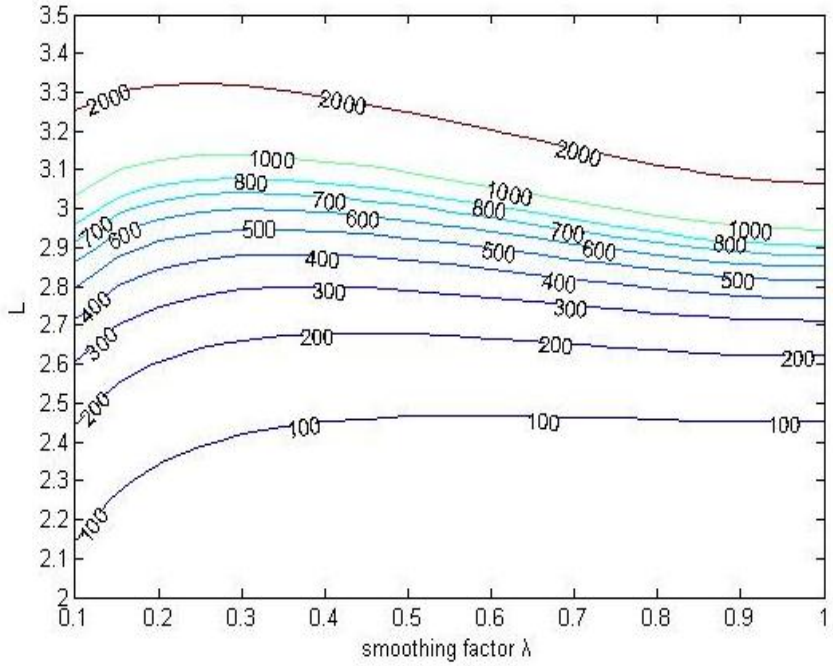

(a) ($0 < \lambda \leq 0.1$)

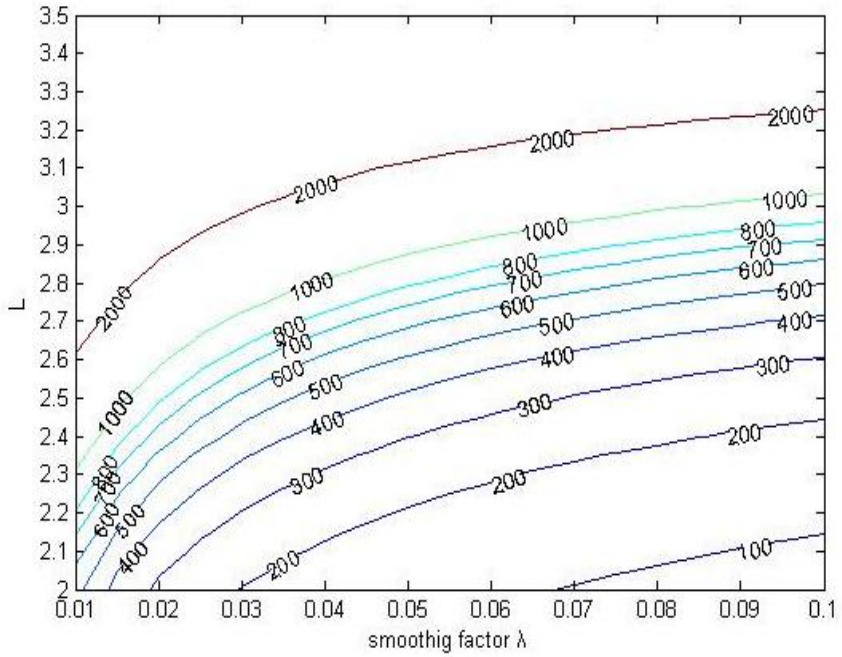

(b) ($0.1 < \lambda \leq 1$)

Figure 3-1 The in-control ARL contour plot of the EWMA chart

Figures 3-1(a) and Figure 3-1(b) provide the contour plots for some commonly used ARL_0 levels. For other ARL_0 values, the relationship of λ and L can be achieved by interpolation. Table 3-1 provides some numerical value of design parameters λ and L according to different ARL_0 levels which would be studied in the optimal design process later.

Table 3-1 The design parameters λ and L combinations of the EWMA chart

ARL_0=100	λ	0.02	0.05	0.1	0.2	0.3	0.4	0.5	0.8	1
	L	1.469	1.880	2.144	2.343	2.420	2.454	2.467	2.458	2.452
ARL_0=300	λ	0.02	0.05	0.1	0.2	0.3	0.4	0.5	0.8	1
	L	2.033	2.396	2.607	2.750	2.793	2.801	2.792	2.732	2.713
ARL_0=370.4	λ	0.02	0.05	0.1	0.2	0.3	0.4	0.5	0.8	1
	L	2.136	2.487	2.688	2.820	2.857	2.861	2.848	2.779	2.758
ARL_0=500	λ	0.02	0.05	0.1	0.2	0.3	0.4	0.5	0.8	1
	L	2.278	2.610	2.798	2.917	2.946	2.944	2.926	2.844	2.818
ARL_0=800	λ	0.02	0.05	0.1	0.2	0.3	0.4	0.5	0.8	1
	L	2.490	2.793	2.961	3.062	3.079	3.067	3.042	2.940	2.906
ARL_0=1000	λ	0.02	0.05	0.1	0.2	0.3	0.4	0.5	0.8	1
	L	2.585	2.876	3.035	3.128	3.140	3.124	3.094	2.983	2.947
ARL_0=2000	λ	0.02	0.05	0.1	0.2	0.3	0.4	0.5	0.8	1
	L	2.862	3.117	3.253	3.321	3.318	3.289	3.249	3.114	3.067

3.3.3 Out-of-control ARL

When the process becomes out-of-control, the ARL_1 value is influenced by the value of Weibull distribution parameters (β_0, η_0) and (β_1, η_1) as well as the design parameters λ and L. The optimal design scheme should have the shortest out-of control ARL at certain ARL_0 length. The difficulty in the studying of out-of-control ARL is that there are two parameters in the Weibull distribution.

We consider the case that the shift level of shape parameter η_1 / η_0 equals 1. This is reasonable since in practical applications the scale parameter is more likely to change due to assignable causes, while the shape parameter is more related to the natural properties of the system and is rather stable. When $\eta_1 / \eta_0 = 1$, we could see from both the formula (B-1) and the calculation results that when keeping the shape parameter η as a constant, the value of ARL_1 of the EWMA chart with transformed Weibull data only depends on the shift level of scale parameter β_1 / β_0. However, different shape parameters η lead to different optimal ARL_1 given a certain scale shift level. In our study, we select some shift levels of scale parameter β_1 / β_0 and use the design parameters provided by Table 3-1 to investigate the property of ARL_1. The shortest out-of-control ARL we obtained is denoted by $ARL_{\min}$.

It can be obviously seen in Table 3-2 that the EWMA charts with smaller λ are more sensitive to small scale shifts (β_1 / β_0 close to 1), while those with larger λ are more effective in detecting larger scale shifts. For small downward shifts (β_1 / β_0 <1), the EWMA charts with large λ between 0.5 and 1.0 may have longer out-of-control ARLs than their ARL_0. The reason behind this is that data after Box-Cox transformation are not exactly symmetric and slightly skewed to the right; meanwhile, as λ approaches 1, an EWMA will approximate to a Shewhart chart, which is sensitive to non-normality. As indicated in bold and italic figures in Table 3-1, the optimal EWMA chart with transformed exponential data for a certain scale shift level β_1 / β_0 should have shortest

ARL_1 among others. Note that, when $\eta_1 / \eta_0 = 1$, the Weibull distribution would reduce to as exponential distribution. The result in Table 3-2 is very similar to the numerical example of EWMA design with transformed exponential data in Liu et al. (2007)'s paper, which implies that the performances of the Box-Cox transformation methods and the double SQRT transformation methods are similar for EWMA design using transformed exponential data.

Some of the optimal design schemes of EWMA control chart with ARL_0 =500 are listed in Table 3-3 according to different shape parameters η and scale shift levels (β_1 / β_0). Only the λ values are listed as the corresponding *L* value could be easily obtained according to Table 3-1. The *ARL* results in Table 3-3 show that the optimal λ increases for a certain amount of scale shift (β_1 / β_0) as the shape parameter η increases. Comparing to smaller scale shift (β_1 / β_0), the optimal λ for larger scale shift level increases more quickly as η increases. However, for small scale shift (β_1 / β_0 close to 1), a smaller λ is always preferred to detect the shift in scale parameter, e.g. the optimal λ for $\beta_1 / \beta_0 = 0.9$ is 0.02 (the smallest λ selected in this study), no matter what the value of shape parameter η is. For small shape parameter η (e.g. $\eta = 0.2, 0.5$), smaller λ is also more effective for detecting the shift in scale parameter. On the other hand, larger λ ($0.5 \le \lambda \le 1$) is more sensitive to large scale shift level and large shape parameter, and the according ARL_1 is rather stable regardless of the value of η and β_1 / β_0. Another observation is that the optimal design parameters λ and L are rather stable for a range of η and scale shift (β_1 / β_0). Hence, it is reasonable to choose a suitable λ value using Table

3-3 even if the desired η and scale shift (β_1 / β_0) is not included. The optimal design schemes of other ARL_0 level are similar.

Table 3-2 The ARLs of some selected EWMA charts with transformed Weibull data. (In-control ARL=500, $\eta_1 = \eta_0 = 1$)

β_1	λ	0.02	0.05	0.1	0.2	0.3	0.4	0.5	0.8	1
β_0	L	2.278	2.610	2.798	2.917	2.946	2.944	2.926	2.844	2.818
0.1		8.52	6.74	5.71	**5.12**	5.21	5.84	7.24	26.66	129.22
0.2		11.41	9.28	**8.23**	8.25	9.71	12.82	18.35	71.62	257.95
0.3		14.88	12.51	**11.76**	13.51	18.25	26.56	39.53	135.74	386.67
0.4		19.53	**17.17**	17.43	23.27	34.55	51.71	75.63	219.64	515.38
0.5		26.34	**24.63**	27.59	42.06	64.64	94.68	132.42	324.13	643.50
0.6		**37.47**	38.18	47.71	78.54	117.92	163.95	216.54	448.83	764.61
0.7		**58.61**	66.72	90.99	148.49	208.10	269.52	333.77	583.00	848.91
0.8		**108.69**	137.11	188.68	276.41	348.08	412.76	474.21	678.24	834.33
0.9		**263.02**	322.12	386.30	456.96	500.24	535.15	565.06	649.82	693.66
1		500.00	499.56	500.28	499.57	499.20	500.38	500.38	500.16	500.91
1.2		**120.71**	134.42	155.69	183.39	199.65	209.85	215.45	220.30	228.37
1.5		41.80	**40.01**	42.38	49.18	55.37	60.62	64.83	74.14	83.79
1.8		25.94	22.93	**22.27**	23.65	25.66	27.68	29.55	34.78	40.83
2		21.10	18.12	**16.97**	17.20	18.16	19.28	20.39	23.91	28.32
2.5		14.96	12.36	10.99	**10.33**	10.35	10.59	10.92	12.35	14.57
3		11.99	9.72	8.42	7.60	7.37	**7.35**	7.41	8.06	9.34
3.5		10.22	8.20	7.00	6.16	5.85	5.73	**5.69**	5.97	6.79
4		9.04	7.20	6.09	5.27	4.94	4.77	**4.69**	4.79	5.35
5		7.54	5.96	4.98	4.24	3.90	3.70	3.58	**3.53**	3.82
10		4.85	3.80	3.15	2.60	2.32	2.16	2.05	**1.92**	1.96

Table 3-3 The optimal design schemes of EWMA chart with transformed Weibull data (ARL_0=500)

β_1/β_0		Shape parameter η									
		0.5	0.8	1	1.5	2	2.5	3	3.5	4	5
0.2	λ	0.05	0.1	0.1	0.2	0.4	0.5	0.5	0.5	0.8	1
	ARL_{min}	20.21	10.77	8.23	4.85	3.44	2.66	2.19	2.01	1.78	1.10
0.5	λ	0.02	0.05	0.05	0.1	0.1	0.2	0.2	0.2	0.3	0.4
	ARL_{min}	60.82	33.79	24.63	14.43	9.82	7.39	5.78	4.83	4.07	3.14
0.8	λ	0.02	0.02	0.02	0.02	0.02	0.05	0.05	0.05	0.05	0.1
	ARL_{min}	248.85	145.19	108.69	63.64	44.16	33.49	25.83	21.00	17.73	13.05
0.9	λ	0.02	0.02	0.02	0.02	0.02	0.02	0.02	0.02	0.02	0.02
	ARL_{min}	413.89	317.92	263.02	168.94	117.19	87.24	68.58	56.15	17.42	36.11
1.2	λ	0.02	0.02	0.02	0.02	0.05	0.05	0.1	0.1	0.2	0.2
	ARL_{min}	259.80	159.28	120.71	70.57	47.16	33.45	25.15	19.42	15.62	10.42
1.5	λ	0.02	0.02	0.05	0.1	0.2	0.3	0.5	0.5	0.8	0.8
	ARL_{min}	105.16	56.15	40.01	21.03	12.84	8.55	6.03	4.49	3.47	2.33
2	λ	0.05	0.1	0.1	0.3	0.5	0.8	0.8	0.8	0.8	1
	ARL_{min}	51.05	24.57	16.97	8.15	4.69	3.06	2.24	1.78	1.52	1.23
3	λ	0.1	0.2	0.4	0.8	0.8	0.8	1	1	1	1
	ARL_{min}	24.97	11.11	7.35	3.37	2.05	1.53	1.28	1.15	1.09	1.03
5	λ	0.2	0.5	0.8	0.8	1	1	1	1	1	1
	ARL_{min}	13.02	5.39	3.53	1.80	1.31	1.13	1.06	1.02	1.01	1.00

Table 3-4 shows the optimal design schemes of a EWMA chart with shape parameter $\eta_1 = \eta_0 = 0.5$ according to different ARL_0 and scale shift level (β_1 / β_0). The results imply that the optimal λ decreases as the ARL_0 increases. However, the optimal λ is rather stable for a range of ARL_0. For example, when scale shift β_1 / β_0 changes from 0.5 to 0.8, the optimal λ is always 0.02 for all the ARL_0 level we studied. Hence, when the shape parameter η is fixed to be 0.5, we could also use Table 3-4 to choose the optimal λ in

application even if the desired ARL_0 level and the shift level (β_1/β_0) are not included. Studies could also be conducted for other values of η, and the results are similar.

Table 3-4 The optimal design schemes of a EWMA chart with transformed Weibull data ($\eta_1=\eta_0=0.5$)

$\frac{\beta_1}{\beta_0}$		In-control ARL						
		100	300	370.4	500	800	1000	2000
0.2	λ	0.05	0.05	0.05	0.05	0.05	0.05	0.05
	ARL_{min}	12.88	17.80	18.79	20.21	22.49	23.61	27.18
0.5	λ	0.02	0.02	0.02	0.02	0.02	0.02	0.02
	ARL_{min}	32.59	50.86	54.87	60.82	70.85	75.87	92.85
0.8	λ	0.02	0.02	0.02	0.02	0.02	0.02	0.02
	ARL_{min}	80.62	177.98	204.71	248.85	336.64	387.83	604.02
1.2	λ	0.05	0.02	0.02	0.02	0.02	0.02	0.02
	ARL_{min}	77.72	181.88	211.18	259.80	356.68	413.07	649.77
1.5	λ	0.05	0.02	0.02	0.02	0.02	0.02	0.02
	ARL_{min}	47.61	84.17	92.47	105.16	127.51	139.20	181.39
2	λ	0.10	0.05	0.05	0.05	0.02	0.02	0.02
	ARL_{min}	27.37	42.55	45.96	51.05	59.02	62.73	74.84
3	λ	0.20	0.10	0.10	0.10	0.05	0.05	0.05
	ARL_{min}	15.06	21.53	22.92	24.97	28.32	29.79	34.55
5	λ	0.30	0.20	0.20	0.20	0.20	0.20	0.10
	ARL_{min}	8.49	11.51	12.12	13.02	14.54	15.31	17.38
10	λ	0.50	0.50	0.50	0.40	0.40	0.30	0.30
	ARL_{min}	4.73	6.05	6.32	6.71	7.34	7.66	8.60

Hence, the recommended optimal design procedure of EWMA charts with a fixed shape parameter is described as follows:

Step1: Specify the desired ARL_0, the fixed shape parameter and the out-of control scale shift level (β_1 / β_0) at the beginning.

Step2: Find the approximate value of the smoothing factor λ according to the optimal design scheme tables mentioned in Section 3.3.2.

Step3: Obtain the approximate corresponding value of L according to the ARL_0 contours figure mentioned in Section 3.3.1.

Step4: Achieve the more accurate ARL_0 and ARL_1 using Markov chain approach to evaluate the performance of the designed EWMA control charts.

When the shape varies, the optimal scheme of design parameters with transformed EWMA chart could also be achieved by choosing the shortest out-of-control ARL value with different design parameters under certain in-control ARL level. However, different combination of shape and scale parameters would lead to different out-of-control ARL value using Markov chain approach, and the optimal design of EWMA should be studied case by case.

Table 3-5 provides an example of the optimal schemes when we fix the scale parameter β to be different value and varies the shape parameter. In this example, the ARL_0 is fixed at 370.4, η_0 is equal to 1 and the shape shift changes from 0.2 to 5. In this case, the optimal λ is rather stable for a range of value of β and η_1 / η_0. For a decrease in shape parameter ($\eta_1 / \eta_0 < 1$), no matter what the value of scale parameter β is, the optimal design scheme would be $\lambda = 1$ and $L = 2.758$. On the other hand, for a increase in

shape parameter ($1 < \eta_1 / \eta_0 \le 5$) with a scale parameter $0.5 \le \beta \le 2$, a EWMA chart with $\lambda = 0.02$ and $L = 2.136$ would be effective to detect the change of shape parameter.

Table 3-5 The optimal design schemes of a EWMA chart with transformed Weibull data (ARL_0=370.4, $\beta_1 = \beta_0$, $\eta_0 = 1$)

β		Shape shift η_1 / η_0								
		0.5	0.8	1.5	2	3	3.5	4	4.5	5
0.1	λ	1	1	0.05	0.1	0.3	0.4	0.4	0.5	0.5
	ARL_{min}	2.84	17.54	23.15	9.99	4.75	3.97	3.00	3.00	2.53
0.2	λ	1	1	0.02	0.05	0.1	0.1	0.1	0.2	0.2
	ARL_{min}	3.42	22.91	46.35	22.58	11.05	8.95	7.84	6.88	6.00
0.5	λ	1	1	0.02	0.02	0.02	0.02	0.02	0.02	0.02
	ARL_{min}	4.44	32.03	156.46	71.38	39.15	33.62	30.03	27.47	25.55
0.9	λ	1	1	0.02	0.02	0.02	0.02	0.02	0.02	0.02
	ARL_{min}	5.35	39.71	290.82	157.99	89.56	77.76	70.42	65.46	61.87
1.2	λ	1	1	0.02	0.02	0.02	0.02	0.02	0.02	0.02
	ARL_{min}	5.90	44.20	309.55	173.37	98.48	84.86	76.20	70.21	65.79
2	λ	1	1	0.02	0.02	0.02	0.02	0.02	0.02	0.02
	ARL_{min}	7.11	53.67	231.97	110.69	53.25	42.82	35.91	30.91	27.08
3	λ	1	1	0.02	0.02	0.02	0.05	0.05	0.1	0.1
	ARL_{min}	8.32	62.81	150.36	64.02	28.41	20.57	15.70	12.04	9.43
5	λ	1	1	0.02	0.02	0.1	0.2	0.3	0.4	0.5
	ARL_{min}	10.236	76.716	84.352	34.353	11.522	7.5245	5.065	3.5218	2.518
10	λ	1	1	0.02	0.1	0.5	0.8	0.8	1	1
	ARL_{min}	13.60	100.20	43.42	14.87	3.67	2.15	1.49	1.21	1.09

3.4 Illustrative example

A simulation example is constructed to illustrate the use of the proposed EWMA chart with transformed Weibull data. We assume that the time between failures of a machine could be described by a Weibull distribution. The first 25 TBE data were generated from a Weibull distribution with shape parameter $\eta_0 = 2$ and scale parameter $\beta_0 = 10$, and the next 15 with shape parameter $\eta_1 = 2$ and scale parameter $\beta_1 = 5$, and in-control ARL=370.4. The design parameters of the EWMA chart are chosen as ($\lambda = 0.1, L = 2.688$) and the starting value Z_0 is estimated from the first 25 samples. The control chart is shown in the Figure 3-2. The procedure becomes out-of-control at the 31th.

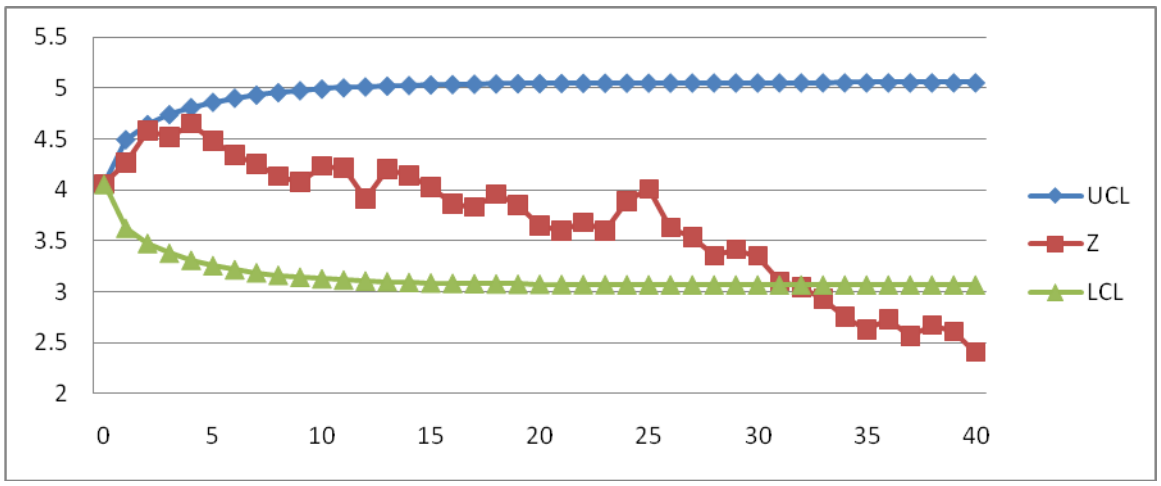

Figure 3-2 The MEWMA chart for the transformed Weibull data

Table 3-6 An example of setting-up EWMA chart with transformed Weibull data

Failure NO	Weibull TBE (X_t)	Transformed Data (Y_t)	EWMA (Z_t)	UCL	LCL
0			4.06	4.06	4.06
1	15.21	6.11	4.27	4.49	3.63
2	20.41	7.45	4.58	4.64	3.48
3	8.35	3.93	4.52	4.74	3.38
4	14.24	5.83	4.65	4.81	3.31
5	5.96	2.98	4.48	4.86	3.26
6	6.13	3.05	4.34	4.90	3.22
7	7.11	3.45	4.25	4.93	3.19
8	6.22	3.08	4.13	4.96	3.16
9	7.36	3.55	4.08	4.98	3.14
10	13.63	5.65	4.23	4.99	3.13
11	8.76	4.08	4.22	5.00	3.12
12	2.52	1.19	3.92	5.01	3.11
13	17.81	6.81	4.20	5.02	3.10
14	7.44	3.58	4.14	5.03	3.09
15	6.07	3.02	4.03	5.03	3.09
16	4.63	2.37	3.86	5.04	3.08
17	7.31	3.53	3.83	5.04	3.08
18	11.87	5.12	3.96	5.04	3.08
19	5.73	2.88	3.85	5.05	3.08
20	3.59	1.83	3.65	5.05	3.07
21	6.30	3.12	3.60	5.05	3.07
22	9.83	4.45	3.68	5.05	3.07
23	5.71	2.86	3.60	5.05	3.07
24	16.64	6.50	3.89	5.05	3.07
25	11.77	5.09	4.01	5.05	3.07
26	1.20	0.19	3.63	5.05	3.07
27	5.34	2.70	3.54	5.05	3.07
28	3.39	1.72	3.35	5.05	3.07
29	8.48	3.97	3.42	5.05	3.07
30	5.52	2.78	3.35	5.05	3.07
31	2.01	0.85	3.10	5.05	3.07
32	5.01	2.55	3.05	5.05	3.07
33	3.65	1.86	2.93	5.05	3.07
34	2.48	1.17	2.75	5.05	3.07
35	3.04	1.52	2.63	5.05	3.07
36	7.51	3.61	2.73	5.05	3.07
37	2.40	1.11	2.57	5.05	3.07
38	7.55	3.62	2.67	5.05	3.07
39	4.05	2.07	2.61	5.05	3.07
40	1.62	0.55	2.41	5.05	3.07

3.5 Conclusions

The proposed EWMA chart with transformed Weibull data provides a more direct and practical way to monitor Weibull TBE data. The results show that the EWMA chart with transformed Weibull data performs well in detecting the shift in scale parameter when the shape parameter is fixed. And the ARL performance discussed in this chapter may provide some guidelines for designing the proposed EWMA chart in practice.

CHAPTER 4 TWO MEWMA CHARTS FOR GUMBEL'S BIVARIATE EXPONENTIAL DISTRIBUTION

The TBE charts have gained popularity for their effectiveness in high quality process monitoring (see Xie et al. 2002). However, all of the TBE charts mentioned in literature focus on univariate cases, assuming that there is only one process characteristic of interest. In reality, the overall quality of a system tends to depend on several quality characteristics that are generally correlated. For example, in reliability analysis, the failure of a system may be caused by the failure of any component within that system; hence the time between failures of one component may be correlated with the time between failures of other components as they are working in a similar environment. While monitoring several correlated TBE variables, the use of separate univariate TBE charts does not account for the correlation between variables, and the results can be very inefficient, sometimes even misleading. Thus it is a practical necessity to develop suitable multivariate TBE control charts that can simultaneously monitor or control two or more related TBE characteristics.

Furthermore, most multivariate control charts, e.g. Hotelling's T^2 charts (Hotelling 1947), the multivariate exponential weighted moving average (MEWMA) charts (Lowry 1992) and the multivariate cumulative sum (MCUSUM) charts (Crosier 1988, Pignatiello and Runger 1990), were developed for multivariate normal data. However, multivariate

TBE data are usually non-normal and highly skewed, as the marginal distributions are usually based on exponential, gamma or Weibull distributions. Similar to the univariate case, the traditional multivariate charts based on the T^2 statistic have been shown to be quite sensitive to non-normality and would face practical difficulties in such a situation, perhaps even losing their efficiency in detecting process shifts.

Various methods have been developed to construct multivariate control charts for skewed populations, some with the help of transformations (Chang and Bai 2004, Chang 2007), while others are based on nonparametric approaches (Qiu and Hawkins 2001, Qiu and Hawkins 2003, Qiu 2008). However, these multivariate non-parametric control charts are usually less powerful, and more computationally intensive. Meanwhile, the MEWMA chart was proposed by various researchers for its effectiveness in monitoring non-normal populations. For recent results, see Hawkins and Maboudou Tchao (2008), Zou and Tsun (2008) and Reynolds and Stoumbos (2008). In particular, Stoumbos and Sullivan (2002) and Testik et al. (2003) showed that the MEWMA control chart with a small smoothing constant is fairly robust to non-normality. These successful applications of MEWMA charts for non-normal data motivate our investigation into the likely benefits of applying MEWMA chart to monitoring of multivariate TBE data.

In this chapter, two MEWMA charts are constructed for the popular Gumbel's bivariate TBE model (Gumbel 1960) in reliability analysis. In the subsequent sections, the Gumbel's bivriate TBE model is introduced, and two MEWMA charts are proposed for the model, one on the raw data and the other on transformed data. Both charts are constructed for monitoring a mean vector shift (or shifts) under the assumption that the

dependence between the two variables remains the same. For MEWMA on the transformed data, we first transform the bivariate exponential data into approximate bivariate normal data using the well-known double square root transformation, and then we apply the MEWMA chart to the transformed data. A numerical example is given to illustrate the use of the MEWMA procedures. The ARL properties of the two MEWMA charts are investigated, and their performances are compared with those of the paired individual *t* charts and the paired individual EWMA charts on both raw and transformed data. The proposed MEWMA charts are shown to generally outperform all the other charts under the circumstances considered. Finally, we briefly discuss the extension of our MEWMA charts to Gumbels's multivariate exponential distribution with more than two variables.

4.1 Two MEWMA charts for Gumbel's lifetime data

4.1.1 Gumbel's bivariate exponential model

Gumbel (1960) first introduced the model with the following joint survival function (1.0 minus the CDF)

$$\bar{F}_{X_1,X_2}(x_1,x_2)=\exp\{-(x_1^m+x_2^m)^{1/m}\},\ x_1,x_2>0,\ m\geq 1. \tag{4-1}$$

A more general expression for the survival function is:

$$\bar{F}_{X_1,X_2}(x_1,x_2)=\exp\left\{-\left[\left(\frac{x_1}{\theta_1}\right)^{\frac{1}{\delta}}+\left(\frac{x_2}{\theta_2}\right)^{\frac{1}{\delta}}\right]^{\delta}\right\},\ x_1,x_2>0,\ \theta_1,\theta_2>0,\ 0<\delta\leq 1. \tag{4-2}$$

Here θ_1 and θ_2 are the scale parameters, δ is the dependence parameter, and δ=1 corresponds to independence. In this chapter, we will refer to this as the GBE model.

Houggard (1986) further studied a bivariate Weibull extension of the GBE model with a common shape parameter γ having the following survival function:

$$\bar{F}_{X_1,X_2}(x_1,x_2)=\exp\{-(\varepsilon_1 x_1^{\gamma}+\varepsilon_2 x_2^{\gamma})^{\alpha}\},\ x_1,x_2>0,\ \varepsilon_1,\varepsilon_2>0,\ 0<\alpha\le 1. \tag{4-3}$$

Here ε_1 and ε_2 are the scale parameters, γ is the shape parameter, α is the dependence parameter, and $\alpha=1$ corresponds to independence. We will refer to it as HBW($\varepsilon_1,\varepsilon_2,\gamma,\alpha$). When $\alpha\gamma=1$, the HBW model reduces to the GBE model. Hougaard (1989) further extended the bivariate Weibull distribution to the multivariate case. Hougaard showed that the HBW model is a meaningful physical model for failure-times analysis derived from consideration of a random environmental stress affecting both components. In other words, the dependence in the GBE model is explained by the random mixing effect of an external stress. This is different from other popular multivariate failure-times models where one could specify the source of dependence. For example, the dependence in the Marshall-Olkin's model (Marshall and Olkin 1967) is explained by a common shock destroying both components, and the dependence in the Freund's model (Freund 1961) is due to a failure event internal to the system.

According to Lee (1979), the bivariate life time (X_1, X_2) of the GBE model can be presented in terms of independent random variables $X_1=\theta_1 U^{\delta}V$ and $X_2=\theta_2(1-U)^{\delta}V$, where U follows a uniform(0,1) distribution, $V=V_{11}+M_{\delta}V_{12}$, each V_{1i} follows an

exponential distribution with mean 1, $M_\delta = 0$ or 1 with probabilities $1-\delta$ and δ, respectively. The random variables U, V_{11}, V_{12}, M_δ are all independent. For more statistical discussions, including the estimators of parameters, one could refer to Lu and Bhattacharyya (1991a, 1991b). Both the GBE model and the HBW model can be easily extended to the multivariate case.

The HBW model and the GBE model have been suggested for different applications in the literature. The HBW model is especially suitable for family data or competing risks data. The family data here refers to the lifetimes of two individuals or components which share some common risk, for example twins, couples or automobile parts with dependent lifetimes. The dependence within a family might be caused by both genetic and environmental factors. For example, Lu and Bhattacharyya (1991a) used the GBE model to analyze paired relief time data collected from headache patients each of whom was given two different treatments. On the other hand, for components in a system, the dependence could be created by the different quality of components from various batches or by the working conditions of the system. For example, Pal and Murthy (2003) fitted the GBE model to the age of motor cycle (in days) and the usage of motor cycle (in kilometers) at the time of registering a warranty claim.

Another interesting type of data is that on competing risks. In competing risk models, the observed system lifetime data can be categorized by the causes of system failure. To analyze competing risks data, one often constructs random variables that denote the lifetimes associated with each cause. To estimate the multivariate distribution with this kind of data, it is necessary to introduce extra dependence assumptions which cannot be

verified, and the estimation results depend very much on the assumptions. Due to the non-identifiability of the dependence assumptions, multivariate lifetime distributions with a specific physical dependence cannot be fitted to competing risks data. On the other hand, the HBW model and the GBE model that assume the dependence caused by random effects can easily be applied in such cases. For example, Houggard (1989) used the HBW model to analyze the time to failure of turn, phase, and ground in 10 motors. One could only first observe the failure of a motor, and then determine the failed motor component or components. In this case, it is impossible to identify any physical dependence between the motor components. It is more likely that the dependence is caused by different working environments for each motor, which suggests a model like the HBW model.

As mentioned above, the GBE model is a typical lifetime model in the reliability applications, and many authors have investigated its properties both theoretically and practically. Thus, it is meaningful and important to develop statistical process control tools for the GBE model. In the following section, two MEWMA charts are proposed for lifetime data with a GBE model.

4.1.2 Construction of a MEWMA chart based on the raw GBE data

Let X_1 and X_2 denote the TBE data of interests. We assume that the joint distribution of (X_1, X_2) follows GBE $(\theta_1, \theta_2, \delta)$ with the survival function as Equation (4-2). It is clear that the marginal distributions of X_1, X_2 are $\exp(\theta_1)$ and $\exp(\theta_2)$, respectively. The mean vector of X_1 and X_2 is given by

$$\boldsymbol{\mu} = \begin{bmatrix} \mu_1 \\ \mu_2 \end{bmatrix} = \begin{bmatrix} \theta_1 \\ \theta_2 \end{bmatrix}. \tag{4-4}$$

Lu and Bhattacharyya (1991a) showed that

$$E(X_1^{k_1} X_2^{k_2}) = \frac{\theta_1^{k_1}\theta_2^{k_2}\Gamma(k_1\delta+1)\Gamma(k_2\delta+1)\Gamma(k_1+k_2+1)}{\Gamma(k_1\delta+k_2\delta+1)},\ k_1, k_2 > 0, \tag{4-5}$$

where $\Gamma(\cdot)$ is the gamma function.

Thus, the correlation coefficient of X_1 and X_2 is given by

$$\rho_X = \frac{2\Gamma^2(\delta+1)}{\Gamma(2\delta+1)} - 1, \tag{4-6}$$

which ranges from 0 to 1 and is monotone decreasing in δ. Let $\boldsymbol{\rho}_X$ denote the correlation coefficient matrix. According to Equation (4-6), $\boldsymbol{\rho}_X$ is dictated by the dependence parameter δ, and is not affected by the value of θ_1 or θ_2. The covariance matrix of (X_1, X_2) becomes

$$\boldsymbol{\Sigma}_X = \begin{bmatrix} \theta_1^2 & \rho_X\theta_1\theta_2 \\ \rho_X\theta_1\theta_2 & \theta_2^2 \end{bmatrix} = \begin{bmatrix} \theta_1^2 & \left(\frac{2\Gamma^2(\delta+1)}{\Gamma(2\delta+1)} - 1\right)\theta_1\theta_2 \\ \left(\frac{2\Gamma^2(\delta+1)}{\Gamma(2\delta+1)} - 1\right)\theta_1\theta_2 & \theta_2^2 \end{bmatrix}. \tag{4-7}$$

First introduced by Lowry et al. (1992), the MEWMA chart is originally constructed for detecting the mean shift (or shifts) for the multivariate normal distribution with an in-control mean vector $\boldsymbol{\mu}_0$ and a constant variance covariance matrix $\boldsymbol{\Sigma}_0$. Let the *i*-th ($i = 1, 2, ...$) observation vector of the process be denoted by $\mathbf{X}_i$ with a vector length of p. According to Lowry et al. (1992), the MEWMA statistic is defined as:

$$\mathbf{z}_i = \mathbf{R}(\mathbf{x}_i - \boldsymbol{\mu}_0) + (\mathbf{I} - \mathbf{R})\mathbf{z}_{i-1} = \sum_{j=1}^{i} \mathbf{R}(\mathbf{I} - \mathbf{R})^{i-j}(\mathbf{x}_j - \boldsymbol{\mu}_0), \tag{4-8}$$

where $\mathbf{R} = diag(r_1, r_2, ..., r_p)$ for some user chosen EWMA parameters $0 \le r_k \le 1$ for $k = 1, 2, \ldots, p$, $\mathbf{z}_0 = 0$ and $\mathbf{I}$ is the identity matrix. The MEWMA chart signals if the charted statistic $E_i^2 = \mathbf{z}_i^T \boldsymbol{\Sigma}_{Z_i}^{-1} \mathbf{z}_i > h$, where $\boldsymbol{\Sigma}_{Z_i}$ is the variance-covariance matrix of $\mathbf{z}_i$, and *h* is the UCL.

When $r_1 = r_2 = \cdots = r_p = r$, with a constant $\boldsymbol{\Sigma}_0$, it can be easily shown that

$$\boldsymbol{\Sigma}_{Z_i} = \frac{(1-(1-r)^{2i})r}{2-r}\boldsymbol{\Sigma}_0 \;\rightarrow\; \frac{r}{2-r}\boldsymbol{\Sigma}_0, \text{for } i \rightarrow +\infty. \tag{4-9}$$

As we have introduced, one important assumption for the traditional MEWMA chart is that the variance-covariance matrix of the underlying multivariate normal distribution remains constant after the process experiences a mean shift. However, obviously, this assumption does not hold for most multivariate exponential distributions which have exponential-type marginal distributions as a shift in the mean also implies a shift in the covariance.

On the other hand, the MEWMA chart based on an asymptotic covariance matrix with a small smoothing factor can be designed to be quite robust to non-normal distributions, (see, e.g., Stoumbos and Sullivan, 2002, Testik et al., 2003). In order to employ the robustness feature of the MEWMA chart, we apply the Lowry's MEWMA charting statistic E_i^2 to the GBE data. Assuming the TBE data (X_1, X_2) follows GBE ($\theta_1, \theta_2, \delta$) and the dependence parameter δ remains constant, the proposed new MEWMA chart for monitoring the mean vector (θ_1, θ_2) is constructed as the following:

Step 1: Calculate the following recursive statistics:

$$\mathbf{z}_i = r(\mathbf{x}_i - \boldsymbol{\mu}_{X_0}) + (1-r)\mathbf{z}_{i-1}, \ i = 1, 2, ..., \tag{4-10}$$

where $\mathbf{x}_i = [X_{1i}, X_{2i}]^T$, $0 < r \leq 1$ is the smoothing factor and $\boldsymbol{\mu}_{X_0}$ is the in-control mean vector of the raw GBE data. The starting value $\mathbf{z}_0$ equals to 0. Note that when *r*=1, the MEWMA chart reduces to the T^2 chart.

Step 2: Set up the MEWMA chart using the following statistics:

$$E_i^2 = \frac{2-r}{r} \mathbf{z}_i^T \boldsymbol{\Sigma}_{X_0}^{-1} \mathbf{z}_i, \tag{4-11}$$

where $\boldsymbol{\Sigma}_{X_0}$ is the in-control variance-covariance matrix of the raw GBE data. Here, we use the asymptotic in-control variance-covariance matrix $\boldsymbol{\Sigma}_Z = \frac{r}{2-r} \boldsymbol{\Sigma}_{X_0}$ and the later comparison study results will show that this implementation is reasonable.

Step 3: The process is considered to be out-of-control when E_i^2 exceeds the decision interval *h*.

In practice, the in-control $\boldsymbol{\mu}_{X_0}$ and $\boldsymbol{\Sigma}_{X_0}$ can be estimated from the in-control historical data using the grand mean vector and sample variance-covariance matrix:

$$\hat{\boldsymbol{\mu}}_{X_0} = \bar{\mathbf{x}} = \frac{1}{n}\sum_{k=1}^{n}\mathbf{x}_k, \tag{4-12}$$

$$\hat{\boldsymbol{\Sigma}}_{X_0} = \frac{1}{n-1}\sum_{k=1}^{n}(\mathbf{x}_k - \bar{\mathbf{x}})(\mathbf{x}_k - \bar{\mathbf{x}})^T. \tag{4-13}$$

Another way to estimate the $\boldsymbol{\mu}_{X_0}$ and $\boldsymbol{\Sigma}_{X_0}$ is to first estimate the in-control parameters $\theta_1, \theta_2, \delta$ of the GBE model, and then calculate $\boldsymbol{\mu}_{X_0}$ and $\boldsymbol{\Sigma}_{X_0}$ according to Equation (4-4) to Equation (4-7).

The design parameters *r* and *h* are determined by Monte Carlo simulation so that the ARL_0 approximately equals to the desired level. Here we use simulation to calculate the ARL values since we encountered difficulties with the published analytical approaches based on the multivariate normal distribution such as the bivariate Markov chain method, the probability limit method, and the integral equation approach. In our study, we first program a subroutine to get the run length for a single charting realization using simulated GBE data. The run length is defined as the number of the plotted points until the charts first signal. Then, 10,000 trials of the run length subroutine are executed and the average of these 10,000 run length values is used to estimate the ARL value. Several commonly used smoothing factor *r* values are selected in this study: *r*=0.01, 0.02, 0.05, 0.1, 0.3, 0.5, 0.8, 1. For each *r* value, the corresponding *h* value is determined so that ARL_0 is the desired value. These *r* and *h* combinations are further used for control chart construction

and performance comparison. The ARL property of the MEWMA chart on raw data will be further analyzed in the later sections.

4.1.3 Construction of a MEWMA chart based on the transformed GBE data

In the literature, there are numerous studies concerning transforming skewed data into approximate normal data before applying control charts. Hence, we investigate the possibility of constructing a multivariate TBE chart based on transformed GBE data.

Again, we assume the joint distribution of TBE data (X_1, X_2) is GBE($\theta_1, \theta_2, \delta$) with the survival function (4-2). We use the double square root transformation on X_1 and X_2 marginally, because the double square root transformation has been recommended by many authors for transforming exponential data to approximately normal; see Kittlitz et al. (1999), Liu et al. (2006), and Liu et al. (2007). Let Y_1 and Y_2 denote the variables after transformation, i.e.

$$Y_1 = X_1^{0.25} \text{ and } Y_2 = X_2^{0.25}. \tag{4-14}$$

The joint survival function of (Y_1, Y_2) becomes

$$\bar{F}_{Y_1,Y_2}(y_1, y_2) = \exp\left\{-\left[\left(\frac{y_1^4}{\theta_1}\right)^{\frac{1}{\delta}} + \left(\frac{y_2^4}{\theta_2}\right)^{\frac{1}{\delta}}\right]^{\delta}\right\},\ y_1, y_2 > 0,\ \theta_1, \theta_2 > 0,\ 0 < \delta \le 1, \tag{4-15}$$

which follows HBW($1/\theta_1^{1/\delta}, 1/\theta_2^{1/\delta}, 4/\delta, \delta$).

The marginal distributions of $Y_i (i = 1, 2)$ follow Weibull distributions $W(\theta_i^{0.25}, 4)$. The mean and standard deviation can be calculated as

$$\mu_{Y_i} = E(Y_i) = \theta_i^{0.25}\Gamma(1+0.25) = 0.9064\theta_i^{0.25} \tag{4-16}$$

and

$$\sigma_{Y_i} = \sqrt{D(Y_i)} = \theta_i^{0.25}\sqrt{\Gamma(1+0.5) - \Gamma^2(1+0.25)} = 0.2543\theta_i^{0.25}. \tag{4-17}$$

According to Equation (4-5),

$$E(Y_1Y_2) = E(X_1^{0.25}X_2^{0.25}) = \frac{\theta_1^{0.25}\theta_2^{0.25}\Gamma(0.25\delta+1)\Gamma(0.25\delta+1)\Gamma(0.25+0.25+1)}{\Gamma(0.25\delta+0.25\delta+1)}. \tag{4-18}$$

So the covariance of Y_1 and Y_2 is

$$\mathrm{cov}(Y_1Y_2) = E(Y_1Y_2) - \mu_{Y_1}\mu_{Y_2} = \left[\frac{\Gamma^2(0.25\delta+1)\Gamma(1.5)}{\Gamma(0.5\delta+1)} - \Gamma^2(1.25)\right]\theta_1^{0.25}\theta_2^{0.25}, \tag{4-19}$$

and the correlation coefficient between Y_1 and Y_2 is

$$\rho_Y = \frac{\mathrm{cov}(Y_1, Y_2)}{\sigma_{Y_1}\sigma_{Y_2}} = \left[\frac{\Gamma^2(0.25\delta+1)\Gamma(1.5)}{\Gamma(0.5\delta+1)} - \Gamma^2(1.25)\right] \Big/ \left[\Gamma(1.5) - \Gamma^2(1.25)\right]. \tag{4-20}$$

Let the correlation coefficient matrix be $\boldsymbol{\rho}_Y$. According to Equation (4-17) and Equation (4-20), $\boldsymbol{\rho}_Y$ is determined by the dependence parameter δ, and does not depend on the value of θ_1 or θ_2. So the covariance matrix of (Y_1, Y_2) becomes

$$\boldsymbol{\Sigma}_Y = \begin{bmatrix} \sigma_{Y_1}^2 & \rho_Y\sigma_{Y_1}\sigma_{Y_2} \\ \rho_Y\sigma_{Y_1}\sigma_{Y_2} & \sigma_{Y_2}^2 \end{bmatrix}. \tag{4-21}$$

In Figure 4-1, some plots are shown for the joint density function of the original distribution, the transformed distribution and the corresponding normal distributions with

the same $\boldsymbol{\mu}$ and $\boldsymbol{\Sigma}$. We can see that the transformed bivariate exponential distribution is quite close to the corresponding bivariate normal distribution but with larger kurtosis.

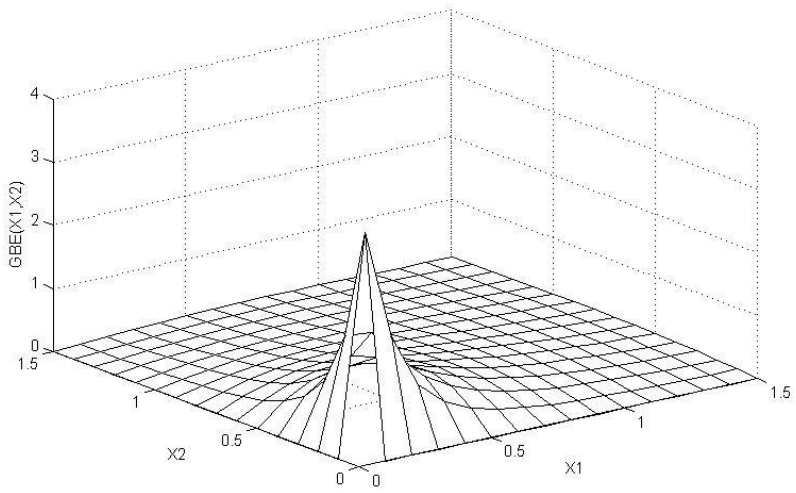

(a) Joint distribution of raw data

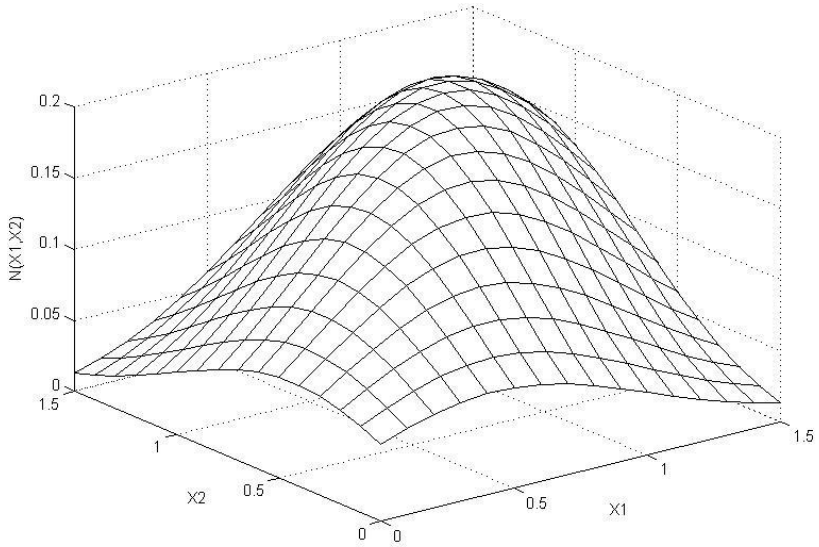

(b) Normal distribution with the same $\boldsymbol{\mu}$ and $\boldsymbol{\Sigma}$ of the raw data

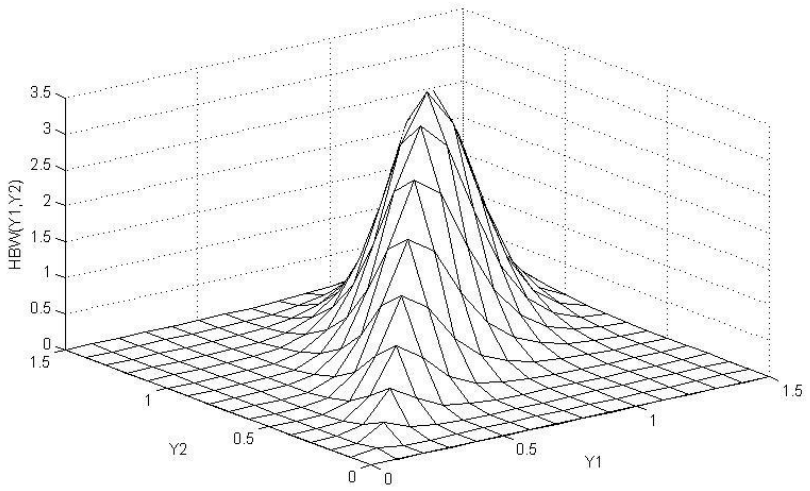

(c) Joint distribution of the transformed data

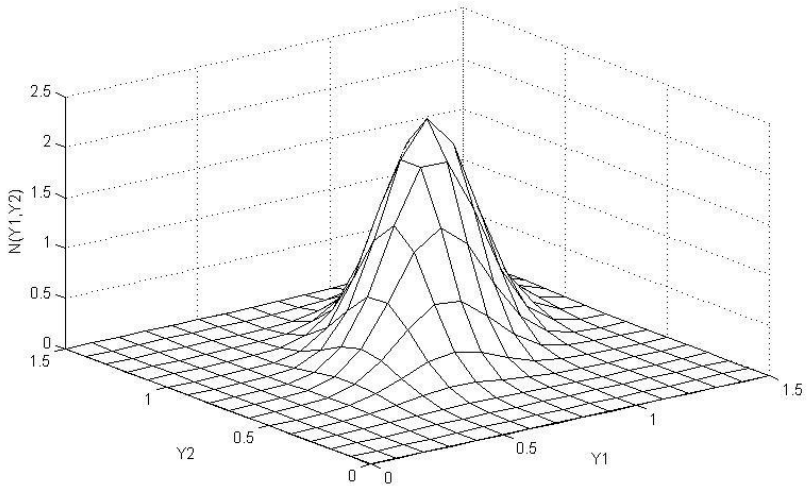

(d) Normal distribution with the same $\boldsymbol{\mu}$ and $\boldsymbol{\Sigma}$ of the transformed data

Figure 4-1 Joint density function plots ($\theta_1=\theta_2=1,\ \delta=0.5$)

Let the *i*-th ($i=1,2,\ldots$) transformed data vector of the process be denoted by $\mathbf{Y}_i$. The proposed MEWMA chart is constructed below:

Step 1: Calculate the following recursion statistics:

$$\mathbf{z}_i = r(\mathbf{y}_i - \boldsymbol{\mu}_{Y_0}) + (1-r)\mathbf{z}_{i-1} = \sum_{j=1}^{i} r(1-r)^{i-j}(\mathbf{y}_j - \boldsymbol{\mu}_{Y_0}), \quad i = 1, 2, ..., \tag{4-22}$$

where $\mathbf{y}_i = [Y_{1i}, Y_{2i}]^T$, $0 < r \leq 1$ is the smoothing factor and $\boldsymbol{\mu}_{Y_0}$ is the in-control mean vector of the transformed GBE data. The starting value $\mathbf{z}_0$ equals 0. Note that when r=1, the MEWMA chart reduces to the T^2 chart.

Step 2: Set up the MEWMA chart on the following statistics:

$$E_i^2 = \frac{2-r}{r}\mathbf{z}_i^T \boldsymbol{\Sigma}_{Y_0}^{-1}\mathbf{z}_i, \tag{4-23}$$

where $\boldsymbol{\Sigma}_{Y_0}$ is the in-control variance-covariance matrix of the transformed GBE data. Again, we directly use the asymptotic in-control variance-covariance matrix $\boldsymbol{\Sigma}_Z = \frac{r}{2-r}\boldsymbol{\Sigma}_{Y_0}$.

Step 3: The process is considered to be out-of-control when E_i^2 exceeds the decision interval h.

In practice, the in-control $\boldsymbol{\mu}_{Y_0}$ and $\boldsymbol{\Sigma}_{Y_0}$ can be estimated from the in-control historical data using the grand mean vector and sample variance-covariance matrix:

$$\hat{\boldsymbol{\mu}}_{X_0} = \bar{\mathbf{y}} = \frac{1}{n}\sum_{k=1}^{n}\mathbf{y}_k, \tag{4-24}$$

$$\hat{\boldsymbol{\Sigma}}_{Y_0} = \frac{1}{n-1}\sum_{k=1}^{n}(\mathbf{y}_k - \bar{\mathbf{y}})(\mathbf{y}_k - \bar{\mathbf{y}})^T. \tag{4-25}$$

Similarly, the design parameters r and h of the MEWMA chart on the transformed data are also determined by Monte Carlo simulation so that the ARL_0 approximately equals the desired level. We first program a subroutine to get the run length for a single

charting realization using simulated GBE data. After that, 10,000 trials of the run length subroutine are executed, and the average of these 10,000 run length values is used to estimate the ARL value. The ARL property of the MEWMA chart on transformed data is analyzed in later sections.

4.1.4 Numerical example

A simulation example is constructed to illustrate the implementation procedure of the proposed MEWMA chart with raw or transformed GBE data. We use the relief time example from Lu and Bhattacharyya (1991a) as the defined in-control process. Each of 10 patients was given two different treatments for headache on separate occasions. The paired data of relief time (in minutes) are: (8.4, 6.9), (7.7, 6.8), (10.1, 10.3), (9.6, 9.4), (9.3, 8.0), (9.1, 8.8) (9.0, 6.1), (7.7, 7.4), (8.1, 8.0) and (5.3, 5.1). These data are transformed by subtracting 5.0 from each point, and then fitting a GBE model. Note that 10 observations are not enough to accurately estimate the parameters, and we only use these numbers as an illustration. We further assume that a new medicine was recently invented and has been used in combination with the two treatments in medical experiments. Due to the effectiveness of the new medicine, the average transformed relief time of the two treatments has been shortened to 20% and 50% of the defined ones, respectively. We use the two proposed MEWMA charts to monitor the transformed patients relief times.

The first 10 paired data in Table 4-1 are the 10 transformed patients relief times mentioned above. The estimated parameters are θ_1=3.43，θ_2=2.68，δ=0.25. According

to the shift assumption we made, the next 15 points are generated with scale parameters (θ_1'=0.2θ_1, θ_2'=0.5θ_2) and the dependence parameters δ=0.25. The design parameters of the MEWMA chart on the raw GBE data are obtained by simulation ($r = 0.02, h = 5.41$) to achieve an in-control ARL=200. The control chart is shown in Figure 4-2. The MEWMA chart on the raw GBE data showed an out of control signal at the 20th point. Similarly, the design parameters of the MEWMA chart on the transformed GBE data are obtained by simulation ($\lambda = 0.02, h = 5.27$) and the control chart is shown in Figure 4-3. The MEWMA chart on the transformed GBE data showed an out of control signal at the 18th point.

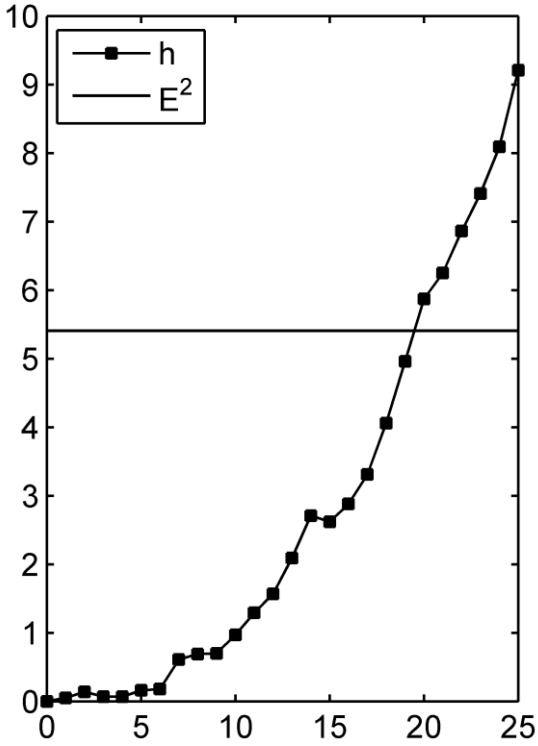

Figure 4-2 An example of constructing MEWMA chart based on raw GBE data

Table 4-1 An example of setting-up MEWMA chart based on raw or transformed GBE data

NO	$MEWMA_{Raw}$					$MEWMA_{Trans}$				
	$\mathbf{x}_i$		$\mathbf{z}_i$		E_i^2	$\mathbf{y}_i$		$\mathbf{z}_i$		E_i^2
0			0	0	0.00			0	0	0.00
1	3.4	1.9	-0.001	-0.031	0.05	1.358	1.174	0.002	-0.001	0.01
2	2.7	1.8	-0.015	-0.063	0.14	1.282	1.158	0.003	-0.003	0.02
3	5.1	5.3	0.019	-0.024	0.07	1.503	1.517	0.009	0.003	0.07
4	4.6	4.4	0.042	-0.004	0.07	1.465	1.448	0.013	0.007	0.18
5	4.3	3	0.058	-0.013	0.16	1.440	1.316	0.017	0.009	0.30
6	4.1	3.8	0.070	-0.005	0.18	1.423	1.396	0.020	0.012	0.45
7	4	1.1	0.080	-0.051	0.61	1.414	1.024	0.024	0.007	0.50
8	2.7	2.4	0.064	-0.071	0.69	1.282	1.245	0.024	0.008	0.52
9	3.1	3	0.056	-0.078	0.70	1.327	1.316	0.026	0.009	0.59
10	0.3	0.1	-0.007	-0.143	0.97	0.740	0.562	0.015	-0.005	0.22
11	0.168	0.186	-0.073	-0.205	1.29	0.640	0.656	0.003	-0.016	0.25
12	0.603	0.810	-0.128	-0.254	1.57	0.881	0.949	-0.004	-0.021	0.43
13	0.096	0.094	-0.192	-0.315	2.09	0.556	0.553	-0.018	-0.035	1.31
14	0.026	0.018	-0.256	-0.377	2.71	0.403	0.366	-0.034	-0.051	3.23
15	1.509	2.535	-0.289	-0.387	2.62	1.108	1.262	-0.036	-0.050	3.18
16	1.038	1.555	-0.331	-0.417	2.88	1.009	1.117	-0.039	-0.051	3.52
17	0.746	1.061	-0.378	-0.456	3.31	0.930	1.015	-0.045	-0.054	4.17
18	0.237	0.258	-0.435	-0.511	4.06	0.698	0.713	-0.055	-0.064	5.91
19	0.013	0.007	-0.494	-0.569	4.96	0.338	0.285	-0.071	-0.081	9.83
20	0.153	0.164	-0.550	-0.623	5.87	0.625	0.636	-0.082	-0.092	12.69
21	1.024	1.519	-0.587	-0.649	6.25	1.006	1.110	-0.085	-0.092	13.17
22	0.664	1.011	-0.631	-0.684	6.86	0.903	1.003	-0.090	-0.095	14.30
23	0.851	1.232	-0.670	-0.714	7.41	0.960	1.054	-0.094	-0.097	15.11
24	0.629	0.948	-0.712	-0.750	8.09	0.890	0.987	-0.099	-0.100	16.37
25	0.127	0.130	-0.764	-0.801	9.21	0.597	0.600	-0.109	-0.110	20.10

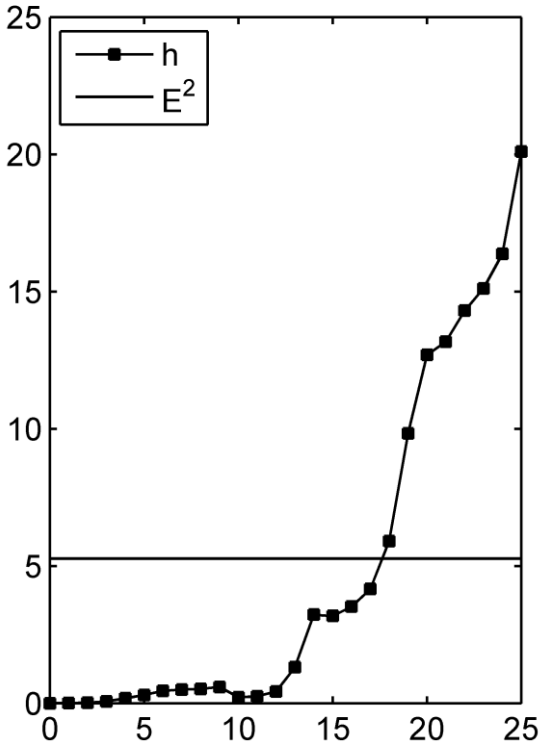

Figure 4-3 An example of constructing MEWMA chart based on transformed GBE

4.2 Average run length and some properties

The ARL is a traditional performance measure for control chart design and comparison. Generally, the ARL is defined as the average number of points that must be plotted before the chart issues an out-of-control signal. For the charts under comparison, the design parameters and control limits are adjusted to achieve a certain ARL_0, and the one with the smallest ARL_1 is considered to be the best.

In this study, we assume the mean vector shift (or shifts) starts (or start) from the very beginning (*i*=1), i.e. we study the "zero state" ARL performance. The in-control process is modeled by GBE ($\theta_1, \theta_2, \delta$), and the out-of-control process modeled by GBE($\theta_1', \theta_2', \delta$). We now show that the ARL performance of the two proposed MEWMA charts on $\mathbf{x}_i$ and $\mathbf{y}_i$ only depends on the marginal mean shift vector ($\theta_1'/\theta_1, \theta_2'/\theta_2$) when the smoothing parameter *r* and the dependency parameter δ are constant. Let $\mathbf{x}_i$ denote the *i*-th observed sample data which follows GBE($\theta_1', \theta_2', \delta$) and $\mathbf{y}_i$ denote the *i*-th transformed sample data while the in-control distribution is denoted by GBE($\theta_1, \theta_2, \delta$). The MEWMA charts are constructed according to Section 4-1 and the out-of-control shift starts from the very beginning that the chart is constructed.

Lemma 1. When the dependency parameter δ remains constant, the initial state ARL performance of the MEWMA chart on $\mathbf{x}_i$ only depends on the marginal mean shift vector ($\theta_1'/\theta_1, \theta_2'/\theta_2$) and the design parameters *r* and *h*.

Proof: According to Section 4.1.2, the charting statistic of the MEWMA chart on $\boldsymbol{X}_i$ is

$$\begin{aligned} E_i^2 &= \frac{2-r}{r}\mathbf{z}_i^T\boldsymbol{\Sigma}_{X_0}^{-1}\mathbf{z}_i \\ &= \frac{2-r}{r}\cdot\left[\sum_{j=1}^{i} r(1-r)^{i-j}\left(\mathbf{x}_j-\boldsymbol{\mu}_X\right)^T\right]\cdot\boldsymbol{\Sigma}_{X_0}^{-1}\cdot\left[\sum_{j=1}^{i} r(1-r)^{i-j}\left(\mathbf{x}_j-\boldsymbol{\mu}_X\right)\right] \\ &= \frac{2-r}{r}\left[\sum_{j=1}^{i} r(1-r)^{i-j}\,\mathbf{v}_i^T\right]\cdot\left[\boldsymbol{\rho}_{X_0}^{-1}\right]\cdot\left[\sum_{j=1}^{i} r(1-r)^{i-j}\,\mathbf{v}_i\right] \\ &\equiv \frac{2-r}{r}\mathbf{m}_i^T\boldsymbol{\rho}_{X_0}^{-1}\mathbf{m}_i \end{aligned} \tag{4-26}$$

where $\mathbf{v}_i = \left(\frac{x_{1i} - \mu_{X_{10}}}{\sigma_{X_{10}}}, \frac{x_{2i} - \mu_{X_{20}}}{\sigma_{X_{20}}} \right)$ is the standardized raw sample data and $\mathbf{m}_i = \sum_{j=1}^{i} r(1-r)^{i-j} \mathbf{v}_i$. The chart issues an out-of-control signal when E_i^2 exceeds the UCL (or h) of the MEWMA chart.

The ARL of the MEWMA chart could be written in the following form

$$ARL = \sum_{i=1}^{\infty} (i-1) \Pr(E_i^2 > h, E_0^2, \ldots, E_{i-1}^2 \le h). \tag{4-27}$$

Since (X_1, X_2) follows the following joint distribution

$$\bar{F}_{X_1,X_2}(x_1, x_2) = \exp\left\{ -\left[\left(\frac{x_1}{\theta_1'} \right)^{\frac{1}{\delta}} + \left(\frac{x_2}{\theta_2'} \right)^{\frac{1}{\delta}} \right]^{\delta} \right\}, x_1, x_2 > 0, \theta_1', \theta_2' > 0, 0 < \delta \le 1,$$

and

$$\mathbf{v} = (v_1, v_2) = \left(\frac{x_1 - \theta_1}{\theta_1}, \frac{x_2 - \theta_2}{\theta_2} \right) = \left(\frac{x_1}{\theta_1} - 1, \frac{x_2}{\theta_2} - 1 \right)$$

$\mathbf{v}$ follows the joint distribution

$$\begin{aligned} \bar{F}_{V_1,V_2}(v_1, v_2) &= \bar{F}_{X_1,X_2}(\theta_1(v_1+1), \theta_2(v_2+1)) \\ &= \exp\left\{ -\left[\left((v_1+1) \frac{\theta_1}{\theta_1'} \right)^{\frac{1}{\delta}} + \left((v_2+1) \frac{\theta_2}{\theta_2'} \right)^{\frac{1}{\delta}} \right]^{\delta} \right\}, v_1, v_2 > 0, \theta_1', \theta_2' > 0, 0 < \delta \le 1. \end{aligned} \tag{4-28}$$

Hence, the joint distribution of $\mathbf{v}$ only depends on the mean shift vector $(\theta_1'/\theta_1, \theta_2'/\theta_2)$ and the dependency parameter δ. As $\mathbf{m}_i = \sum_{j=1}^{i} r(1-r)^{i-j} \mathbf{v}_i (i = 1, 2, \ldots)$, $\mathbf{m}_i$ is also decided by the mean shift vector $(\theta_1'/\theta_1, \theta_2'/\theta_2)$.

From Equation 4-6, it is known that the correlation coefficient matrix $\boldsymbol{\rho}_X$ only depends on the dependency parameter δ. Thus, when the dependency parameter δ remains as a constant, the distribution of the E^2 statistic on $\mathbf{x}_i$ only depends on the marginal mean shift vector ($\theta_1'/\theta_1, \theta_2'/\theta_2$). Therefore, the ARL performance of the MEWMA chart on $\mathbf{x}_i$ only depends on marginal mean shift vector ($\theta_1'/\theta_1, \theta_2'/\theta_2$) and the design parameters *r* and *h*.

Lemma 2. When the dependency parameter δ remains as a constant, the ARL performance of the MEWMA chart on $\mathbf{y}_i$ only depends on the marginal mean shift vector ($\theta_1'/\theta_1, \theta_2'/\theta_2$) and the design parameters *r* and *h*.

Proof: According to section 4.1.3, the charting statistic of the MEWMA chart on $\mathbf{y}_i$ is

$$\begin{aligned} E_i^2 &= \mathbf{z}_i^T \boldsymbol{\Sigma}_{\mathbf{z}_i}^{-1} \mathbf{z}_i = \frac{2-r}{r} \mathbf{z}_i^T \boldsymbol{\Sigma}_{Y_0}^{-1} \mathbf{z}_i \\ &= \frac{2-r}{r} \cdot \left[\sum_{j=1}^{i} r(1-r)^{i-j} \left(\mathbf{y}_j - \boldsymbol{\mu}_Y \right)^T \right] \cdot \boldsymbol{\Sigma}_{Y_0}^{-1} \cdot \left[\sum_{j=1}^{i} r(1-r)^{i-j} \left(\mathbf{y}_j - \boldsymbol{\mu}_Y \right) \right] \\ &= \frac{2-r}{r} \left[\sum_{j=1}^{i} r(1-r)^{i-j} \mathbf{w}_i^T \right] \cdot \left[\boldsymbol{\rho}_{Y_0}^{-1} \right] \cdot \left[\sum_{j=1}^{i} r(1-r)^{i-j} \mathbf{w}_i \right] \\ &\equiv \frac{2-r}{r} \mathbf{n}_i^T \boldsymbol{\rho}_{X_0}^{-1} \mathbf{n}_i \end{aligned} \tag{4-28}$$

where $\mathbf{n}_i = \sum_{j=1}^{i} r(1-r)^{i-j} \mathbf{w}_i$ and $\mathbf{w}_i = \left(\frac{y_{1i} - \mu_{Y_{10}}}{\sigma_{Y_{10}}}, \frac{y_{2i} - \mu_{Y_{20}}}{\sigma_{Y_{20}}} \right)$ is the standardized transformed sample data. The chart issues an out-of-control signal when E_i^2 exceeds the *h* value.

The ARL of the MEWMA chart could be written in the following form

$$ARL = \sum_{i=1}^{\infty} (i-1) \Pr(E_i^2 > h, E_0^2, \ldots, E_{i-1}^2 \le h).$$

Since (Y_1, Y_2) follows the joint distribution

$$\bar{F}_{Y_1,Y_2}(y_1, y_2) = \exp\left\{-\left[\left(\frac{y_1^4}{\theta_1'}\right)^{\frac{1}{\delta}} + \left(\frac{y_2^4}{\theta_2'}\right)^{\frac{1}{\delta}}\right]^{\delta}\right\}, y_1, y_2 > 0, \theta_1', \theta_2' > 0, 0 < \delta \le 1,$$

and

$$\begin{aligned}\mathbf{w} = (w_1, w_2) &= \left(\frac{y_1 - \theta_1^{0.25}\Gamma(1.25)}{\theta_1^{0.25}\sqrt{\Gamma(1.5) - \Gamma^2(1.25)}}, \frac{y_2 - \theta_2^{0.25}\Gamma(1.25)}{\theta_2^{0.25}\sqrt{\Gamma(1.5) - \Gamma^2(1.25)}}\right), \\ &= \left(\frac{y_1}{0.2543\theta_1^{0.25}} - 3.5643, \frac{y_2}{0.2543\theta_2^{0.25}} - 3.5643\right)\end{aligned} \quad (4\text{-}29)$$

we have that $\mathbf{w}$ follows the joint distribution

$$\begin{aligned}&\bar{F}_{W_1,W_2}(w_1, w_2) = \bar{F}_{Y_1,Y_2}(0.2543\theta_1^{0.25}(w_1 + 3.5643), 0.2543\theta_2^{0.25}(w_2 + 3.5643)) \\ &= \exp\left\{-\left[\left(0.2543^4(w_1 + 3.5643)^4 \cdot \frac{\theta_1}{\theta_1'}\right)^{\frac{1}{\delta}} + \left(0.2543^4(w_2 + 3.5643)^4 \cdot \frac{\theta_2}{\theta_2'}\right)^{\frac{1}{\delta}}\right]^{\delta}\right\}, \quad (4\text{-}30) \\ &w_1, w_2 > 0, \theta_1', \theta_2' > 0, 0 < \delta \le 1.\end{aligned}$$

Hence, the joint distribution of $\mathbf{w}$ only depends on the marginal mean shift vector $(\theta_1'/\theta_1, \theta_2'/\theta_2)$ and the dependency parameter δ. As $\mathbf{n}_i = \sum_{j=1}^{i} r(1-r)^{i-j}\mathbf{w}_i$, $\mathbf{n}_i$ is also decided by mean shift vector $(\theta_1'/\theta_1, \theta_2'/\theta_2)$.

Referring to Equation 4-20, we can see that the correlation coefficient matrix $\boldsymbol{\rho}_Y$ only depends on the dependency parameter δ. Thus, when the dependency parameter δ remains as a constant, the distribution of the E^2 statistic on $\mathbf{y}_i$ only depends on the mean shift vector $(\theta_1'/\theta_1, \theta_2'/\theta_2)$. Therefore, the ARL performance of the MEWMA chart on $\mathbf{y}_i$ only depends on the mean shift vector $(\theta_1'/\theta_1, \theta_2'/\theta_2)$ and the design parameters *r* and *h*.

Thus, when the process is in control, i.e. $\theta_1' = \theta_1$, $\theta_2' = \theta_2$, the ARL_0 of the two MEWMA charts only depends on the design parameters *r* and *h*. Hence, without loss of generality, we could study the ARL_0 performance of GBE (1, 1, δ) to determine the *r* and *h* combinations. The *r* and *h* values we get could be applied to any GBE distribution with the same δ . Given the design parameter *r* and *h*, the ARL_1 of the two charting processes only depends on mean shift vector ($\theta_1' / \theta_1, \theta_2' / \theta_2$). Thus, to decide the most efficient chart or parameter combination, we only need to identify the mean shift (or shifts) level.

Figure 4-4(a) and 4-4(b) illustrate the ARL_0 curves of MEWMA charts when δ =0.5 with the following *r* values: 0.01, 0.02, 0.05, 0.1, 0.3, 0.5, 0.8, 1. The curves are plotted with an increasing *h* step of 0.25, and are located from left to right as the *r* value increases from 0.01 to 1. Once the *r* and δ values are determined, one could easily obtain the approximate *h* value to achieve a desired ARL_0 with the help of interpolation. The exact *h* values can be achieved by the following steps: 1) specify the ARL_0 , *r*; 2) find the approximate range of *h* values from the ARL_0 plots; 3) calculate the ARL_0 values against the *h* values within that range with an increasing step of 0.01; 4) find the *h* value which gives an ARL_0 value closest to the target one; 5) if the closest ARL_0 value deviates by more than +2% or －2% from the target value, decrease or increase the obtained *h* value by 0.005 accordingly. The simulation results show such an *h* value would provide an ARL_0 within the range of target ARL ±2%, which is accurate enough in most applications.

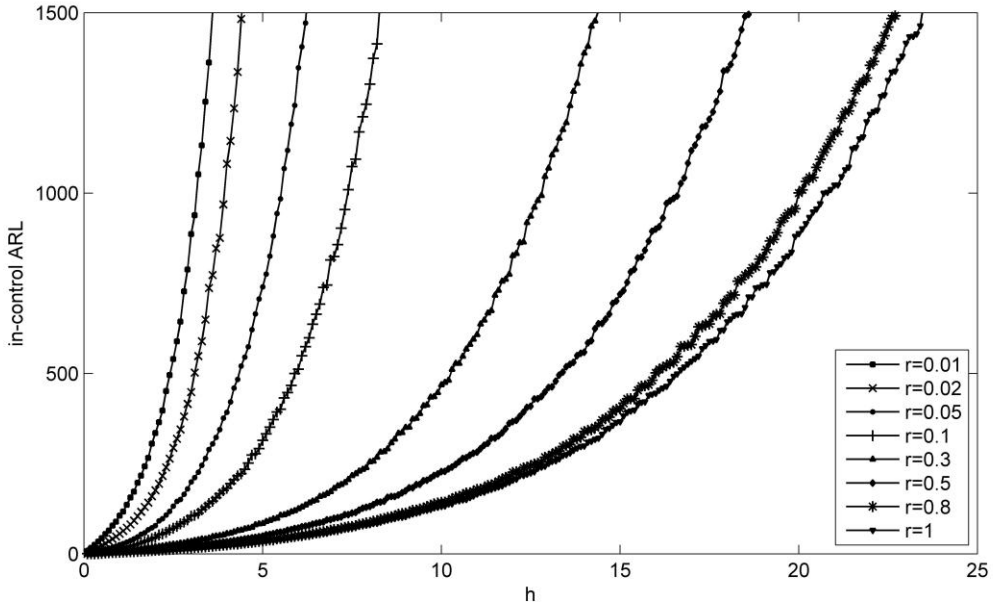

Figure 4-4(a) The in-control ARL for the MEWMA chart based on raw data when δ=0.5

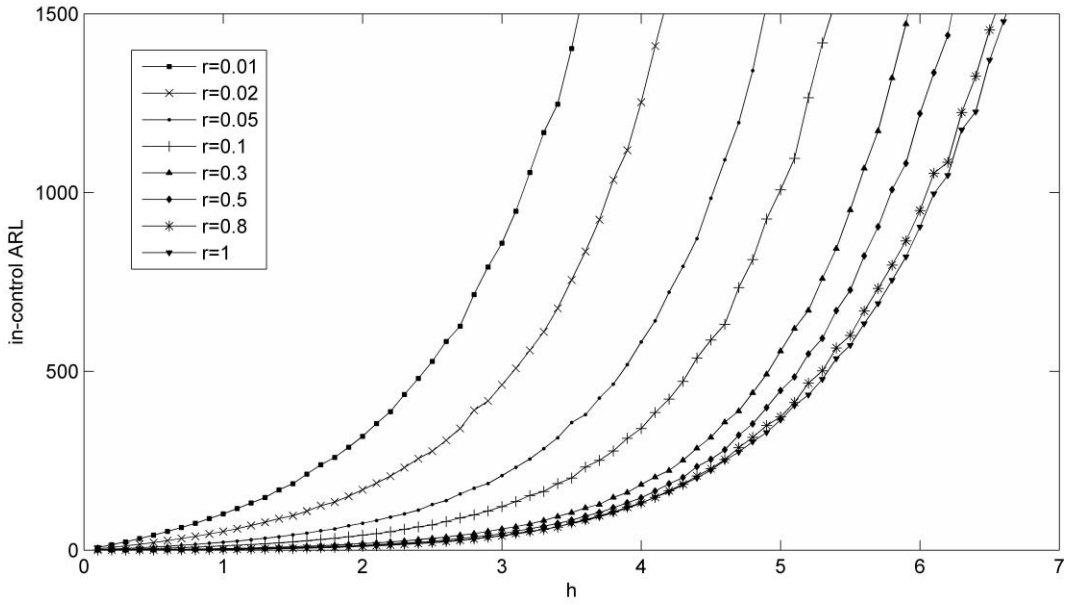

Figure 4-4 (b) The in-control ARL for the MEWMA chart based on transformed data when δ=0.5

4.3 Comparison studies

The effectiveness of five control charts (the MEWMA chart based on raw data, the MEWMA chart based on transformed data, the paired individual *t* charts, the paired individual EWMA charts based on raw data, and the paired individual EWMA charts based on transformed data) are compared in this section. An acceptable ARL_0 is specified at the beginning to determine the probability of false alarm, and the chart that provides the shortest ARL_1 is considered to be the best. Three types of shifts are considered: the downside-downside (D-D) shift ($\theta_1'/\theta_1 < 1$, $\theta_2'/\theta_2 \le 1$), the upside-upside (U-U) shift ($\theta_1'/\theta_1 > 1, \theta_2'/\theta_2 \ge 1$) and the downside-upside (D-U) shift ($\theta_1'/\theta_1 < 1, \theta_2'/\theta_2 > 1$). We first introduce the paired individual *t* charts, and then compare its performance to the two MEWMA charts we have proposed earlier.

4.3.1 Paired individual t charts

The paired individual *t* charts run two *t* charts simultaneously, one for X_1 and the other for X_2. The *t* chart was first introduced by Xie et al. (2002) which directly monitors the TBE data based on the probability limit method. Assume the TBE data follow an exponential distribution, with survival function

$$\bar{F}_X(x) = \exp(-x/\theta), x > 0. \tag{4-31}$$

Given the Type I error of a one-sided *t* chart (α_t), the UCL and the LCL are

$$\begin{aligned} UCL_t &= -\theta \ln(\alpha_t), \\ LCL_t &= -\theta \ln(1-\alpha_t). \end{aligned} \tag{4-32}$$

Again, the in-control process (X_1, X_2) is assumed to follow the GBE($\theta_1, \theta_2, \delta$) model and the out-of-control process is modeled by the GBE($\theta_1', \theta_2', \delta$) model. Let UCL_i and LCL_i ($i = 1, 2$) be the control limits for the two *t* charts. In this study, we equally allocate the Type I error for the two *t* charts, i.e. $\alpha_1 = \alpha_2 = \alpha_t$.

To detect the D-D shift ($\theta_1'/\theta_1 < 1, \theta_2'/\theta_2 \le 1$), the paired individual *t* charts use two lower-side *t* charts. It produces an out of control signal if X_1 falls below LCL_1 and/or X_2 falls below LCL_2 . To detect the U-U shift ($\theta_1'/\theta_1 > 1$, $\theta_2'/\theta_2 \ge 1$), the paired individual *t* charts use two upper-side *t* charts. It produces an out of control signal if X_1 goes above UCL_1 and/or X_2 goes above UCL_2 . To detect the D-U shift ($\theta_1'/\theta_1 < 1$, $\theta_2'/\theta_2 > 1$), the paired individual *t* charts use one lower-side *t* chart and one upper-side *t* chart. It produces an out of control signal if X_1 falls below LCL_1 and/or X_2 goes above UCL_2 . The calculation of the control limits and ARL values is discussed next.

For detecting the D-D shift ($\theta_1'/\theta_1 < 1, \theta_2'/\theta_2 \le 1$), the paired individual *t* charts use two lower-side *t* charts. It produces an out of control signal if X_1 falls below LCL_1 and/or X_2 falls below LCL_2 . Thus, the total ARL of the paired individual *t* charts is calculated as

$$ARL = 1/\Pr[(x_1 < LCL_1) \bigcup (x_2 < LCL_2)], \tag{4-33}$$

where

$$
\begin{aligned}
&\Pr[(x_1 < LCL_1) \bigcup (x_2 < LCL_2)] \\
&= 1 - \Pr[(x_1 > LCL_1) \bigcap (x_2 > LCL_2)] \\
&= 1 - \bar{\bar{F}}_{X_1, X_2}(LCL_1, LCL_2) \qquad (4\text{-}34) \\
&= 1 - \exp\left\{ -\left[\left(\frac{LCL_1}{\theta_1'} \right)^{1/\delta} + \left(\frac{LCL_2}{\theta_2'} \right)^{1/\delta} \right]^{\delta} \right\} \\
&= 1 - \exp\left\{ -\left[\left(-\frac{\theta_1}{\theta_1'} \cdot \ln(1-\alpha_t) \right)^{1/\delta} + \left(-\frac{\theta_2}{\theta_2'} \cdot \ln(1-\alpha_t) \right)^{1/\delta} \right]^{\delta} \right\}.
\end{aligned}
$$

Thus, the ARL_0 of the paired individual *t* charts is

$$ARL_0 = 1 \Big/ \left\{ 1 - (1-\alpha_t)^{2^{\delta}} \right\} = 1/\alpha \ , \qquad (4\text{-}35)$$

where α is the total Type I error of the paired individual *t* charts. Specifying ARL_0 and δ, one could solve Equation 4-35 to get α_t, and further calculate the control limits according to Equation 4-32. The ARL_1 value could be obtained using Equation 4-33 and Equation 4-34.

For detecting the U-U shift ($\theta_1'/\theta_1 > 1, \theta_2'/\theta_2 \geq 1$), the individual *t* chart pair uses two upper-side *t* charts. It produces an out of control signal if X_1 goes above UCL_1 and/or X_2 goes above UCL_2. Thus, the total ARL of the paired individual *t* charts is calculated as

$$ARL = 1/\Pr[(x_1 > UCL_1) \bigcup (x_2 > UCL_2)], \qquad (4\text{-}36)$$

where

$$
\begin{aligned}
&\Pr[(x_1 > UCL_1) \bigcup (x_2 > UCL_2)] \\
&= \Pr(x_1 > UCL_1) + \Pr(x_2 > UCL_2) - \Pr[(x_1 > UCL_1) \bigcap (x_2 > UCL_2)] \\
&= \bar{\bar{F}}_{X_1}(UCL_1) + \bar{\bar{F}}_{X_2}(UCL_2) - \bar{\bar{F}}_{X_1,X_2}(UCL_1, UCL_2) \qquad (4\text{-}37) \\
&= \exp\left(-\frac{UCL_1}{\theta_1'}\right) + \exp\left(-\frac{UCL_2}{\theta_2'}\right) - \exp\left\{-\left[\left(\frac{UCL_1}{\theta_1'}\right)^{1/\delta} + \left(\frac{UCL_2}{\theta_2'}\right)^{1/\delta}\right]^{\delta}\right\} \\
&= \alpha_t^{\left(\frac{\theta_1}{\theta_1'}\right)} + \alpha_t^{\left(\frac{\theta_2}{\theta_2'}\right)} - \exp\left\{-\left[\left(-\frac{\theta_1}{\theta_1'} \cdot \ln(\alpha_t)\right)^{1/\delta} + \left(-\frac{\theta_2}{\theta_2'} \cdot \ln(\alpha_t)\right)^{1/\delta}\right]^{\delta}\right\}.
\end{aligned}
$$

The ARL_0 of the paired individual *t* charts becomes

$$ARL_0 = 1 \Big/ \left\{2\alpha_t - (\alpha_t)^{2^{\delta}}\right\} = 1/\alpha, \qquad (4\text{-}38)$$

where α is the total Type I error of the paired individual *t* charts. Specifying ARL_0 and δ, one could solve Equation 4-38 to get α_t, and further calculate the control limits according to Equation 4-27. The ARL_1 value could be obtained using Equation 4-36 and Equation 4-37.

For detecting the D-U shift ($\theta_1'/\theta_1 < 1, \theta_2'/\theta_2 > 1$), the paired individual *t* charts use one lower-side *t* chart and one upper-side *t* chart. It produces an out of control signal if X_1 falls below LCL_1 and/or X_2 goes above UCL_2. Thus, the total ARL of the individual *t* charts is calculated as

$$ARL = 1/\Pr[(x_1 < LCL_1) \bigcup (x_2 > UCL_2)], \qquad (4\text{-}39)$$

where

$$
\begin{aligned}
&\Pr[(x_1 < LCL_1) \bigcup (x_2 > UCL_2)] \\
&= \Pr(x_1 < LCL_1) + \Pr[(x_1 > LCL_1) \bigcap (x_2 > UCL_2)] \\
&= 1 - \bar{F}_{X_1}(LCL_1) + \bar{F}_{X_1,X_2}(LCL_1, UCL_2) \\
&= 1 - \exp\left(-\frac{LCL_1}{\theta_1'}\right) + \exp\left\{-\left[\left(\frac{LCL_1}{\theta_1'}\right)^{1/\delta} + \left(\frac{UCL_2}{\theta_2'}\right)^{1/\delta}\right]^{\delta}\right\} \\
&= 1 - (1-\alpha_t)^{\left(\frac{\theta_1}{\theta_1'}\right)} + \exp\left\{-\left[\left(-\frac{\theta_1}{\theta_1'} \cdot \ln(1-\alpha_t)\right)^{1/\delta} + \left(-\frac{\theta_2}{\theta_2'} \cdot \ln(\alpha_t)\right)^{1/\delta}\right]^{\delta}\right\}
\end{aligned}
\tag{4-40}
$$

The ARL_0 of the paired individual *t* charts becomes

$$
ARL_0 = 1 \Big/ \left\{\alpha_t + \exp\left\{-[(-\ln(1-\alpha_t))^{1/\delta} + (-\ln \alpha_t)^{1/\delta}]^{\delta}\right\}\right\} = 1/\alpha, \tag{4-41}
$$

where α is the total Type I error of the *t* & *t* chart. Specifying ARL_0 and δ, one could solve Equation 4-41 to get α_t, and further calculate the control limits according to Equation 4-27. The ARL_1 value could be obtained using Equation 4-39 and Equation 4-40.

4.3.2 Paired individual EWMA charts

The paired individual EWMA charts on the raw data run two two-sided EWMA charts for X_1 and X_2 simultaneously, while the paired individual EWMA charts on the transformed data run two two-sided EWMA charts for Y_1 and Y_2. Similar to the paired individual *t* charts, we equally allocate the Type I error between the two EWMA charts. Let the paired individual EWMA charts on raw data be denoted by $EWMA_{Raw}$ and the paired individual

EWMA charts on transformed data be denoted by $EWMA_{Trans}$ .The steady state control limits are used:

$$EWMA_{Raw}:\begin{cases} UCL_{EWMA_{Raw}} = \mu_{X_0} + L\sigma_{X_0}\sqrt{r/(2-r)} \\ LCL_{EWMA_{Raw}} = \mu_{X_0} + L\sigma_{X_0}\sqrt{r/(2-r)} \end{cases}$$
$$EWMA_{Trans}:\begin{cases} UCL_{EWMA_{Trans}} = \mu_{Y_0} + L\sigma_{Y_0}\sqrt{r/(2-r)} \\ LCL_{EWMA_{Trans}} = \mu_{Y_0} + L\sigma_{Y_0}\sqrt{r/(2-r)} \end{cases} \quad (4\text{-}42)$$

where r is the smoothing factor and L is the width of the control limits. 10000 runs of simulation are used to calculate the ARL value of the paired individual EWMA charts.

4.3.3 Detection of the D-D shifts

When both X_1 and X_2 experience a downward shift ($\theta_1'/\theta_1 < 1, \theta_2'/\theta_2 \le 1$), it is called a D-D shift. The D-D shift is critical when the events we are interested in are negative ones, e.g. the failure of an engine, the collapse of a computer, or the breakout of an infection.

Let the MEWMA chart based on raw data be denoted by $MEWMA_{Raw}$ and the MEWMA chart based on transformed data be denoted by $MEWMA_{Trans}$. Without loss of generality, the comparison is conducted with the following condition:

$$\theta_1 = 1, \theta_2 = 1, \delta = 0.5, ARL_0 = 200 .$$

Four commonly used smoothing factor r values are selected in this study for the MEWMA charts and the paired individual EWMA charts: r=0.02, 0.1, 0.5, 1. Note that the MEWMA chart reduces to the traditional T^2 chart and the EWMA charts pair reduces to $\bar{X}$ charts pair when r=1.

Table 4-2 shows the numerical values of ARL_1 for the five charts under selected D-D shift levels including the case in which only θ_1 shifts and the case in which both θ_1 and θ_2 shift. For each pair of shift levels, the numbers of the first row are the ARL_1 values of the MEWMA charts and the paired individual *t* charts, while the numbers of the second row are the ARL_1 values of the paired individual EWMA charts. The values in bold are the optimal ARL_1 of the $MEWMA_{Raw}$, $MEWMA_{Trans}$, $EWMA_{Trans}$ and $EWMA_{Trans}$ under specific shift (or shifts) setting. The control limits or design parameters for the five charts are listed in the first three rows of the table. We can observe that:

(1) The $MEWMA_{Raw}$, $MEWMA_{Trans}$, $EWMA_{Raw}$ and $EWMA_{Trans}$ with a small smoothing factor (e.g. r=0.02) outperform the paired individual *t* charts across the whole shift domain. Note that the control limit h for the $MEWMA_{Raw}$ when r=0.02 is quite close to that of the $MEWMA_{Trans}$, which shows the robustness of MEWMA chart to non-normality.

(2) The T^2 based on transformed data (the $MEWMA_{Trans}$ with r=1) is only effective for detecting large downward shifts, i.e. the shifts that are far away from 1, while the T^2 based on raw data (the $MEWMA_{Raw}$ with r=1) totally loses its effectiveness. This shows the sensitivity of T^2 to non-normality.

(3) With the same smoothing factor, the $MEWMA_{Trans}$ (or the $EWMA_{Trans}$) is more effective than $MEWMA_{Raw}$ (or the $EWMA_{Raw}$) in all cases. With the same smoothing factor, the performances of the MEWMA charts and the paired individual EWMA charts are similar. An interesting finding is that the $MEWMA_{Trans}$ (or the $MEWMA_{Raw}$)

seems to be slightly more effective for detecting single mean shifts while the $EWMA_{Trans}$ (or the $EWMA_{Raw}$) works better when both of the means shifted. The possible reason is that when δ=0.5, the correlation coefficient between X_1 and X_2 is 0.8541 which is a positive value close to 1. As the MEWMA chart takes the correlation between variables into account, on one hand, it is more sensitive when θ_1'/θ_1 departs from θ_2'/θ_2, as the effect of the mean shift (shifts) is opposite to the effect of positive correlation in this case. On the other hand, it is less sensitive when θ_1'/θ_1 is close to θ_2'/θ_2, as the effect of the mean shift (shifts) is confounded with the effect of positive correlation in this case.

(4) For specific shift (or shifts) settings, the relative difference between the optimal ARL_1 of the $MEWMA_{Trans}$ (or the $MEWMA_{Raw}$) and the $EWMA_{Trans}$ (or the $EWMA_{Raw}$) are calculated as $Diff = \frac{Min(ARL_{MEWMA}) - Min(ARL_{EWMA})}{Min(ARL_{EWMA})} \times 100\%$. The average of the 16 *Diff* values is -9.72% which may indicate that the overall performance of the MEWMA charts are better than the paired individual EWMA charts.

Table 4-2 The out-of-control ARLs for D-D shifts when δ =0.5 and $ARL_0 = 200$

		$MEWMA_{Raw}$ ($EWMA_{Raw}$)				$MEWMA_{Trans}$ ($EWMA_{Trans}$)				*t* & *t*
$\left(\frac{\theta_1'}{\theta_1}, \frac{\theta_2'}{\theta_2}\right)$	*r*	0.02	0.1	0.5	1	0.02	0.1	0.5	1	LCL_1 0.0035
	h	5.29	10.35	23.58	29.56	5.42	8.7	10.71	10.99	LCL_2 0.0035
	L	2.072	2.901	4.431	4.962	2.07	2.66	2.84	2.756	
(1,1)	*ARL*	200	200	200	200	200	200	200	200	200
	(*ARL*)	200	200	200	200	200	200	200	200	
(0.1,1)	*ARL*	9.98	**8.89**	77.83	145.76	4.01	1.94	**1.25**	7.98	28.58
	(*ARL*)	11.48	**11.10**	*	*	5.66	**3.33**	4.14	50.23	
(0.2,1)	*ARL*	11.54	**11.29**	102.05	177.76	5.90	3.39	**4.23**	23.25	55.83
	(*ARL*)	**13.40**	14.96	*	*	8.26	**5.61**	11.80	94.79	
(0.5,1)	*ARL*	**20.83**	38.06	*	*	15.12	**12.29**	39.74	112.19	126.68
	(*ARL*)	**24.64**	84.59	*	*	**21.05**	21.42	76.16	191.66	
(0.8,1)	*ARL*	**66.53**	178.56	*	*	**55.89**	75.56	164.22	*	176.75
	(*ARL*)	**77.61**	*	*	*	**75.83**	111.29	188.47	*	
(0.1,0.1)	*ARL*	11.27	**10.84**	*	*	5.89	**3.37**	5.85	*	20.45
	(*ARL*)	11.33	**10.98**	*	*	5.34	**3.00**	3.08	38.13	
(0.2,0.2)	*ARL*	**13.13**	14.62	*	*	8.48	**5.68**	18.89	*	40.40
	(*ARL*)	**13.06**	14.35	*	*	7.70	**4.97**	8.80	77.31	
(0.5,0.5)	*ARL*	**24.24**	111.55	*	*	**21.35**	21.49	142.19	*	100.25
	(*ARL*)	**22.79**	79.16	*	*	18.78	**17.83**	56.86	194.16	
(0.8,0.8)	*ARL*	**81.10**	*	*	*	**78.82**	117.47	*	*	160.10
	(*ARL*)	**71.25**	*	*	*	**69.11**	95.41	183.99	*	

* The ARL values are larger than 200 and are not listed here.

4.3.4 Detection of the U-U shifts

When both X_1 and X_2 experience an upward shift ($\theta_1'/\theta_1 > 1, \theta_2'/\theta_2 \geq 1$), it is called a U-U shift. The U-U shift is critical when the events we are interested in are positive ones, e.g. the purchase order of a product, the arrival of a scarce service, or the completion of a maintenance project.

For U-U shift, the comparison is conducted under the same specification: $\theta_1 = 1$, $\theta_2 = 1, \delta = 0.5$, $ARL_0 = 200$, r=0.02, 0.1, 0.5, 1. Table 4-3 shows the numerical values of the ARL_1 for the five charts under selected U-U shift levels. We can find that:

(1) The $MEWMA_{Raw}$, $MEWMA_{Trans}$, $EWMA_{Raw}$ and $EWMA_{Trans}$ with a small smoothing factor (e.g. r=0.02) outperform the paired individual t charts across the whole shift domain.

(2) The T^2 based on transformed data ($MEWMA_{Trans}$ with r=1) and the T^2 based on raw data ($MEWMA_{Raw}$ with r=1) are quite effective for detecting upward shifts. The difference between the results for U-U shift and D-D shift is due to the factors that the MEWMA charts including the T^2 cases are not directional invariant to skewed populations like the exponential distribution, and the double square root transformation is not an accurate transformation method.

(3) With the same smoothing factor, the $MEWMA_{Trans}$ is slightly more effective than $MEWMA_{Raw}$ in all of the cases.

(4) With the same smoothing factor, the performances of the MEWMA charts and the paired individual EWMA charts are similar. But the $MEWMA_{Trans}$ (or the $MEWMA_{Raw}$) seems to be slightly more effective for detecting single mean shifts, while the $EWMA_{Trans}$ (or the $EWMA_{Raw}$) works better when both of the means shift.

(5) The average of the relative difference between the MEWMA chart and the corresponding EWMA charts pair is -6.48% which also indicates the superiority of the MEWMA charts.

Table 4-3 The out-of-control ARLs for U-U shifts when δ =0.5 and $ARL_0 = 200$

		$MEWMA_{Raw}$（$EWMA_{Raw}$）				$MEWMA_{Trans}$（$EWMA_{Trans}$）				*t* & *t*
$\left(\frac{\theta_1'}{\theta_1}, \frac{\theta_2'}{\theta_2}\right)$	*R*	0.02	0.1	0.5	1	0.02	0.1	0.5	1	UCL_1 5.948
	h	5.29	10.35	23.58	29.56	5.42	8.7	10.71	10.99	UCL_2 5.948
	L	2.072	2.901	4.431	4.962	2.07	2.66	2.84	2.756	
(1,1)	*ARL*	200	200	200	200	200	200	200	200	200
	(*ARL*)	200	200	200	200	200	200	200	200	
(1.5,1)	*ARL*	21.77	**20.22**	34.72	44.59	24.45	**22.18**	39.61	65.73	48.11
	(*ARL*)	25.17	**23.28**	37.05	46.62	33.52	**33.07**	50.50	67.03	
(2,1)	*ARL*	9.86	**7.62**	11.49	15.93	12.33	**8.72**	11.78	22.52	19.08
	(*ARL*)	11.42	**9.03**	12.93	17.10	16.88	**13.42**	16.41	24.07	
(5,1)	*ARL*	1.70	**1.01**	1.03	1.33	3.49	1.62	**0.88**	1.39	3.28
	(*ARL*)	2.01	**1.29**	1.30	1.55	5.01	2.80	**1.67**	1.96	
(10,1)	*ARL*	0.47	0.25	**0.23**	0.28	1.66	0.48	**0.14**	0.21	1.81
	(*ARL*)	0.59	0.34	**0.31**	0.36	2.56	1.10	**0.43**	0.46	
(1.5,1.5)	*ARL*	21.17	**17.31**	23.90	28.71	31.87	**29.34**	45.23	63.20	29.19
	(*ARL*)	19.61	**15.63**	22.17	27.74	29.03	**25.72**	32.35	40.59	
(2,2)	*ARL*	9.55	**6.80**	8.15	10.26	16.34	**12.19**	14.71	25.07	11.46
	(*ARL*)	8.73	**6.16**	7.80	9.56	14.59	**10.63**	10.40	13.97	
(5,5)	*ARL*	1.49	0.82	**0.71**	0.84	4.88	2.48	**1.36**	1.86	2.37
	(*ARL*)	1.37	0.74	**0.68**	0.78	4.30	2.15	**1.00**	1.03	
(10,10)	*ARL*	0.39	0.20	**0.16**	0.17	2.51	0.94	**0.30**	0.37	1.49
	(*ARL*)	0.34	0.17	**0.14**	0.16	2.15	0.77	0.22	**0.20**	

4.3.5 Detection of the D-U shifts

When one of X_1 and X_2 experiences a downward shift and the other one experiences an upward shift ($\theta_1'/\theta_1 < 1, \theta_2'/\theta_2 > 1$), it is called a D-U shift. The D-U shift is critical when one of the events we are interested in is positive and the other one is negative.

For D-U shift, the comparison is conducted under the same specification: $\theta_1 = 1$, $\theta_2 = 1, \delta = 0.5$, $ARL_0 = 200$, *r*=0.02, 0.1, 0.5, 1. Table 4-4 shows the numerical values of

ARL_1 for the five charts under selected D-U shift levels. We have the following observations:

(1) The $MEWMA_{Raw}$, $MEWMA_{Trans}$, $EWMA_{Raw}$ and $EWMA_{Trans}$ with a small smoothing factor (e.g. r=0.02) outperform the paired individual t charts across the whole shift domain.

(2) The T^2 based on transformed data ($MEWMA_{Trans}$ with r=1) and the T^2 based on raw data ($MEWMA_{Raw}$ with r=1) are also effective for detecting downward-upward shifts. These are the combination results of the shift directions, i.e. one downward and one upward.

(3) With the same smoothing factor, it is difficult to decide which one of $MEWMA_{Trans}$ and $MEWMA_{Raw}$ is more effective. The reason is the same as (2).

(4) With the same smoothing factor, the performances of the MEWMA charts are significantly better than the paired individual EWMA charts. This large improvement may be due to the fact that θ_1'/θ_1 always shifts in the opposite direction of θ_2'/θ_2 in the D-U shifts setting.

(5) After checking the relative difference between the optimal ARL_1 of the $MEWMA_{Trans}$ (or the $MEWMA_{Raw}$) and the $EWMA_{Trans}$ (or the $EWMA_{Raw}$), we found that the smallest percentage of improvement of MEWMA chart is –32.53%. The average of the relative difference between MEWMA charts and EWMA charts is –58.12% which shows a strong evidence of the superiority of the MEWMA charts.

Table 4-4 The out-of-control ARLs for D-U shifts when δ =0.5 and $ARL_0 = 200$

		$MEWMA_{Raw}$ ($EWMA_{Raw}$)				$MEWMA_{Trans}$ ($EWMA_{Trans}$)				t & t
$\left(\frac{\theta_1'}{\theta_1}, \frac{\theta_2'}{\theta_2}\right)$	R	0.02	0.1	0.5	1	0.02	0.1	0.5	1	LCL_1 0.0025
	h	5.29	10.35	23.58	29.56	5.42	8.7	10.71	10.99	UCL_2 5.9915
	L	2.072	2.901	4.431	4.962	2.07	2.66	2.84	2.756	
(1,1)	ARL	200	200	200	200	200	200	200	200	200
	(ARL)	200	200	200	200	200	200	200	200	
(0.8,1.5)	ARL	16.33	**15.77**	31.61	43.64	16.18	**13.01**	24.09	49.70	46.42
	(ARL)	**23.38**	23.68	40.11	49.32	28.14	**27.79**	47.86	68.26	
(0.5,2)	ARL	6.66	**4.89**	8.51	13.19	6.22	**3.67**	3.71	9.14	18.18
	(ARL)	10.72	**8.96**	12.99	17.48	12.95	**9.26**	13.81	23.98	
(0.2,5)	ARL	1.33	**0.76**	0.81	1.07	1.65	0.44	**0.08**	0.20	3.18
	(ARL)	1.98	**1.26**	1.27	1.62	4.51	2.29	**1.23**	1.99	
(0.1,10)	ARL	0.41	0.20	**0.18**	0.26	0.61	0.05	**0.00**	0.01	1.74
	(ARL)	0.62	0.34	**0.31**	0.37	2.43	0.93	**0.24**	0.42	

4.4 Extension to Gumbel's multivariate exponential distribution

The GBE distribution can be easily extended to the multivariate setting with the following survival function.

$$\bar{F}_{X_1,X_2,\ldots,X_p}(x_1,x_2,\ldots,x_p) = \exp\left\{-\left[\left(\frac{x_1}{\theta_1}\right)^{1/\delta} + \left(\frac{x_2}{\theta_2}\right)^{1/\delta} + \cdots + \left(\frac{x_p}{\theta_p}\right)^{1/\delta}\right]^{\delta}\right\}, \qquad (4\text{-}29)$$

$$x_1, x_2, \ldots, x_p > 0,\ \theta_1, \theta_2, \ldots, \theta_p > 0,\ 0 < \delta \le 1.$$

Here $\theta_i (i = 1, \ldots, p)$ are the scale parameters, δ is the dependence parameter, and δ=1 corresponds to independence. The marginal distributions of $X_1, \ldots, X_p$ are $\exp(\theta_1),\ ..., \exp(\theta_p)$ respectively.

The distribution is symmetrical in $X_1,\ldots,X_p$, and the correlation coefficient of any combination of $(X_i, X_j),\ i \neq j, i, j \in \{1,...,p\}$ is independent of *i* and *j*:

$$\rho_{X_{ij}} = \frac{2\Gamma^2(\delta+1)}{\Gamma(2\delta+1)} - 1. \tag{4-30}$$

Apparently, the proposed MEWMA charts for the GBE model can be directly applied to the Gumbel's multivariate exponential distribution. It is also not difficult to generalize Lemma 1 and 2 in Section 4.2. Thus the ARL performance of the MEWMA charts only depends on the marginal mean shift vector (θ_1'/θ_1, … , θ_p'/θ_p) while the smoothing parameter *r* and the dependency parameter δ are constant. In practice, the in-control $\boldsymbol{\mu}_0$ can be estimated using Equation (4-12) or (4-24), and $\boldsymbol{\Sigma}_0$ can be estimated using Equation (4-13) or (4-25).

However, with the increased complexity of the GBE model, large sample sizes would be required to accurately estimate the in-control parameters. In addition, significant computational effort is required to provide design suggestions, as simulation is the only way to calculate statistical measurements of the control chart, e.g. the ARL. Moreover, the dependence parameter may not be stable, due to the nature of specific applications, and thus robustness of the performance, with respect to the dependence parameter, should be investigated further.

4.5 Conclusions

In this chapter, we proposed two MEWMA TBE charts for monitoring the mean shift (or shifts) of a process that can be modeled by the well-known GBE model. For the MEWMA chart applied to the transformed data, the bivariate exponential data values are first transformed into approximate bivariate normal data using the double square root transformation, and then monitored by the MEWMA chart. The proposed methodologies could easily be extended to higher dimensions.

We further compared the zero-state ARL performance of the two MEWMA charts, the paired individual *t* charts, and the paired individual EWMA charts. The results showed that the MEWMA charts with a small smoothing factor are more favorable than the paired individual *t* charts. As a special case of the MEWMA charts, the T^2 charts are effective for detecting upward shifts, but totally lose their effectiveness for detecting downward shifts. Considering the whole shift domain, the performances of the MEWMA charts are better than the paired individual EWMA charts especially for detecting mean shifts with opposite shift directions.

This chapter demonstrates the potential use of the MEWMA charts for the GBE TBE model. Multivariate control chart techniques are required as various existing multivariate TBE models lack efficient monitoring in applications such as manufacturing system monitoring, spatiotemporal healthcare management and service system evaluation. It is hoped that this illustration of the MEWMA chart's benefits would encourage researchers and practitioners to pay more attention to the chart's usage.

CHAPTER 5 DESIGN OF THE MEWMA CHART FOR RAW GUMBEL'S BIVARIATE EXPONENTIAL DATA

In this chapter, the statistical design of the aforementioned MEWMA chart based on raw GBE data is investigated. The properties of both in-control and out-of-control ARL are studied using simulation. Some general guidelines are provided for designing the optimal MEWMA chart to monitor the GBE TBE data. A simulation study is conducted to examine the robustness of the chart to the estimation errors of the dependent parameter. Finally, a numerical example is given to illustrate the effectiveness of the proposed chart.

5.1 Preliminaries

In this section, we summarize the procedure to construct a MEWMA chart based on raw GBE data according to Chapter 4. The concept of ARL is also briefly introduced.

5.1.1 The GBE distribution

In a two-component system, we assume the time between failures of each component can be described by an exponential distribution. Let X_1 and X_2 denote the time between failures

of component 1 and component 2, respectively, and the joint distribution of component lifetimes (X_1, X_2) follows the underlying survival function:

$$\bar{F}(x_1, x_2) = \exp\left\{-\left[(x_1/\theta_1)^{1/\delta} + (x_2/\theta_2)^{1/\delta}\right]^{\delta}\right\} \tag{5-1}$$

where θ_1, $\theta_2 > 0$ are scale parameters and $0 < \delta \leq 1$ is the dependence parameter which is usually determined by the environmental stress level. Since it is first introduced by Gumbel (1960), we will call it the Gumbel's biveriate exponential (GBE) distribution. The marginal distributions of X_1 and X_2 are EXP(θ_1) and EXP(θ_2), respectively, and the mean vector of X_1 and X_2 is given by

$$\boldsymbol{\mu} = \begin{bmatrix} \mu_1 \\ \mu_2 \end{bmatrix} = \begin{bmatrix} \theta_1 \\ \theta_2 \end{bmatrix}. \tag{5-2}$$

According to Lu and Bhattacharyya (1991a), the correlation coefficient is given by

$$\rho = \frac{2\Gamma^2(\delta+1)}{\Gamma(2\delta+1)} - 1. \tag{5-3}$$

The physical justification of this model was given by Hougaard (1986). Some applications of this model in failure time data analysis can be found in Pal and Murthy (2003).

5.1.2 Setting up a MEWMA chart with raw GBE data

The procedure to set up such a MEWMA chart is proposed in Chapter 4 as follows:

At time t, t = 1, 2, … , observe $\boldsymbol{X}_t$ = (X_{1t}, X_{2t}). Calculate the following recursive

statistics:

$$\boldsymbol{z}_t = r\left(X_t - \boldsymbol{\mu}_{X_0}\right) + (1-r)\boldsymbol{z}_{i-1} \tag{5-7}$$

Where $0 < r \leq 1$ is the smoothing factor and $\boldsymbol{\mu}_{X_0}$ is the in-control mean vector of the raw data. The starting value of $\mathbf{z}_0$ equals 0.

Set up the MEWMA chart using the following statistics:

$$E_t^2 = \frac{2-r}{r}\boldsymbol{z}_t^T \Sigma_{X_0}^{-1} \boldsymbol{z}_t, \tag{5-8}$$

where Σ_{X_0} is the in-control variance-covariance matrix of the raw data.

The process is considered to be out-of-control when E_t^2 exceeds the decision interval *h*.

5.1.3 Average run length

In evaluating multivariate control charts, the ARL has been the most commonly used one in literature. For the MEWMA chart based on raw GBE data, we have proved in Section 4.2 that given the constant dependence parameter δ, the ARL value depends only on the design parameters (*r* and *h*), and the mean shift ratio $(\theta_1'/\theta_1, \theta_2'/\theta_2)$, where θ_1 and θ_2 are the scale parameters of the in-control process and θ_1' and θ_2' are the scale parameters of the out-of-control process.

In this study, we calculate the zero-state ARL values using simulation. 10,000 trials of the subroutine for run length are run to obtain each ARL value. The general

design parameter combinations could be obtained by calculating the ARL value of any in-control processes.

5.2 Optimal design of the MEWMA charts

In this section, we use simulation to compute the ARL_0 for some typical combinations of (δ , r). Given a pre-specified ARL_0, the optimal combinations of (r, h) that results in the shortest ARL_1 can then be identified. Based on these results, a procedure is suggested to guide the optimal design.

5.2.1 In-control ARL

Assuming the dependence parameter δ is constant, the ARL_0 only depends on the two design parameters r and h. Without loss of generality, we evaluate the ARL_0 of the MEWMA chart for GBE(1,1, δ) against the combination of r and h with the following δ values: δ = 0.1, 0.3, 0.5, 0.8, 1. The following commonly used r values are chosen for this study: 0.01, 0.02, 0.05, 0.1, 0.3, 0.5, 0.8, 1. Under each combination (δ , r), the ARL_0 for each h value is obtained through simulation. The ARL_0 plot curves are depicted in Figure 5-1 to Figure 5-5. We can see that the ARL_0 plot curves lie from left to right as r value increases from 0.01 to 1.

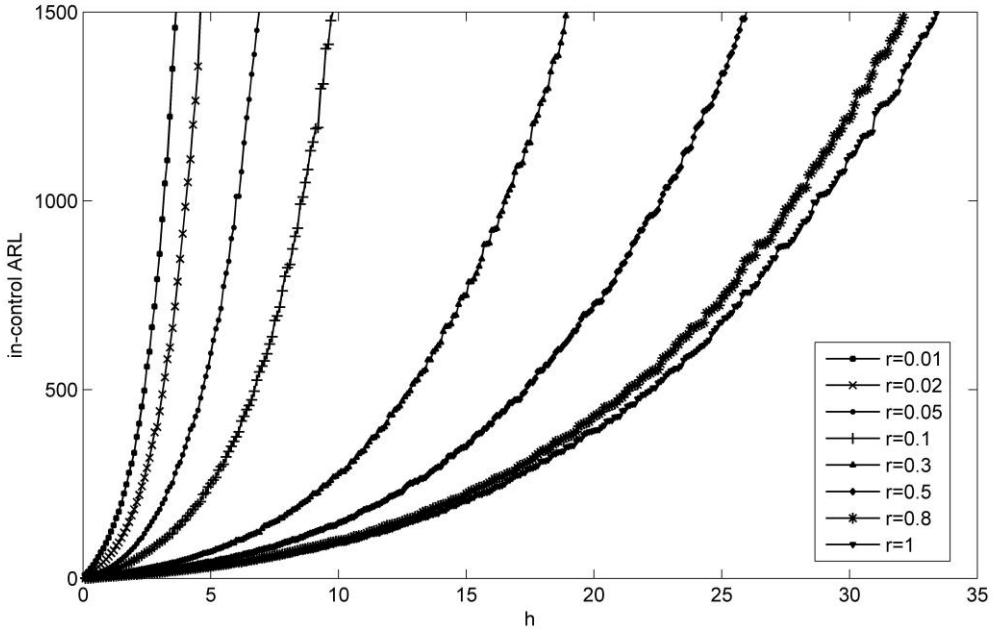

Figure 5-1 The ARL_0 curve for the $MEWMA_{Raw}$ chart when $\delta = 0.1$

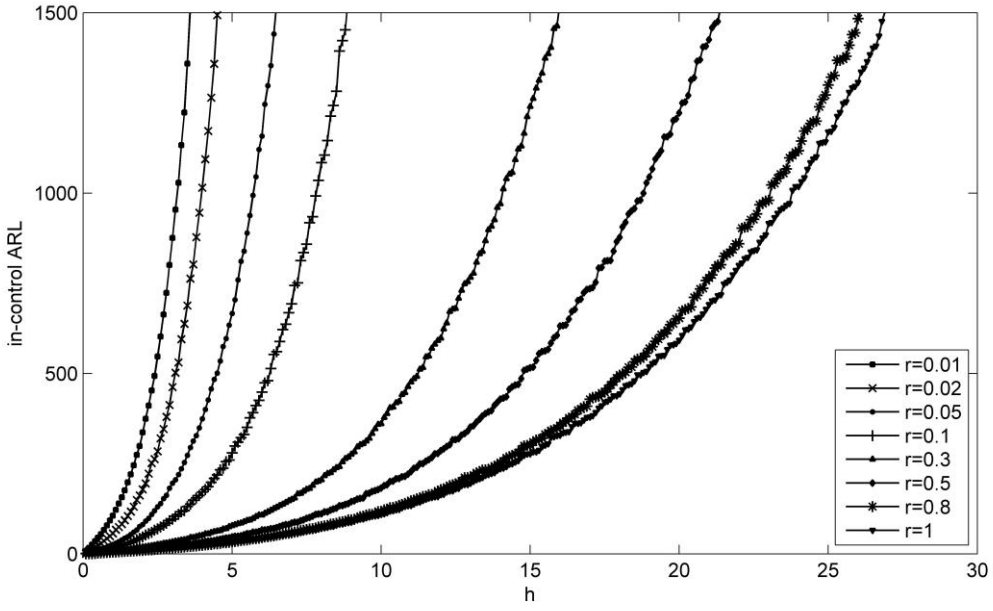

Figure 5-2 The ARL_0 curve for the $MEWMA_{Raw}$ chart when $\delta = 0.3$

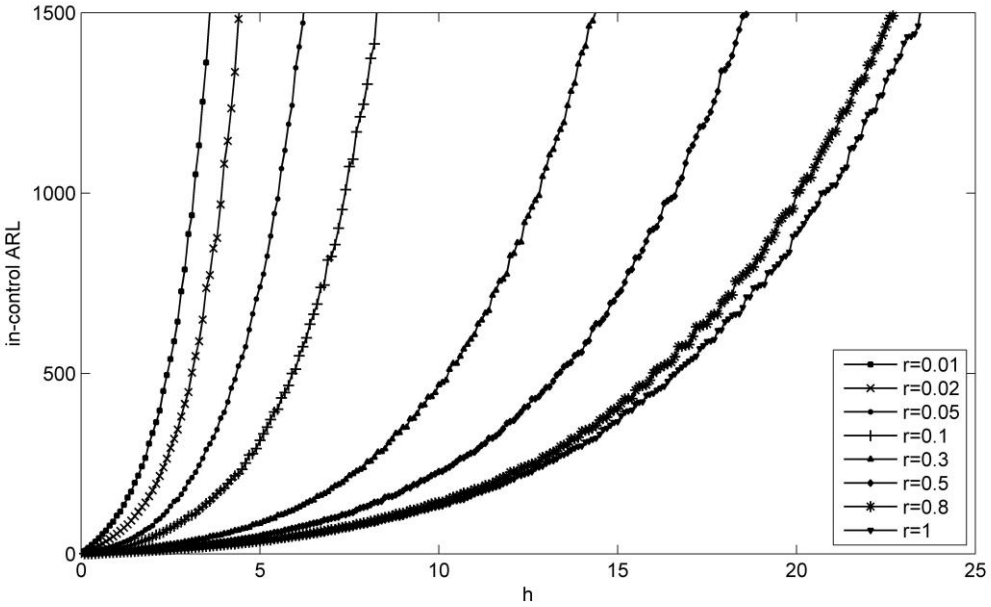

Figure 5-3 The ARL_0 curve for the $MEWMA_{Raw}$ chart when $\delta = 0.5$

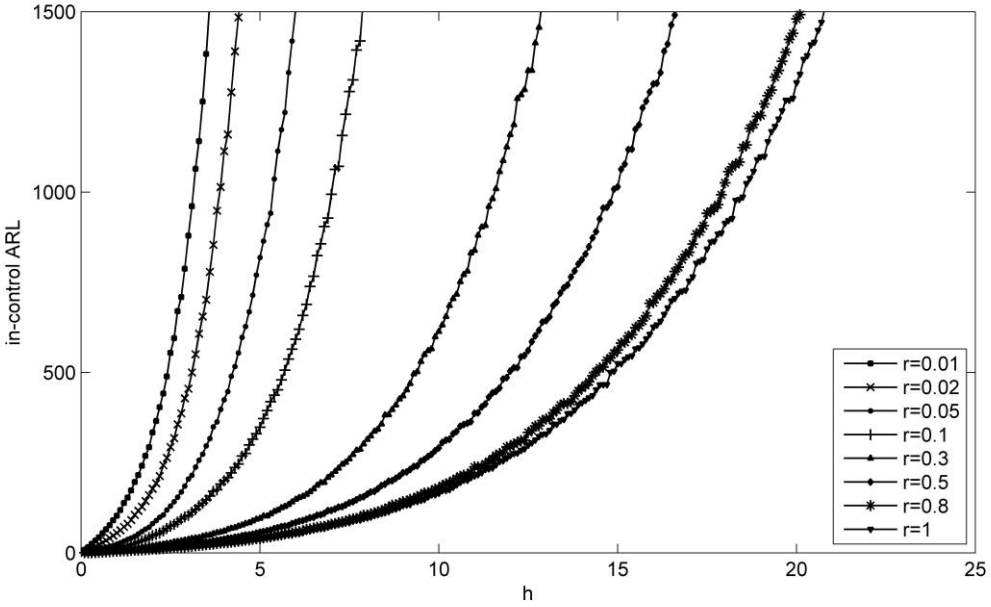

Figure 5-4 The ARL_0 curve for the $MEWMA_{Raw}$ chart when $\delta = 0.8$

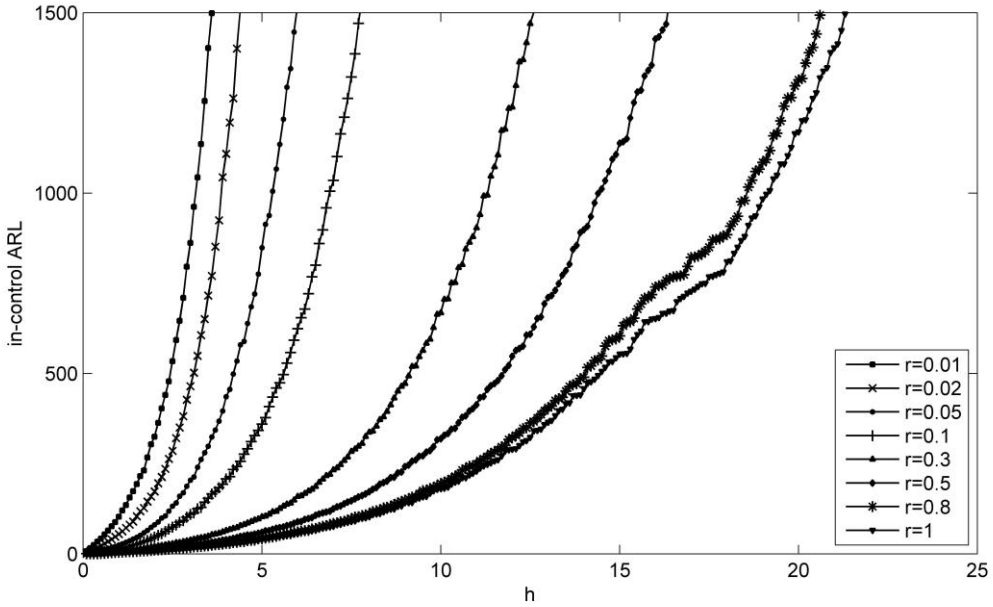

Figure 5-5 The ARL_0 curve for the $MEWMA_{Raw}$ chart when $\delta = 1$

Some observations can be made from these figures:

(1) There are some fluctuations in these curves. This is because for each combination of r and h, the ARL_0 is obtained through simulation.

(2) When r is small, say $r \leq 0.05$, the ARL_0 is fairly insensitive to the dependence parameter δ. Nevertheless, the effect of δ becomes more and more significant when r gets larger.

(3) Given a desired ARL_0 value, the h value under the selected combination of r and δ can be obtained directly from the ARL_0 curves. The h values for other combinations of r and δ can be achieved by interpolation.

Table 5-1 provides some numerical values of combinations of *r* and *h* according to different ARL_0 levels. These combinations of *r* and *h* are used in the following optimal statistical design study.

Table 5-1 The design parameter combinations for of $MEWMA_{Raw}$ chart

ARL_0=100	*r*	0.01	0.02	0.05	0.1	0.3	0.5	0.8	1
$\delta = 0.1$	*h*	2.37	3.6	5.5	7.8	15.08	20.28	25.16	26
$\delta = 0.3$	*h*	2.38	3.65	5.55	7.63	14.37	18.95	22.99	23.78
$\delta = 0.5$	*h*	2.41	3.66	5.54	7.5	13.56	17.58	21.12	22
$\delta = 0.8$	*h*	2.43	3.7	5.56	7.26	12.61	16.38	19.6	20.27
$\delta = 1$	*h*	2.42	3.66	5.55	7.3	12.34	15.96	18.95	19.5
ARL_0=200	*r*	0.01	0.02	0.05	0.1	0.3	0.5	0.8	1
$\delta = 0.1$	*h*	3.72	5.22	7.72	11.31	21.45	29.1	35.77	36.79
$\delta = 0.3$	*h*	3.78	5.29	7.63	10.87	19.67	25.86	31.63	32.65
$\delta = 0.5$	*h*	3.81	5.29	7.53	10.35	18.33	23.58	28.77	29.56
$\delta = 0.8$	*h*	3.83	5.32	7.49	10.03	17.05	21.68	25.99	26.72
$\delta = 1$	*h*	3.82	5.32	7.44	9.83	16.63	21.14	25.1	26.13
ARL_0=370	*r*	0.01	0.02	0.05	0.1	0.3	0.5	0.8	1
$\delta = 0.1$	*h*	5.225	6.93	10.31	14.84	28.17	38.1	46.9	48.6
$\delta = 0.3$	*h*	5.25	6.92	9.95	13.94	25.16	33.12	40.52	41.98
$\delta = 0.5$	*h*	5.26	6.93	9.67	13.3	23.05	29.89	36.25	37.55
$\delta = 0.8$	*h*	5.3	6.89	9.52	12.77	21.22	27.12	32.49	33.74
$\delta = 1$	*h*	5.27	6.9	9.5	12.6	20.74	26.43	31.58	32.58
ARL_0=500	*r*	0.01	0.02	0.05	0.1	0.3	0.5	0.8	1
$\delta = 0.1$	*h*	6	7.82	11.67	16.75	31.77	43.05	53.1	55.25
$\delta = 0.3$	*h*	6.03	7.76	11.23	15.63	28.02	37.03	45.34	46.96
$\delta = 0.5$	*h*	6.04	7.76	10.91	14.84	25.54	33.28	39.99	41.44
$\delta = 0.8$	*h*	6.04	7.75	10.65	14.16	23.39	29.98	36.06	37.21
$\delta = 1$	*h*	6.05	7.72	10.54	13.97	22.81	29.27	35.07	36.07

5.2.2 Out-of-control ARL

The ARL_1 is influenced by the value of mean shift vector $(\theta_1'/\theta_1, \theta_2'/\theta_2)$ as well as the design parameters *r* and *h*. The optimal statistical design scheme should have the shortest ARL_1 at certain ARL_0 value. After we specify an in-control ARL (ARL_0), possible combinations of the design parameters (*r*, *h*) can be read from Figure 5-2 to Figure 5-5 or Table 5-1. The optimal design combination is the one yields the shortest ARL_1 which is denoted by ARL_{opt}.

In our study, the listed combinations of *r* and *h* in Table 5-1 were used to calculate the ARL_1 values. Different shift vectors $(\theta_1'/\theta_1, \theta_2'/\theta_2)$ lead to different optimal settings of the design parameters. Table 5-2 to Table 5-4 show the optimal design schemes for the $MEWMA_{Raw}$ charts with δ = 0.5 and ARL_0 = 100, 200, 370.4, 500. (The optimal design schemes for δ =0.1, 0.3, 0.8, 1 are given in Appendix B.) In these tables, we consider the cases of the downward-downward shift (D-D shift), the upward-upward shift (U-U shift) and the downward-upward shifts (D-U shift). Then, to further examine the effects of δ on the optimal design, we fix ARL_0 = 200 and depict the optimal design schemes under δ =0.1, 0.3, 0.5, 0.8, 1, as are given in Table 5-5. Only the values of smoothing factor *r* and the optimal ARL_1 values are listed in the tables as we could easily get the corresponding UCL *h* values according to Table 5-1.

- Detection of the D-D Shift

A D-D shift denotes the situation that both X_1 and X_2 are shifting downward $(\theta_1'/\theta_1 < 1, \theta_2'/\theta_2 \leq 1)$.

Table 5-2 shows the optimal design schemes of $MEWMA_{Raw}$ chart under selected D-D shift levels. Some interesting conclusions can be made from Table 5-2:

1) The optimal *r* value ranges from 0.02 to 0.1. These *r* values are comparatively small indicating that the raw GBE data are highly skewed data.

2) The optimal *r* values are rather stable for a wide range of ARL_0 specifications. Hence, it is reasonable to choose a suitable *r* value using Table 5-2 even if the desired ARL_0 and mean shift $(\theta_1'/\theta_1, \theta_2'/\theta_2)$ is not included.

3) To detect a small shift, i.e. θ_i'/θ_i close to 1, it is preferable to use a small value of *r*. For example, the optimal *r* for detecting $(\theta_1'/\theta_1, \theta_2'/\theta_2)$ = (0.8, 1) or (0.9, 1) is 0.01 no matter what the dependence parameter δ is. Nevertheless, a large *r* is more effective in detecting large shifts. This is similar to the univariate cases as the EWMA chart with a small smoothing factor has long been considered highly effective for detecting small sustained shifts.

4) Comparing the single shift and double shifts situation, we can see that the optimal ARL values for detecting double shifts is larger than the one for detecting the single shift with the same shift value. It is due to the confounding effect of the mean shift (shifts) and the positive correlation between variables.

Table 5-2 The optimal design schemes of $MEWMA_{Raw}$ chart for D-D shifts when $\delta = 0.5$

$(\theta_1'/\theta_1, \theta_2'/\theta_2)$	ARL_0	100	200	370	500
(0.1,1)	R	0.1	0.05	0.05	0.05
	ARL_{opt}	6.38	8.27	10.09	11.10
(0.2,1)	R	0.05	0.05	0.05	0.05
	ARL_{opt}	7.69	9.79	12.10	13.34
(0.3,1)	R	0.05	0.05	0.05	0.05
	ARL_{opt}	9.40	12.03	14.94	16.76
(0.4,1)	R	0.05	0.05	0.05	0.02
	ARL_{opt}	11.73	15.31	19.36	21.57
(0.5,1)	R	0.05	0.05	0.02	0.02
	ARL_{opt}	15.22	20.55	25.41	27.54
(0.6, 1)	R	0.02	0.02	0.02	0.02
	ARL_{opt}	21.05	27.92	34.09	37.35
(0.7,1)	R	0.02	0.02	0.02	0.02
	ARL_{opt}	29.48	39.80	50.78	56.63
(0.8,1)	R	0.01	0.01	0.01	0.01
	ARL_{opt}	45.07	64.86	83.91	94.95
(0.9,1)	R	0.01	0.01	0.01	0.01
	ARL_{opt}	75.02	124.59	184.34	216.75
(0.1,0.1)	R	0.5	0.05	0.05	0.05
	ARL_{opt}	7.52	9.54	11.63	12.85
(0.2,0.2)	R	0.05	0.05	0.05	0.05
	ARL_{opt}	9.06	11.51	14.12	15.70
(0.5,0.5)	R	0.02	0.02	0.02	0.02
	ARL_{opt}	18.85	24.21	29.39	31.91
(0.8,0.8)	R	0.01	0.01	0.01	0.01
	ARL_{opt}	52.08	74.69	98.08	111.23

- Detection of the U-U Shift

A U-U shift denotes the situation that both X_1 and X_2 are shifting upward $(\theta_1'/\theta_1 > 1,\ \theta_2'/\theta_2 \geq 1)$.

Table 5-3 shows the optimal design schemes under selected U-U shift levels. Some interesting conclusions can be made from Table 5-3:

1) The optimal *r* value ranges from 0.02 to 0.3.
2) The optimal design parameters *r* and *h* are rather stable for a range of mean vector shifts according to different ARL_0 specifications.
3) A small value of *r* is preferred for detecting a small shift and vice versa.
4) Same to the case of D-D shifts, the confounding effect caused the optimal ARL values of double shifts larger than the ones of single shift with the same shift value.

- Detection of the D-U Shift

A D-U shift denotes the situation that one of X_1 and X_2 is shifting upward and the other one is shifting downward $(\theta_1'/\theta_1 < 1,\ \theta_2'/\theta_2 \geq 1)$.

Table 5-4 shows the optimal design schemes under selected D-U shift levels. Some interesting conclusions can be made from Table 5-4:

1) The optimal *r* value ranges from 0.05 to 0.3.
2) The optimal design parameters *r* and *h* are rather stable for a range of mean vector shifts according to different ARL_0 specifications.
3) A small value of *r* is preferred for detecting a small shift and vice versa.
4) Comparing the double shifts values in Table 5-2 to Table 5-4, we can see that the MEWMA chart is most effective for detecting D-U shifts. For example, the

optimal ARL values for mean shifts (0.5, 0.5), (0.5, 1), (0.5, 2), (2, 1), (2, 2) are 24.21, 20.55, 5.02, 7.62, and 6.81 when ARL_0 =200. The MEWMA chart has the smallest optimal ARL value for mean shifts (0.5, 2). The optimal ARL value decreases when θ_1'/θ_1 departs from θ_2'/θ_2 due to the confounding effect of the mean shift direction and the positive correlation between variables.

Table 5-3 The optimal design schemes of $MEWMA_{Raw}$ chart for U-U shifts when δ = 0.5

$(\theta_1'/\theta_1, \theta_2'/\theta_2)$	ARL_0	100	200	370	500
(1.2,1)	r	0.05	0.05	0.02	0.02
	ARL_{opt}	40.53	57.68	78.12	87.93
(1.5,1)	r	0.1	0.05	0.05	0.05
	ARL_{opt}	14.84	19.19	23.86	26.34
(1.8,1)	r	0.1	0.1	0.05	0.05
	ARL_{opt}	8.08	10.58	12.75	13.78
(2,1)	r	0.1	0.1	0.1	0.1
	ARL_{opt}	5.97	7.62	9.37	10.17
(2.5,1)	r	0.1	0.1	0.1	0.1
	ARL_{opt}	3.49	4.32	5.24	5.67
(3, 1)	r	0.1	0.1	0.1	0.1
	ARL_{opt}	2.31	2.94	3.44	3.76
(4,1)	r	0.3	0.3	0.3	0.3
	ARL_{opt}	1.24	1.51	1.85	2.01
(5,1)	r	0.3	0.3	0.3	0.3
	ARL_{opt}	0.72	0.97	1.13	1.21
(10,1)	r	0.3	0.5	0.3	0.3
	ARL_{opt}	0.18	0.23	0.26	0.29
(1.5,1.5)	r	0.1	0.1	0.05	0.05
	ARL_{opt}	12.40	17.12	22.02	24.92
(2,2)	r	0.1	0.1	0.1	0.1
	ARL_{opt}	5.17	6.81	8.36	9.02
(5,5)	r	0.5	0.3	0.3	0.3
	ARL_{opt}	0.53	0.71	0.85	0.96
(10,10)	r	0.5	0.3	0.3	0.3
	ARL_{opt}	0.11	0.16	0.18	0.21

Table 5-4 The optimal design schemes of $MEWMA_{Raw}$ chart for D-U shifts when $\delta = 0.5$

$(\theta_1'/\theta_1, \theta_2'/\theta_2)$	ARL_0	100	200	370	500
(0.8,1.5)	r	0.05	0.05	0.05	0.05
	ARL_{opt}	11.43	14.56	17.55	19.79
(0.5,2)	r	0.1	0.1	0.1	0.1
	ARL_{opt}	3.90	5.02	6.05	6.62
(0.2,5)	r	0.3	0.3	0.3	0.3
	ARL_{opt}	0.55	0.69	0.90	0.96
(0.1,10)	r	0.3	0.3	0.3	0.3
	ARL_{opt}	0.13	0.18	0.23	0.25

- Optimal Design under Different δ Value

Table 5-5 shows the optimal design schemes under δ=0.1, 0.3, 0.5, 0.8, 1 when ARL_0 = 200. We can find the following observations from Table 5-5:

1) The optimal design parameters r and h are rather stable for a range of mean vector shifts according to different correlation parameter δ.

2) A small value of r is preferred for detecting a small shift and vice versa.

3) Another interesting feature observed from Table 5-5 is that the optimal design parameters r and h are also stable for a range of δ values. Thus, it is also reasonable to find an r value with good performance using Table 5-2 to Table 5-5 even if the desired δ is not listed.

Table 5-5 The optimal design schemes for $MEWMA_{Raw}$ chart when $ARL_0 = 200$

$(\theta_1'/\theta_1, \theta_2'/\theta_2)$	δ	0.1	0.3	0.5	0.8	1
(0.2,1)	r	0.1	0.05	0.05	0.05	0.05
	ARL_{opt}	1.62	6.46	9.79	12.44	12.76
(0.4,1)	r	0.1	0.05	0.05	0.05	0.05
	ARL_{opt}	2.54	9.81	15.31	19.94	20.25
(0.6, 1)	r	0.1	0.05	0.02	0.02	0.02
	ARL_{opt}	4.93	18.00	27.92	34.41	35.16
(0.8,1)	r	0.5	0.02	0.01	0.01	0.01
	ARL_{opt}	13.16	44.72	64.86	77.80	78.66
(1.5,1)	r	0.1	0.05	0.05	0.05	0.05
	ARL_{opt}	3.64	13.28	19.19	23.19	23.55
(2,1)	r	0.1	0.1	0.1	0.1	0.1
	ARL_{opt}	1.23	5.18	7.62	9.25	9.29
(3, 1)	r	0.3	0.1	0.1	0.1	0.3
	ARL_{opt}	0.35	1.79	2.94	3.58	3.58
(5,1)	r	0.3	0.3	0.3	0.3	0.3
	ARL_{opt}	0.10	0.55	0.97	1.22	1.21
(0.2,0.2)	r	0.05	0.05	0.05	0.05	0.05
	ARL_{opt}	14.14	13.03	11.51	9.36	8.01
(0.8,0.8)	r	0.01	0.01	0.01	0.01	0.01
	ARL_{opt}	83.30	80.30	74.69	64.70	56.78
(2,2)	r	0.1	0.1	0.1	0.1	0.1
	ARL_{opt}	8.59	7.76	6.81	5.49	4.73
(5,5)	r	0.3	0.3	0.3	0.5	0.3
	ARL_{opt}	1.10	0.90	0.71	0.45	0.31
(0.2, 5)	r	0.3	0.3	0.3	0.3	0.3
	ARL_{opt}	0.07	0.37	0.69	1.04	1.17
(0.8,1.5)	r	0.1	0.05	0.05	0.05	0.05
	ARL_{opt}	2.10	8.98	14.56	20.47	22.74

5.2.3 Procedure for optimal design of the MEWMA chart

Based on the aforementioned results, we recommend the following procedure for the optimal design of the MEWMA chart based on the raw GBE TBE data:

Step 1: Specify the desired ARL_0 value, the constant dependence parameter δ and the

out-of control mean shift vector $(\theta_1'/\theta_1, \theta_2'/\theta_2)$ at the beginning.

Step 2: Find the approximate value of the smoothing factor *r* according to the optimal design schemes in Tables 5-2 to 5-5.

Step 3: Locate the corresponding *h* value according to the ARL_0 contour plots in Figure 5-1 to Figure 5-5.

Step 4: Use simulation to achieve the more accurate in-control and ARL_0 to evaluate the performance of the designed $MEWMA_{Raw}$ chart.

5.3 Robustness study

In the former study, we have used the dependence parameter δ as if it is known and remains constant through the whole monitoring process. In practice, this dependence parameter δ is estimated from past data, or from expert opinion, and thus is subject to estimation errors and biases. Moreover, in real applications, it is very possible for δ to experience small random drifts due to the fluctuations of circumstance stress level. In order to account for the estimation deviations and the possible natural instability, we need to examine the sensitivity of this chart to the departure of δ from the estimated value.

For each combination $(\theta_1'/\theta_1, \theta_2'/\theta_2)$ in the first column of Table 5-6, we use the estimated $\delta_{est} = 0.5$ to derive the 'estimated' optimal settings given the pre-specified $ARL_0 = 200$. Assume that this estimated optimal setting is used but the true values of δ is $\delta_{true} = 0.3, 0.8$, respectively. The actual values of ARL_0 and ARL_1, denoted as $ARL_0^{(true)}$ and $ARL_1^{(true)}$, are then computed via simulation. For comparison purpose, the optimal settings

$ARL_{opt}^{(\text{true})}$ derived from the true values of δ, given the pre-specified ARL_0 = 200, are also given in the table.

From Table 5-6, we find the following observations:

1) For a range of mean shift values, the ARL_1 is not sensitive to the dependent parameter δ. Hence, it is reasonable for us to use the optimal design results in Section 5.2 as guidelines in real applications.

2) When $\theta_i'/\theta_i \ll 1$, and, i =1, 2, $ARL_1^{(\text{true})}$ is quite close to $ARL_{opt}^{(\text{true})}$ and $ARL_0^{(\text{true})}$ is quite close to 200 except for the only case of $(\theta_1'/\theta_1, \theta_2'/\theta_2)$ = (0.8, 0.8). This means that the effect of estimation error tends to be quite small when we are interested in shifts with downside shifts. In the special case of $(\theta_1'/\theta_1, \theta_2'/\theta_2)$ = (0.8, 0.8), the $ARL_0^{(\text{true})}$ deviates from 200. This may due to the fact that with such small shifts, the optimal r value becomes very small (r=0.01) and has a comparatively steeper ARL_0 curve which causes the $ARL_0^{(\text{true})}$ to deviate from 200.

3) When $\theta_i'/\theta_i \gg 1$ and, i =1, 2, $ARL_0^{(\text{true})}$ is inclined to be further away from 200. This result prompts us to give more attention to the estimation accuracy of δ when we would like to detect upside shifts.

Table 5-6 Estimated ARL_1 of $MEWMA_{Raw}$ chart based on δ_{est} = 0.5 and δ_{true} = 0.3, 0.8

$(\theta_1'/\theta_1, \theta_2'/\theta_2)$	$ARL_{opt}^{(est)}$	δ_{true} = 0.3			δ_{true} = 0.8		
		$ARL_1^{(true)}$	$ARL_0^{(true)}$	$ARL_{opt}^{(true)}$	$ARL_1^{(true)}$	$ARL_0^{(true)}$	$ARL_{opt}^{(true)}$
(0.1,1)	8.27	5.43	194.24	5.49	10.45	202.40	10.38
(0.2,1)	9.79	6.39	194.24	6.46	12.54	202.40	12.44
(0.3,1)	12.03	7.81	194.24	7.85	15.50	202.40	15.47
(0.4,1)	15.31	9.71	194.24	9.81	19.96	202.40	19.94
(0.5,1)	20.55	12.57	194.24	12.89	27.37	202.40	25.87
(0.6,1)	27.92	18.79	199.96	18.00	34.25	201.18	34.41
(0.7,1)	39.8	26.78	199.96	26.80	49.39	201.18	49.65
(0.8,1)	64.84	45.73	202.86	44.72	76.98	198.15	77.80
(0.9,1)	124.59	94.35	202.86	94.41	139.78	198.15	139.21
(1.2,1)	57.68	41.76	194.24	42.82	67.55	202.40	67.02
(1.5, 1)	19.19	12.97	194.24	13.28	23.28	202.40	23.19
(1.8,1)	10.58	6.86	183.35	7.14	12.85	215.75	12.61
(2,1)	7.62	4.93	183.35	5.18	9.44	215.75	9.25
(2.5,1)	4.32	2.72	183.35	2.84	5.50	215.75	5.26
(3,1)	2.94	1.81	183.35	1.79	3.74	215.75	3.58
(4,1)	1.51	0.86	164.73	0.93	2.04	244.61	1.89
(5,1)	0.97	0.51	164.73	0.55	1.26	244.61	1.22
(10,1)	0.23	0.11	159.99	0.11	0.32	245.02	0.30
(0.1,0.1)	9.54	10.65	194.24	10.76	7.87	202.40	7.84
(0.2,0.2)	11.51	12.89	194.24	13.03	9.38	202.40	9.36
(0.5,0.5)	24.21	26.61	199.96	26.44	20.36	201.18	19.99
(0.8,0.8)	74.69	80.55	202.86	80.30	63.99	198.15	64.70
(1.5,1.5)	17.12	18.78	183.35	19.35	15.52	215.75	14.41
(2,2)	6.81	7.50	183.35	7.76	5.67	215.75	5.49
(5,5)	0.71	0.87	164.73	0.90	0.48	244.61	0.45
(10,10)	0.16	0.21	164.73	0.22	0.08	244.61	0.07
(0.2,0.2)	14.56	8.77	194.24	8.98	20.48	202.40	20.47
(0.8,0.8)	5.02	2.74	183.35	2.87	7.57	215.75	7.44
(0.8,1.5)	0.69	0.35	164.73	0.37	1.12	244.61	1.04
(0.5,2)	0.18	0.08	164.73	0.09	0.29	244.61	0.25

5.4 Illustrative example

A simulation example is constructed to illustrate the use of the proposed MEWMA chart with raw GBE data from the model. The first 15 TBE data are generated from a GBE distribution with scale parameters $\theta_1 = \theta_2 = 1$ and the dependence parameter $\delta = 0.5$, and the next 15points with scale parameters $\theta_1 = 1$, $\theta_2 = 0.5$ and the dependence parameter $\delta = 0.5$.

Under ARL_0 =370.4, the design parameters of the MEWMA chart on the GBE data are chosen following the design procedures above ($r = 0.02, h = 6.93$) and the control chart is shown in the Figure 5-6. The MEWMA chart on the GBE data becomes out of control at the 21st point which is the 6th point after the process has shifted. We could see that the performance of the proposed MEWMA chart is pretty good even though the optimal ARL_1 values from our optimal design table are not so small (25.41 for optimal initial state ARL_1). It is due to the fact that our optimal designs are based on the assumption that the process becomes out of control from the very beginning. The performances of the proposed charts will be much better if it is allowed to warm up for a few points.

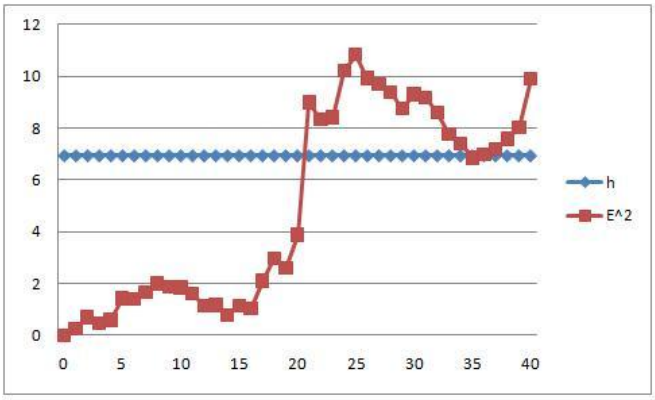

Figure 5-6 A MEWMA TBE chart based on raw GBE data

Table 5-7 An example of setting-up MEWMA chart with raw GBE data

Failure NO	X_t		Z_t		E_i^2
0			0.00	0.00	0.00
1	2.05	3.40	0.02	0.05	0.23
2	0.56	2.37	0.01	0.07	0.68
3	1.90	0.65	0.03	0.07	0.44
4	1.99	1.60	0.05	0.08	0.58
5	1.91	3.25	0.07	0.12	1.42
6	2.00	0.97	0.08	0.12	1.40
7	2.66	0.97	0.12	0.11	1.67
8	0.94	2.18	0.11	0.14	1.99
9	0.21	1.14	0.09	0.14	1.85
10	0.66	1.18	0.09	0.14	1.84
11	0.94	0.63	0.08	0.13	1.59
12	0.19	0.20	0.07	0.11	1.15
13	0.76	1.15	0.06	0.11	1.16
14	0.15	0.09	0.04	0.09	0.78
15	2.07	2.02	0.06	0.11	1.13
16	0.22	0.80	0.04	0.10	1.02
17	0.19	2.72	0.03	0.13	2.09
18	0.17	1.86	0.01	0.15	2.95
19	0.23	0.27	0.00	0.13	2.59
20	2.10	3.21	0.02	0.17	3.87
21	0.80	5.31	0.01	0.25	8.98
22	0.13	0.30	0.00	0.24	8.32
23	0.14	0.79	-0.02	0.23	8.42
24	1.37	2.68	-0.01	0.26	10.20
25	0.47	1.33	-0.02	0.26	10.83
26	0.22	0.18	-0.04	0.24	9.93
27	0.16	0.52	-0.06	0.22	9.70
28	0.09	0.38	-0.07	0.20	9.39
29	0.07	0.06	-0.09	0.18	8.74
30	0.29	1.06	-0.10	0.18	9.30
31	0.65	0.86	-0.11	0.17	9.16
32	0.15	0.08	-0.12	0.15	8.60
33	2.57	2.00	-0.09	0.17	7.75
34	0.12	0.20	-0.10	0.15	7.40
35	0.33	0.14	-0.12	0.13	6.84
36	0.40	0.78	-0.13	0.12	6.99
37	0.02	0.41	-0.14	0.11	7.19
38	0.78	1.37	-0.14	0.11	7.58
39	1.81	2.46	-0.12	0.14	8.02
40	0.73	2.44	-0.13	0.16	9.91

5.5 Conclusions

This chapter explores the optimal design issue of the MEWMA chart based on raw GBE data for monitoring mean shift(s). An optimal design procedure was provided to guide the real applications. To facilitate the potential users, we give the optimal design schemes in Appendix B for the MEWMA charts with δ = 0.1, 0.3, 0.5, 0.8, 1, and ARL_0 = 100, 200, 370.4, 500. A rough estimate of the optimal schemes for scenarios not included in these tables could be obtained from extrapolation.

Robustness of the chart to the estimation errors of the dependence parameter δ was examined. We found that the effect of estimation errors was small when we were interested in detecting moderately small shifts or large downward shifts. On the other hand, when we are interested in large upward shifts, we should look to the estimation accuracy since the ARL_0 tends to be sensitive to the estimation errors.

CHAPTER 6 DESIGN OF THE MEWMA CHART FOR TRANSFORMED GUMBEL'S BIVARIATE EXPONENTIAL DATA

In this chapter, an optimal design procedure is provided for the MEWMA chart based on the transformed GBE data proposed in Chapter 4. The optimal design is based on the ARL statistic. The robustness of the optimal design is conducted to examine the effect of estimation errors of the correlation parameter δ. The remainder of the chapter is as follows. Section 6-1 briefly introduces the GBE distribution, the data transformation technique and the procedure to set up the MEWMA chart. Section 6-2 investigates properties of the ARL_0 and ARL_1 via simulation, after which the optimal design procedure is proposed. In section 6-3, a simulation study is conducted to examine the robustness of the chart to the estimation errors of the dependent parameter. A numerical example is shown in Section 6-4 to illustrate the optimal design procedure of the chart. Finally, we give the conclusion in Section 6-5.

6.1 Preliminaries

In this section, we summarize the procedure to construct a MEWMA chart based on transformed data according to Xie et al. (2002).

6.1.1 The GBE distribution

In a two-component system, let X_1 and X_2 denote the time between failures of component 1 and component 2, respectively. We assume the joint distribution of component lifetimes (X_1, X_2) can be described by the Gumbel's bivariate exponential distribution with the underlying survival function:

$$\bar{F}(x_1, x_2) = \exp\left\{-\left[(x_1/\theta_1)^{1/\delta} + (x_2/\theta_2)^{1/\delta}\right]^{\delta}\right\}, \tag{6-1}$$

where θ_1, $\theta_2 > 0$ are scale parameters and $0 < \delta \leq 1$ is the dependence parameter which is usually determined by the environmental stress level.

6.1.2 Transform the GBE data into approximately normal

The double square root transformation (SQRT) method has been recommended in literature for transforming exponential distributed data to approximately normal (e.g. Liu et al. 2007). We apply the double SQRT method to the marginal distributions of X_1 and X_2. Let Y_1 and Y_2 denote the variables after transformation, then

$$Y_1 = X_1^{0.25} \text{ and } Y_2 = X_2^{0.25}. \tag{6-2}$$

The joint survival function of (Y_1, Y_2) becomes

$$\bar{G}(y_1, y_2) = \exp\left\{-\left[\left(y_1^4/\theta_1\right)^{1/\delta} + \left(y_2^4/\theta_2\right)^{1/\delta}\right]^{\delta}\right\} \tag{6-3}$$

This is a bivariate Weibull extension to the GBE model proposed by Hougaard [24]. The marginal distributions of Y_1 and Y_2 follow the Weibull distribution. Let $\boldsymbol{\mu}_Y$ and Σ_Y denote the mean vector and the variance-covariance matrix of (Y_1, Y_2). According to Hougaard (1986), the covariance of Y_1 and Y_2 is

$$\operatorname{cov}(Y_1, Y_2) = E(Y_1 Y_2) - \mu_{Y_1}\mu_{Y_2} = \left[\frac{\Gamma^2(0.25\delta+1)\Gamma(1.5)}{\Gamma(0.5\delta+1)} - \Gamma^2(1.25)\right]\theta_1^{0.25}\theta_2^{0.25} \tag{6-4}$$

Goodness of the normal approximation was examined in Chapter 4.

6.1.3 Setting up a MEWMA chart with transformed GBE data

The MEWMA chart was originally introduced by Lowry et al. (1992) for detecting the mean shift or shifts of the multivariate normal distribution. According to Chapter 4, we first transform the GBE data to be approximately normal, and then construct a MEWMA chart based on the transformed data. The procedure to set up such a MEWMA chart is as follows.

At time t, $t = 1, 2, \ldots$, observe $\boldsymbol{X}_t = (X_{1t}, X_{2t})$ and transform X_{1t} and X_{2t} with the double SQRT method to obtain $\boldsymbol{Y}_t = (Y_{1t}, Y_{2t})^T$.

Calculate the following recursion statistics:

$$\boldsymbol{z}_t = r\left(\boldsymbol{Y}_t - \boldsymbol{\mu}_{\boldsymbol{Y}_0}\right) + (1-r)\boldsymbol{z}_{i-1} \tag{6-5}$$

where $0 < r \leq 1$ is the smoothing factor and $\boldsymbol{\mu}_{Y_0}$ is the in-control mean vector of the transformed data. The starting value of $\boldsymbol{z}_0$ equals 0.

Set up the MEWMA chart based on the following statistics:

$$E_t^2 = \frac{2-r}{r} \boldsymbol{z}_t^T \Sigma_{\boldsymbol{Y}_0}^{-1} \boldsymbol{z}_t, \tag{6-6}$$

where Σ_{Y_0} is the in-control variance-covariance matrix of the transformed data.

The process is considered to be out-of-control when E_t^2 exceeds the decision interval *h*.

6.1.4 ARL

For the MEWMA chart based on transformed GBE data, in section 4.2 we had shown that given the constant dependence parameter δ, the ARL value depends only on the design parameters (*r* and *h*), and the mean shift ratio $(\theta_1'/\theta_1, \theta_2'/\theta_2)$, where θ_1 and θ_2 are the scale parameters of the in-control process and θ_1' and θ_2' are the scale parameters of the out-of-control process.

We calculate the zero-state ARL values using simulation. 10,000 trials of the subroutine for run length are run to obtain each ARL value and the average of these run length values are calculated to estimate the ARL. According to Section 4.2, the design parameter combinations obtained by calculating the ARL value of any in-control processes would be the same.

6.2 Optimal design of the MEWMA charts

In this section, we use simulation to compute the ARL_0 of the MEWMA chart based on transformed GBE data for some typical combinations of (δ, r). Given a pre-specified ARL_0, the optimal combinations of (r, h) that results in the shortest ARL_1 can then be identified. The optimal statistical design procedure is suggested to guide future practice.

6.2.1 In-control ARL

Again, the dependence parameter δ is assumed to be constant. The ARL_0 only depends on the two design parameters r and h. Without loss of generality, we evaluate the ARL_0 of the $MEWMA_{Trans}$ chart for GBE(1,1, δ) against the combination of r and h with the following δ values: δ = 0.1, 0.3, 0.5, 0.8, 1. The following r values are chosen in this study: 0.01, 0.02, 0.05, 0.1, 0.3, 0.5, 0.8, 1. Under each combination (δ, r), the ARL_0 for each h value is obtained through simulation. The ARL_0 plot curves are depicted in Figure 6-1 to Figure 6-5.

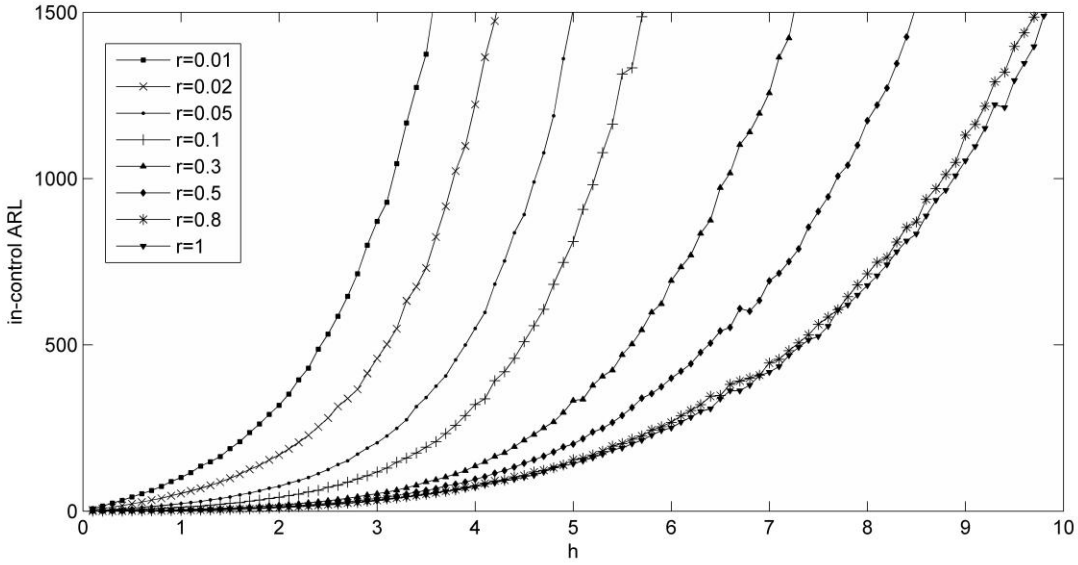

Figure 6-1 The ARL_0 curve for the $MEWMA_{Trans}$ chart when $\delta = 0.1$

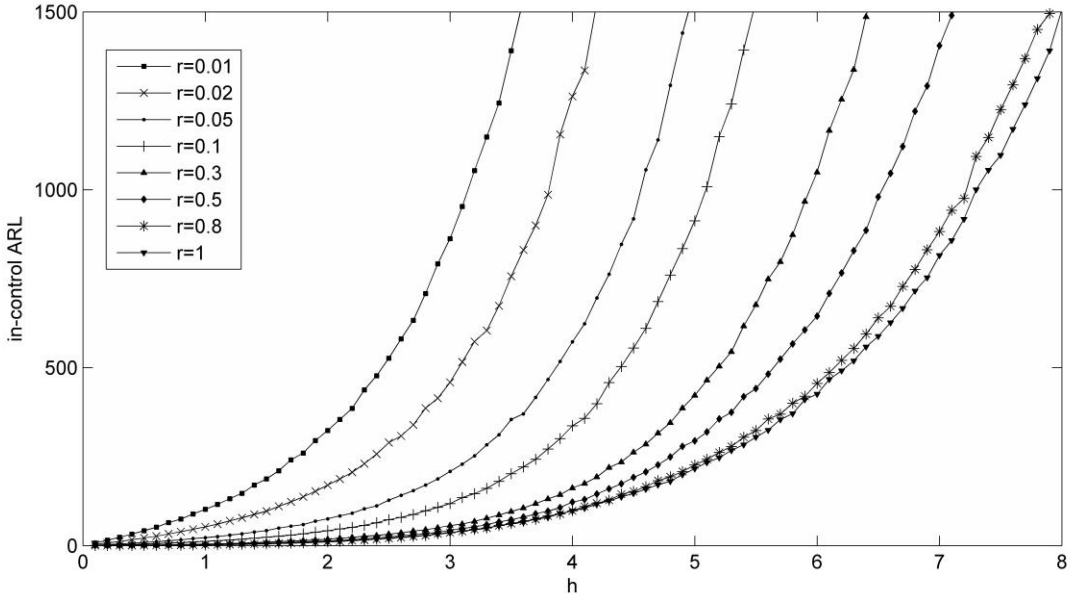

Figure 6-2 The ARL_0 curve for the $MEWMA_{Trans}$ chart when $\delta = 0.3$

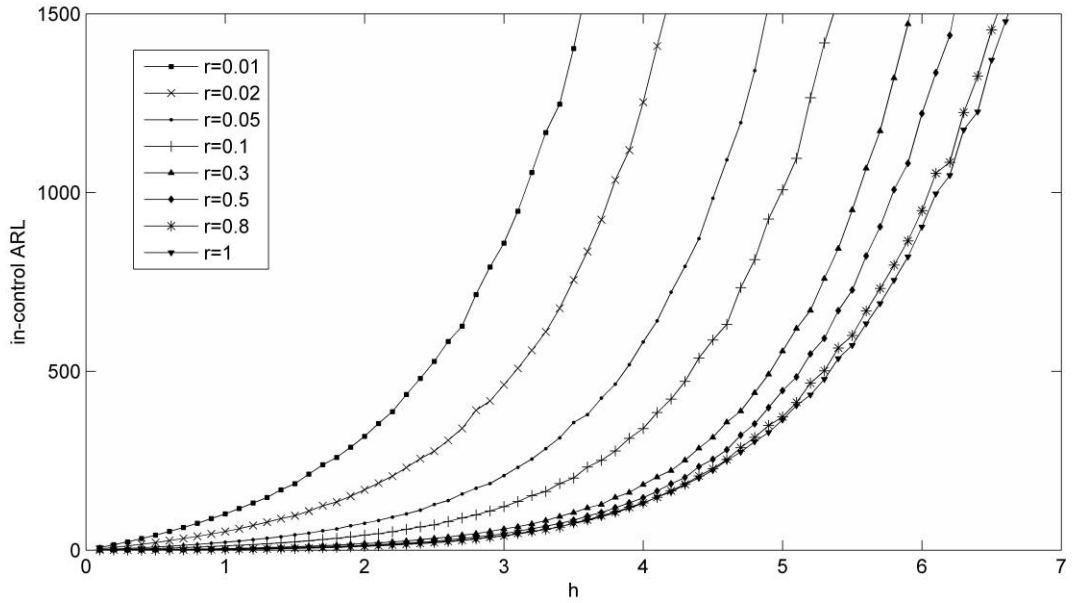

Figure 6-3 The ARL_0 curve for the $MEWMA_{Trans}$ chart when $\delta = 0.5$

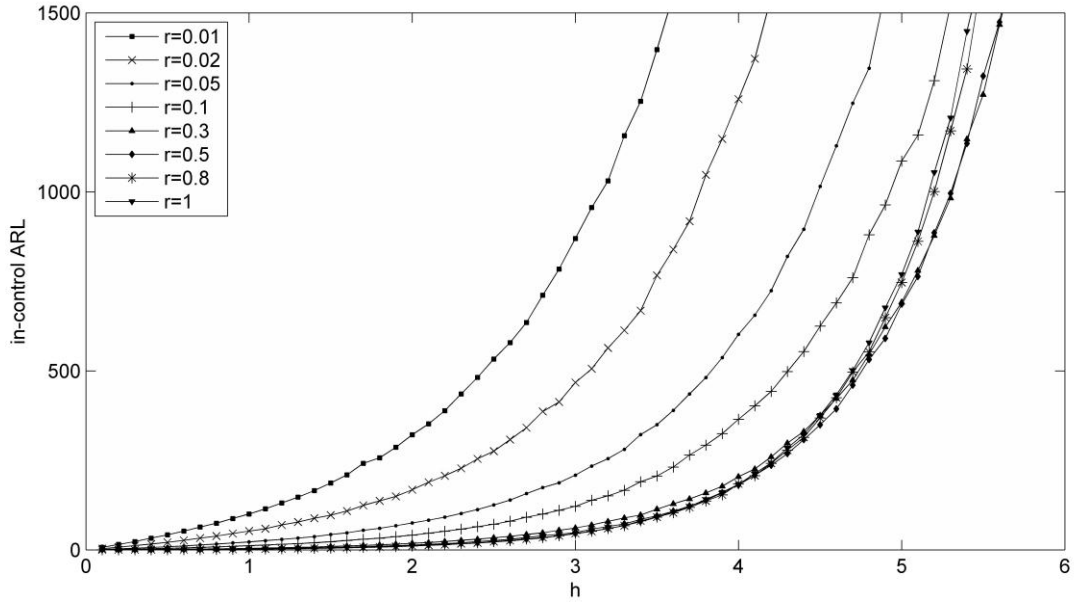

Figure 6-4 The ARL_0 curve for the $MEWMA_{Trans}$ chart when $\delta = 0.8$

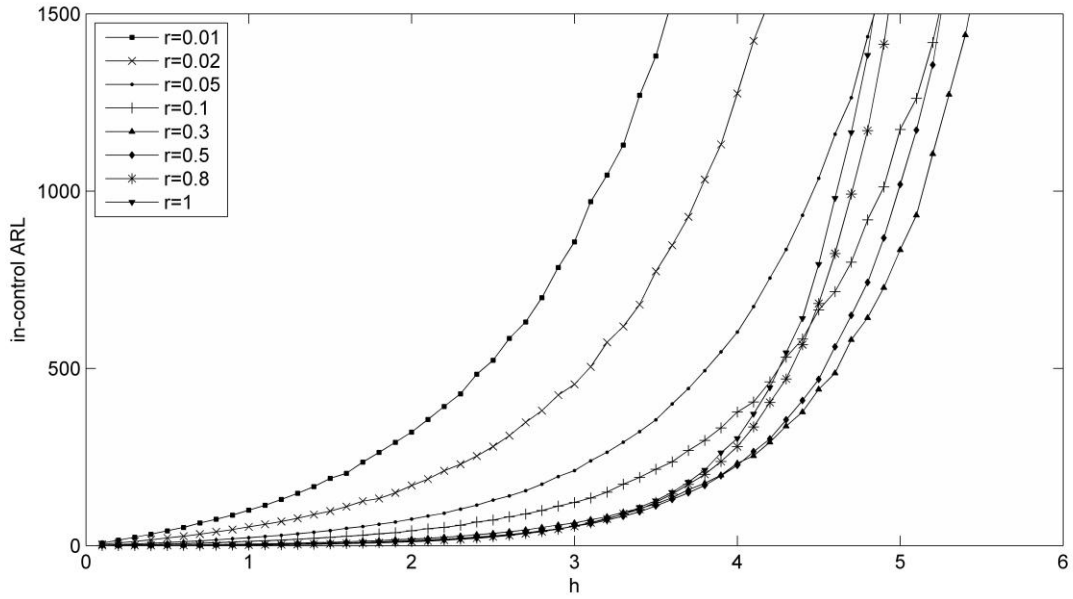

Figure 6-5 The ARL_0 curve for the $MEWMA_{Trans}$ chart when $\delta = 1$

Some observations are discovered after carefully examining these figures:

(1) There are some fluctuations in these curves. This is because for each combination of r and h, the ARL_0 is obtained through simulation.

(2) When δ is large, say $\delta > 0.5$, the ARL_0 is first increasing and then decreasing in r, as can be observed from Figure 6-4 and Figure 6-5.

(3) When r is small, say $r \leq 0.05$, the ARL_0 is fairly insensitive to the dependence parameter δ. Nevertheless, the effect of δ becomes more and more significant when r gets larger.

(4) Given a desired ARL_0 value, the h value under the selected combination of r and δ can be obtained directly from the ARL_0 curves. The h values for other

combinations of r and δ can be achieved by interpolation.

Table 6-1 provides some numerical values of combinations of r and h according to different ARL_0 levels. These combinations of r and h are used in the following optimal statistical design study.

Table 6-1 The design parameter combinations for $MEWMA_{Trans}$ chart

ARL_0=100	r	0.01	0.02	0.05	0.1	0.3	0.5	0.8	1
$\delta = 0.1$	h	2.47	3.78	5.72	7.11	9.15	10.12	10.92	11.11
$\delta = 0.3$	h	2.47	3.78	5.72	7.08	8.85	9.56	10.03	10.12
$\delta = 0.5$	h	2.49	3.79	5.69	6.74	8.68	9.15	9.38	9.38
$\delta = 0.8$	h	2.49	3.8	5.73	7.08	8.53	8.84	8.93	8.93
$\delta = 1$	h	2.49	3.8	5.68	6.99	8.39	8.59	8.46	8.41
ARL_0=200	r	0.01	0.02	0.05	0.1	0.3	0.5	0.8	1
$\delta = 0.1$	h	3.87	5.41	7.41	8.84	11.08	12.41	13.66	13.96
$\delta = 0.3$	h	3.88	5.41	7.39	8.72	10.57	11.38	12.12	12.26
$\delta = 0.5$	h	3.9	5.42	7.41	8.7	10.24	10.71	10.94	10.99
$\delta = 0.8$	h	3.89	5.43	7.41	8.65	9.96	10.19	10.18	10.17
$\delta = 1$	h	3.89	5.43	7.37	8.61	9.76	9.71	9.49	9.39
ARL_0=370	r	0.01	0.02	0.05	0.1	0.3	0.5	0.8	1
$\delta = 0.1$	h	5.34	6.94	8.98	10.43	12.95	14.68	16.48	16.87
$\delta = 0.3$	h	5.34	6.94	8.92	10.26	12.17	13.17	14.2	14.43
$\delta = 0.5$	h	5.35	6.94	8.91	10.13	11.61	12.09	12.45	12.52
$\delta = 0.8$	h	5.36	6.94	8.89	10.09	11.23	11.38	11.28	11.23
$\delta = 1$	h	5.36	6.95	8.84	10.08	11.23	11.36	11.28	11.22
ARL_0=500	r	0.01	0.02	0.05	0.1	0.3	0.5	0.8	1
$\delta = 0.1$	h	6.11	7.69	9.73	11.19	13.96	15.92	17.89	18.37
$\delta = 0.3$	h	6.09	7.71	9.67	10.98	12.94	14.08	15.29	15.55
$\delta = 0.5$	h	6.11	7.71	9.67	10.87	12.29	12.82	13.23	13.31
$\delta = 0.8$	h	6.12	7.71	9.61	10.74	11.86	11.94	11.79	11.77
$\delta = 1$	h	6.11	7.69	9.57	10.7	11.54	11.35	10.81	10.66

6.2.2 Out-of-control ARL

Under the constant dependence parameter assumption, the ARL_1 of the $MEWMA_{Trans}$ chart is influenced by the value of mean shift vector $(\theta_1'/\theta_1, \theta_2'/\theta_2)$ as well as the design parameters *r* and *h*. The optimal statistical design scheme should have the shortest ARL_1 at certain in-control ARL value. After we specify an ARL_0, possible combinations of the design parameters (*r, h*) can be read from Figure 6-1 to Figure 6-5 or Table 6-1. The optimal design combination is the one yields the shortest ARL_1 which is denoted by ARL_{opt}.

The listed combination of *r* and *h* in Table 6-1 were used to calculate the out-of-control ARL values. Different shift vectors lead to different optimal settings of the design parameters. Table 6-2 to 6-4 show the optimal design schemes for the MEWMA charts on transformed GBE data with δ = 0.5 and ARL_0 = 100, 200, 370.4, 500. (The optimal design schemes for δ =0.1, 0.3, 0.8, 1 with ARL_0 = 100, 200, 370.4, 500 are listed in Appendix C.) In these tables, we consider the cases of the downward-downward shift (D-D shift), the upward-upward shift (U-U shift) and the downward-upward shifts (D-U shift). Then, to further examine the effects of δ on the optimal design, we fix ARL_0 = 200 and the optimal design schemes under δ =0.1, 0.3, 0.5, 0.8, 1, as are given in Table 6-5. Only the values of smoothing factor *r* and the optimal ARL_1 values are listed in the tables since we could easily get the corresponding UCL *h* values according to Table 6-1.

- Detection of the D-D Shift

A D-D shift denotes the situation that both X_1 and X_2 are shifting downward $(\theta_1'/\theta_1 < 1, \theta_2'/\theta_2 \leq 1)$. The D-D shift is of interests when we are facing negative effect events which would cause social and economic loss and the decreasing TBE indicates the deterioration. Some of these negative events are of high severity and closely monitoring may create great benefit in human life. Such examples include the occurrence of a traffic accident, the collapse of a computer network, and the recrudescing of a disease.

Table 6-2 shows the optimal design schemes of $MEWMA_{Trans}$ chart under selected D-D shift levels. Some interesting conclusions can be made from Table 6-2:

1) The optimal *r* value ranges from 0.01 to 0.3. These *r* values are comparatively small indicating that the size of the D-D shift of the transformed data is not so large, i.e. the effect of D-D shift has been reduced after the double SQRT transformation.

2) The optimal *r* values are rather stable for different ARL_0 specifications especially when the shift level is large. Hence, it is reasonable to choose a suitable *r* value using Table 6-2 even if the desired ARL_0 and mean shift $(\theta_1'/\theta_1, \theta_2'/\theta_2)$ is not included.

3) To detect a small shift, i.e. θ_i'/θ_i close to 1, it is preferable to use a small value of *r*. For example, the optimal *r* for detecting $(\theta_1'/\theta_1, \theta_2'/\theta_2)$ = (0.8, 1) is 0.01, 0.02, or 0.05 no matter what the dependence parameter δ is. Nevertheless, a large *r* is more effective in detecting large shifts. This is similar to the univariate cases as the

EWMA chart with a small smoothing factor has long been considered highly effective for detecting small sustained shifts.

4) Comparing the single shift and double shifts situation, we can see that the optimal ARL values for detecting double shifts is larger than the one for detecting the single shift with the same shift value. It is due to the confounding effect of the mean shift (shifts) and the positive correlation between variables.

Table 6-2 The optimal design schemes of $MEWMA_{Trans}$ chart for D-D shifts when $\delta = 0.5$

$(\theta_1'/\theta_1, \theta_2'/\theta_2)$	ARL_0	100	200	370	500
(0.1,1)	R	0.3	0.3	0.3	0.3
	ARL_{opt}	0.79	1.12	1.43	1.58
(0.2,1)	R	0.3	0.3	0.3	0.3
	ARL_{opt}	2.09	2.77	3.45	3.81
(0.3,1)	R	0.1	0.1	0.1	0.1
	ARL_{opt}	4.12	5.18	6.00	6.44
(0.4,1)	R	0.1	0.1	0.1	0.1
	ARL_{opt}	6.10	7.90	9.17	9.94
(0.5,1)	R	0.1	0.1	0.1	0.05
	ARL_{opt}	9.29	12.29	14.56	16.08
(0.6, 1)	R	0.1	0.05	0.05	0.05
	ARL_{opt}	14.64	19.19	23.02	25.01
(0.7,1)	R	0.05	0.05	0.02	0.02
	ARL_{opt}	23.51	32.13	39.41	43.13
(0.8,1)	R	0.02	0.02	0.02	0.02
	ARL_{opt}	39.72	55.89	71.04	80.48
(0.9,1)	R	0.01	0.01	0.01	0.01
	ARL_{opt}	70.99	114.27	164.18	193.90
(0.1,0.1)	R	0.3	0.3	0.3	0.3
	ARL_{opt}	2.28	2.99	3.75	4.17
(0.2,0.2)	R	0.1	0.1	0.1	0.1
	ARL_{opt}	4.46	5.65	6.54	6.97
(0.5,0.5)	R	0.05	0.05	0.05	0.05
	ARL_{opt}	15.47	19.75	23.68	25.68
(0.8,0.8)	R	0.01	0.01	0.01	0.01
	ARL_{opt}	52.88	77.37	101.41	114.67

- Detection of the U-U Shift

A U-U shift denotes the situation that both X_1 and X_2 are shifting upward $(\theta_1'/\theta_1 > 1, \theta_2'/\theta_2 \geq 1)$. The U-U shift is interested when the events occurring have positive effects in human life and the increasing TBE indicates the deterioration. The example events include the failure of an engine, the collapse of a computer, and the breakout of an infection.

Table 6-3 shows the optimal design schemes under selected U-U shift levels. Some interesting conclusions can be made from Table 6-3:

1) The optimal *r* value ranges from 0.1 to 0.8. These *r* values are located throughout the range of 0 to 1 indicating that the effect of U-U shift has not been reduced after the double SQRT transformation.
2) The optimal design parameters *r* and *h* are rather stable for a range of mean vector shifts according to different ARL_0 specifications.
3) A small value of *r* is preferred for detecting a small shift and vice versa.
4) Same to the case of D-D shifts, the confounding effect caused the optimal ARL values of double shifts larger than the ones of single shift with the same shift value.

Table 6-3 The optimal design schemes of $MEWMA_{Trans}$ chart for U-U shifts when $\delta = 0.5$

$(\theta_1'/\theta_1, \theta_2'/\theta_2)$	ARL_0	100	200	370	500
(1.2,1)	R	0.1	0.02	0.02	0.02
	ARL_{opt}	43.23	63.82	83.82	94.56
(1.5,1)	R	0.1	0.05	0.05	0.05
	ARL_{opt}	16.04	22.01	26.53	28.87
(1.8,1)	R	0.1	0.1	0.1	0.1
	ARL_{opt}	9.00	11.72	13.73	14.82
(2,1)	R	0.1	0.1	0.1	0.1
	ARL_{opt}	6.95	8.72	10.30	11.00
(2.5,1)	R	0.3	0.3	0.3	0.3
	ARL_{opt}	3.77	4.78	5.74	6.27
(3, 1)	R	0.3	0.3	0.3	0.3
	ARL_{opt}	2.43	2.93	3.60	3.83
(4,1)	R	0.5	0.5	0.5	0.3
	ARL_{opt}	1.17	1.53	1.87	1.97
(5,1)	R	0.5	0.5	0.5	0.5
	ARL_{opt}	0.66	0.88	1.07	1.22
(10,1)	R	0.5	0.5	0.5	0.5
	ARL_{opt}	0.10	0.14	0.19	0.21
(1.5,1.5)	R	0.1	0.05	0.05	0.05
	ARL_{opt}	20.17	29.59	36.80	40.04
(2,2)	R	0.1	0.1	0.1	0.1
	ARL_{opt}	9.09	12.05	14.39	15.51
(5,5)	R	0.5	0.5	0.5	0.5
	ARL_{opt}	1.03	1.37	1.69	1.87
(10,10)	R	0.8	0.8	0.5	0.5
	ARL_{opt}	0.23	0.30	0.40	0.44

- Detection of the D-U Shift

A D-U shift denotes the situation that one of X_1 and X_2 is shifting upward and the other one is shifting downward $(\theta_1'/\theta_1 < 1, \theta_2'/\theta_2 \geq 1)$. The D-U shift is interested when one of the event occurring has positive effect and the other one has negative effect in human life.

Table 6-4 shows the optimal design schemes under selected D-U shift levels. Some interesting conclusions can be made from Table 6-4:

1) The optimal *r* value ranges from 0.1 to 0.5. The range of *r* values indicates that the effect of downside shift and upside shift after the double SQRT transformation has been confounded.

2) The optimal design parameters *r* and *h* are rather stable for a range of mean vector shifts according to different ARL_0 specifications.

3) A small value of *r* is preferred for detecting a small shift and vice versa.

4) Comparing the double shifts values in Table 6-2 to Table 6-4, we can see that the MEWMA chart is most effective for detecting D-U shifts. For example, the optimal ARL values for mean shifts (0.5, 0.5), (0.5, 1), (0.5, 2), (2, 1), (2, 2) are 19.75, 12.29, 3.02, 8.72, and 12.05. The MEWMA chart has the smallest optimal ARL value for mean shifts (0.5, 2). The optimal ARL value decreases when θ_1'/θ_1 departs from θ_2'/θ_2 due to the confounding effect of the mean shift direction and the positive correlation between variables.

Table 6-4 The optimal design schemes of $MEWMA_{Trans}$ chart for D-U shifts when $\delta = 0.5$

$(\theta_1'/\theta_1, \theta_2'/\theta_2)$	ARL_0	100	200	370	500
(0.8,1.5)	*r*	0.1	0.1	0.3	0.1
	ARL_{opt}	9.88	12.96	15.48	17.06
(0.5,2)	*r*	0.3	0.3	0.5	0.3
	ARL_{opt}	2.30	3.02	3.62	3.98
(0.2,5)	*r*	0.5	0.5	0.5	0.5
	ARL_{opt}	0.05	0.08	0.12	0.14
(0.1,10)	*r*	0.5	0.5	0.5	0.5
	ARL_{opt}	0.00	0.00	0.00	0.01

- Optimal Design under Different δ Value

Table 6-5 shows the optimal design schemes under δ=0.1, 0.3, 0.5, 0.8, 1 when ARL_0 = 200.

Table 6-5 The optimal design schemes of $MEWMA_{Trans}$ chart when ARL_0 = 200

$(\theta_1'/\theta_1, \theta_2'/\theta_2)$	Δ	0.1	0.3	0.5	0.8	1
(0.2,1)	r	0.3	0.3	0.3	0.1	0.1
	ARL_{opt}	0.00	0.72	2.77	5.63	6.12
(0.4,1)	r	0.5	0.3	0.1	0.1	0.1
	ARL_{opt}	0.01	3.42	7.90	13.26	14.40
(0.6, 1)	r	0.3	0.1	0.05	0.05	0.05
	ARL_{opt}	0.79	9.60	19.19	29.89	32.28
(0.8,1)	r	0.1	0.05	0.02	0.01	0.01
	ARL_{opt}	6.43	32.92	55.89	76.27	80.21
(1.5,1)	r	0.3	0.1	0.05	0.05	0.05
	ARL_{opt}	1.29	11.38	22.01	31.80	34.92
(2,1)	r	0.3	0.3	0.1	0.1	0.1
	ARL_{opt}	0.08	3.97	8.72	13.67	14.57
(3, 1)	r	0.5	0.3	0.3	0.3	0.3
	ARL_{opt}	0.00	1.04	2.93	5.17	5.51
(5,1)	r	0.1	0.5	0.5	0.5	0.5
	ARL_{opt}	0.00	0.15	0.88	1.80	1.83
(0.2,0.2)	r	0.1	0.1	0.1	0.1	0.3
	ARL_{opt}	6.57	6.24	5.65	4.46	2.78
(0.8,0.8)	r	0.01	0.01	0.01	0.01	0.02
	ARL_{opt}	82.33	80.70	77.37	66.93	57.05
(2,2)	r	0.1	0.1	0.1	0.3	0.3
	ARL_{opt}	13.88	12.96	12.05	9.82	7.43
(5,5)	r	0.3	0.5	0.5	0.5	0.8
	ARL_{opt}	2.15	1.76	1.37	0.84	0.48
(0.2, 5)	r	≥0.05	0.5	0.5	0.5	0.5
	ARL_{opt}	0.00	0.00	0.08	0.68	1.17
(0.8,1.5)	r	0.3	0.1	0.1	0.1	0.05
	ARL_{opt}	0.23	6.03	12.96	24.10	30.39

We can find the following observations from Table 6-5:

1) The optimal design parameters r and h are rather stable for a range of mean vector shifts according to different correlation parameter δ.

2) A small value of *r* is preferred for detecting a small shift and vice versa.

3) Another interesting feature observed from Table 6-5 is that the optimal design parameters *r* and *h* are also stable for a range of δ values. Thus, it is also reasonable to find an *r* value with good performance using Table 6-2 to Table 6-5 even if the desired δ is not listed.

6.2.3 Procedure for optimal design of the MEWMA chart

Based on the aforementioned results, we recommend the following procedure for the optimal design of the MEWMA chart based on the transformed GBE TBE data:

Step 1: Specify the desired ARL_0 value, the constant dependence parameter δ and the out-of control mean shift vector $(\theta_1'/\theta_1, \theta_2'/\theta_2)$ at the beginning.

Step 2: Find the approximate value of the smoothing factor *r* according to the optimal design schemes in Tables 6-2 to 6-5.

Step 3: Locate the corresponding *h* value according to the ARL_0 contour plots in Figure 6-1 to Figure 6-5.

Step 4: Use simulation to achieve the more accurate ARL_0 and ARL_1 to evaluate the performance of the designed $MEWMA_{Trans}$ chart.

6.3 Robustness study

In Section 6.2, we assume the dependence parameter δ is known and remains constant through the whole monitoring process. In practice, this dependence parameter δ is subject to estimation errors and moreover faces small random drifts. In order to account for the

estimation deviations and the possible natural instability, we need to examine the sensitivity of the $MEWMA_{Trans}$ chart to the departure of δ from the estimated value.

For each combination $(\theta_1'/\theta_1, \theta_2'/\theta_2)$ in the first column of Table 6-6, we use the estimated δ_{est} = 0.5 to derive the 'estimated' optimal settings given the pre-specified ARL_0 = 200. Assume that this estimated optimal setting is used but the true values of δ is δ_{true} = 0.3, 0.8, respectively. The actual values of ARL_0 and ARL_1, denoted as $ARL_0^{(true)}$ and $ARL_1^{(true)}$, are then computed via simulation. For comparison purpose, the optimal settings $ARL_{opt}^{(true)}$ derived from the true values of δ, given the pre-specified ARL_0 = 200, are also given in the table.

From Table 6-6, we observe the following phenomenon:

1) For a range of mean shift values, the ARL_1 is not sensitive to the dependent parameter δ. Hence, it is reasonable for us to use the optimal design results in Section 6.2 as guidelines in real applications.

2) When the shift is not too large, say $0.3 \le \theta_i'/\theta_i \le 2$, i =1, 2, ($ARL_0^{(\text{true})}$, $ARL_1^{(\text{true})}$) is quite close to (200, $ARL_{opt}^{(\text{true})}$). This means that the effect of estimation error tends to be quite small when we are interested in shifts with small size.

3) When $\theta_i'/\theta_i \gg 1$ and $\theta_i'/\theta_i \ll 1$, i =1, 2, $ARL_0^{(\text{true})}$ is inclined to be far removed from 200. This result prompts us to give more attention to the estimation accuracy of δ when we would like to detect extremely large shifts.

Table 6-6 Estimated ARL_1 s of $MEWMA_{Trans}$ chart based on δ_{est} = 0.5 and δ_{true} = 0.3, 0.8

$(\theta_1'/\theta_1, \theta_2'/\theta_2)$	$ARL_{\text{opt}}^{(est)}$	δ_{true} = 0.3			δ_{true} = 0.8		
		$ARL_1^{(\text{true})}$	$ARL_0^{(\text{true})}$	$ARL_{\text{opt}}^{(\text{true})}$	$ARL_1^{(\text{true})}$	$ARL_0^{(\text{true})}$	$ARL_{\text{opt}}^{(\text{true})}$
(0.1,1)	0.40	0.10	173.94	0.09	2.89	226.37	2.76
(0.2,1)	1.12	0.67	173.94	0.72	6.60	226.37	5.61
(0.3,1)	2.77	2.42	198.23	1.71	8.67	205.92	8.65
(0.5,1)	7.90	5.85	198.23	5.87	20.79	205.92	19.54
(0.7,1)	19.19	17.03	204.75	17.01	48.65	203.25	46.44
(0.9,1)	55.89	79.47	206.08	76.70	139.82	199.12	139.12
(1.2,1)	197.73	39.31	201.59	39.09	85.72	200.04	85.02
(1.5,1)	63.82	12.30	204.75	11.38	32.76	203.25	32.31
(1.8,1)	22.01	5.97	198.23	5.96	18.33	205.92	18.02
(2,1)	11.72	4.46	198.23	3.97	13.63	205.92	13.63
(3, 1)	4.78	0.99	173.94	1.04	5.42	226.37	5.20
(5,1)	0.88	0.14	159.09	0.15	1.96	261.17	1.79
(2,2)	12.05	12.95	198.23	12.96	10.14	205.92	9.82
(5,5)	1.37	1.57	159.09	1.76	0.92	261.17	0.84
(0.2,0.2)	5.65	6.19	198.23	6.24	4.46	205.92	4.46
(0.8,0.8)	77.37	80.25	206.08	80.70	67.30	199.12	66.93
(0.8,1.5)	12.96	6.06	198.23	6.03	24.94	205.92	24.10
(0.5,2)	3.02	0.73	173.94	0.76	8.08	226.37	7.33

6.4 Illustrative example

We assume that, in a two-component system, the time between failures of each component follows exponential distribution and the joint distribution of the time between failures for the two components follows GBE model. A simulation example is constructed to illustrate the optimal design of the MEWMA chart based on transformed data and use it to detect the mean shifts of the time between failures. The generated data are listed in Table 6-7. The first 15 pairs of TBE data follow a GBE (1, 1, 0.5), and the next 15 pairs follow a GBE (1, 0.5, 0.5).

Table 6-7 An example of setting-up MEWMA chart with transformed GBE data

No	x_i		y_i		z_i		E_i^2
					0	0	0
1	2.05	3.40	1.20	1.36	0.03	0.05	0.60
2	0.56	2.37	0.87	1.24	0.02	0.07	2.14
3	1.90	0.65	1.17	0.90	0.05	0.07	1.27
4	1.99	1.60	1.19	1.12	0.07	0.08	2.03
5	1.91	3.25	1.18	1.34	0.09	0.12	4.03
6	2.00	0.97	1.19	0.99	0.11	0.11	4.29
7	2.66	0.97	1.28	0.99	0.14	0.11	5.52
8	0.94	2.18	0.98	1.22	0.13	0.13	5.84
9	0.21	1.14	0.68	1.03	0.09	0.13	4.98
10	0.66	1.18	0.90	1.04	0.08	0.13	5.06
11	0.94	0.63	0.98	0.89	0.08	0.12	3.96
12	0.19	0.20	0.66	0.67	0.05	0.08	1.94
13	0.76	1.15	0.93	1.04	0.05	0.09	2.24
14	0.15	0.09	0.62	0.55	0.01	0.04	0.62
15	2.07	2.02	1.20	1.19	0.04	0.07	1.27
16	0.22	0.80	0.68	0.95	0.02	0.06	1.63
17	0.19	2.72	0.66	1.28	-0.01	0.09	6.05
18	0.17	1.86	0.64	1.17	-0.04	0.11	11.19
19	0.23	0.27	0.69	0.72	-0.05	0.08	9.11
20	2.10	3.21	1.20	1.34	-0.02	0.12	9.87
21	0.80	5.31	0.95	1.52	-0.01	0.17	17.89
22	0.13	0.30	0.60	0.74	-0.04	0.13	15.89
23	0.14	0.79	0.61	0.94	-0.07	0.12	18.28
24	1.37	2.68	1.08	1.28	-0.04	0.15	19.11
25	0.47	1.33	0.83	1.07	-0.05	0.15	20.14
26	0.22	0.18	0.68	0.65	-0.06	0.11	15.16
27	0.16	0.52	0.63	0.85	-0.08	0.09	15.74
28	0.09	0.38	0.55	0.79	-0.11	0.07	16.95
29	0.07	0.06	0.51	0.49	-0.14	0.02	14.47
30	0.29	1.06	0.73	1.01	-0.14	0.03	16.35

Given a pre-specified $ARL_0 = 370.4$, the optimal design parameters can be obtained from Table 6-2, which are given by (r, h) = (0.1, 10.13). A MEWMA chart based

on the transformed data can be constructed by following the set-up procedure described in Section 6.2. We can see from Figure 6-6 that the MEWMA chart signals the out of control situation at the 18th point which is the third point after the underlying process has been shifted. Thus, the proposed MEWMA chart is quite effective according to the simulation example.

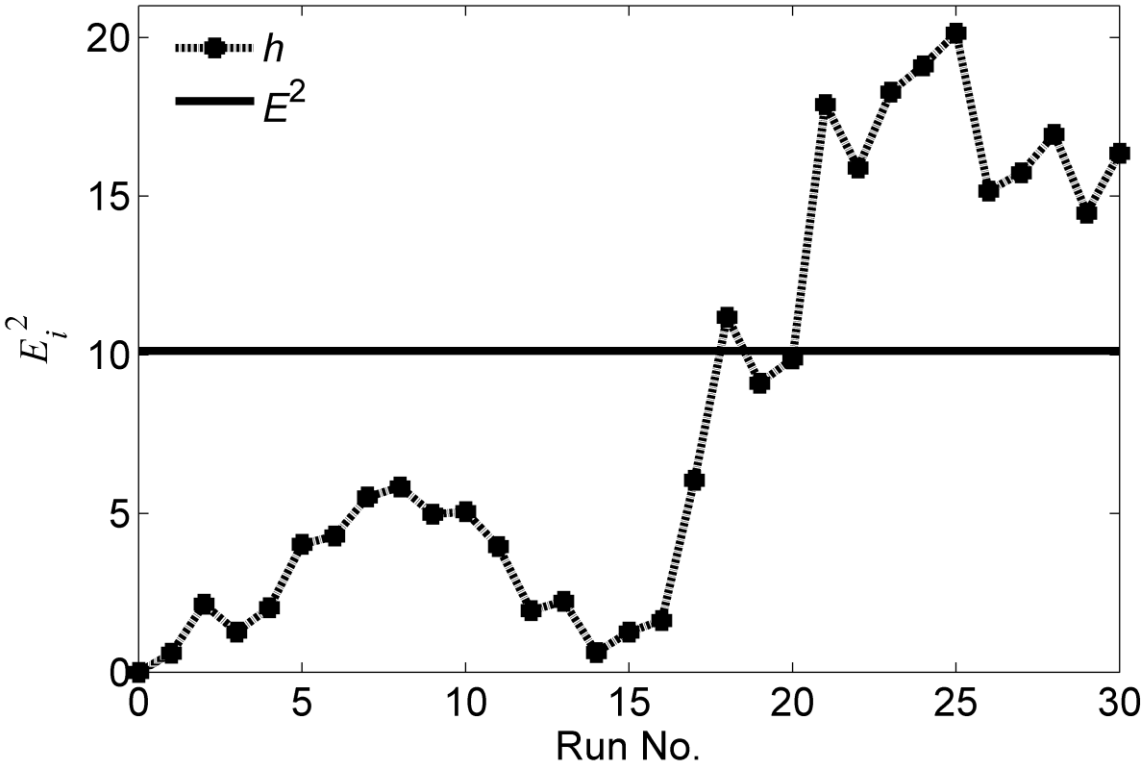

Figure 6-6 A MEWMA TBE chart based on transformed GBE data

6.5 Conclusions

In this chapter we investigated the optimal design problem of the MEWMA chart based on transformed GBE data for monitoring mean shift(s). The optimal design procedure was

provided and the optimal design schemes are given in Appendix C to guide the future study. A rough estimate of the optimal schemes for scenarios not included in these tables could be obtained from extrapolation. Robustness study of the $MEWMA_{Trans}$ charts to the estimation errors of the dependence parameter δ showed that the effect of estimation errors was small when we were interested in detecting moderately small shifts. However, we should pay attention to the estimation accuracy if the circumstances of large upward shifts or extremely large downward shifts of the dependence parameter δ existed.

CHAPTER 7 CONCLUSIONS AND FUTURE WORKS

The results and contributions of the research works included in this dissertation are summarized in this chapter. The limitations of current works are discussed and some future works are suggested.

7.1. Summary

TBE charts were shown to be highly effective in both industry system improvement and human management. The example areas of applications of the TBE charts include the manufacturing systems, the reliability and maintenance monitoring problem, the human health surveillance, the service improvement. Despite its effectiveness and generality of applications, the current TBE chart techniques are facing more and more challenges as the implementing circumstance become more complex and the needs for multivariate charting techniques become greater. This thesis expanded the application area of the TBE charts by developing an EWMA TBE control chart based on the more generalized Weibull distribution and proposing two MEWMA chart for the multivariate GBE distribution.

Chapter 3 develops an EWMA chart for transformed Weibull-distributed TBE data. The Weibull distribution is a more reasonable assumption for lifetime data as it can describe not only the circumstances with a constant failure rate but also the ones with an increasing failure rate or a decreasing failure rate. The Box-Cox transformation method is

adopted to transform the Weibull-distributed data into approximately normal. Then an EWMA chart is constructed based on the transformed data. The statistical design of the proposed chart is using ARL criteria applying Markov chain calculation. It is proved that the in-control ARLs of the EWMA charts with transformed Weibull data only depend on the design parameters of the control charts and are irrelevant to the distribution parameters. The guidelines for optimal statistical design of the EWMA chart are given to promote the use of the chart in real applications.

Charter 4 proposed two MEWMA control charts for the Gumbel's bivariate exponential (GBE) distributed data, one based on the raw GBE data, the other based on the transformed data. Both charts are constructed for monitoring a mean vector shift (or shifts) under the assumption that the dependence between the two variables remains the same. For MEWMA on the transformed data, we first transform the bivariate exponential data into approximate bivariate normal data using the well-known double square root transformation, and then we apply the MEWMA chart to the transformed data. The ARL performance of the two MEWMA charts are compared with those of the paired individual *t* charts and the paired individual EWMA charts on both raw and transformed data. The results showed that the proposed MEWMA charts generally outperform all the other charts under all the circumstances considered. This prompts us to explore the potential applications of multivariate TBE charts in the future.

Chapter 5 and Chapter 6 study the optimal design for the MEWMA charts based on raw GBE data and on transformed GBE data, separately. The optimal design procedure was provided and the optimal design schemes were examined. Results showed that the optimal design parameters are quite constant for a range of mean shift or shifts. Thus a

rough estimate of the optimal schemes for scenarios not included in these tables could be obtained from extrapolation. Another general guideline is that a smaller smoothing factor *r* is more preferred for small shift or shifts levels and vice versa which is quite similar to the case of design of the EWMA chart for univariate distributed data. The robustness of the two control charts to the estimation errors of the dependence parameter was also examined. Robustness study of the $MEWMA_{Raw}$ and $MEWMA_{Trans}$ charts to the estimation errors of the dependence parameter δ showed that the effect of estimation errors is small when we are interested in detecting moderately small shifts. However, we should pay attention to the estimation accuracy if the circumstances of large upward shifts or extremely large downward shifts of the dependence parameter δ existed.

Results from each chapter showed that the control charts proposed in this thesis did improve the effectiveness of the TBE charting technique and make it more practical for complex TBE data monitoring. However, this thesis also has its limitations which along with future research direction are discussed in the next section.

7.2. Future works

In Chapter 3, it was assumed that the shape parameter of the Weibull distribution is known. However, in practice, the shape parameter is subject to estimation error and random drifts. It would be interesting to examine the robustness of the EWMA chart to the estimation error of the shape parameter. Moreover, Chapter 3 mainly dealt with the statistical design of the EWMA charts. Another widely studied method for designing control charts is the economic approach. The pioneering work done in this area was due to Duncan (1956) and

Lorenzen and Vance (1986). In the recent years, considerable research has been devoted to the economic design for univariate TBE charts e.g. Zhang et al. (2008). it would be interesting to investigate the economic design of the proposed EWMA chart based on transformed Weibull data.

In Chapter 4, 5 and 6, it was assumed that the dependence parameter of the GBE distribution was known and remained constant through the whole monitoring process. It would be a challenging problem to develop charting techniques for monitoring both the dependence parameter and the mean vector. Another thing is that the ARL values that calculated are zero-state ARLs. Further studies might examine the performance of the proposed charts for stable-state ARLs.

Chapter 5 and Chapter 6 discussed about the statistical design of the proposed MEWMA charts based on raw and transformed GBE data. As we know, economic design is another important design approach of control charts. Although its complexity methodology and the lack of general accepted multivariate cost function limited its application in the multivariate control charting research area, people are still paying attention to this area. For example, Linderman and Love (2000) extended the economic design to the MEWMA chart under multivariate normal assumption. We may further investigate the performance of the proposed charts under economic consideration. The comparison of the economic design and the statistical design of the MEWMA charts may provide us some insight in designing a TBE chart for different purposes. The computation complexity of different methods could be compared.

Moreover, there were lots of other multivariate attribute or variable TBE models with important applications in literature. As mentioned before, multivariate TBE charts for monitoring several TBE quantities at the same time have been rarely studied. Although some authors have developed various non-parametric control charts for multivariate data, the performance of such charts are usually poor comparing to distribution-based control charts. To improve the effectiveness of the control charts and overcome the weakness of univariate TBE charts for correlated quantities, it would be beneficial to extend the univariate TBE charts for some common multivariate TBE data, e.g. the famous Marshall-Olkin's multivariate exponential distribution, the Freund's multivariate exponential model and so on.

REFERENCES

Albers W. (2010). The optimal choice of negative binomial charts for monitoring high-quality processes. *J Stat Plan Inference*, 140,214–225.

Albert M. (2011). Control charts for health care monitoring under overdispersion. *Metria*, 74(1), 67-87.

Alt F.B. (1985). Multivariate quality control. *The Encyclopedia of Statisticla Sciences*, Kotz S., Johnson N.L., Read CR(eds). Wiley:New Yourk, 110-122.

Alt, F.B. and Smith, M.D. (1988). Multivariate process control. *Handbook of Statistics*, Krishnaiah, P.R. and Rao, C.R., (eds) Elsevier Science Publishers, New York, 333-351.

Aparisi, F., Jabaloyes, J. and Carrion, A. (1999). Statistical properties of the |S| multivariate control chart. *Communications in Statistics – Theory and Methods*, 28, 2671-2686.

Bai, D.S. and Choi, I.S. (1995). $\bar{X}$ and *R* chart for skewed population. *Journal of Quality Technology*, 27(2), 120-131.

Ben K.I. and Limam M. (2008). Support vector regression based residual MCUSUM control chart for autocorrelated process control chart for autocorrelated process. *Applied Mathematics and Computation*, 201, 565–574.

Bourke, P.D. (1991). Detecting a shift in fraction nonconforming using run-length control charts with 100% inspection. *Journal of Quality Technology*, 23(3), 225-238.

Bourke, P.D. (2001). The geometric CUSUM chart with sampling inspection for monitoring fraction defective. *Journal of Applied Statistics*, 28(8), 951-972.

Borror, C.M., Champ, C.W. and Rigdon, S.E. (1998). Poisson EWMA control charts. *Journal of Quality Technology*, 30(4), 352 – 361.

Borror C.M., Montgomery D.C. and Runger G.C. (1999). Robustness of the EWMA control charts to non-normality. *Journal of Quality Technology*; 31, 309 – 316.

Borror, C.M., Keats, J.B. and Montgomery, D.C. (2003). Robustness of the time between events CUSUM. *International Journal of Production Research*, 41(15), 3435-3444.

Box, George E. P. and Cox, D. R. (1964). An analysis of transformations. *Journal of the Royal Statistical Society, Series B,* 26, 211–246.

Brook, D. and Evans, D.A. (1972). An Approach to the Probability Distribution of CUSUM Run Length. *Biometrika*, 59(3), 539 – 549.

Calvin, T.W. (1983). Quality control techniques for "zero defects". *IEEE Transactions on Components, Hybrids, and Manufacturing Technology*, 6, 323-328.

Capizzi, G. and Masarotto, G. (2010). Self-starting CUSCORE control charts for multivariate individual observations. *Journal of Quality Technology*, 42, 136-151.

Chan, L.K. and Zhang J. (2001) Cumulative sum control charts for the covariance matrix. *Statistica Sinica*; 11, 767–790.

Chang, T.C. and Gan, F.F. (2001) Cumulative sum charts for high yield processes. *Statistica Sinica*, 11, 791-805.

Chang, Y.S. (2007). Multivariate CUSUM and EWMA control charts for skewed populations using weighted standard deviations. *Communications in Statistics—Simulation and Computation*, 36, 921–936.

Chang, Y.S. and Bai, D.S. (2001). Control Charts for Positively-skewed Populations with Weighted Standard Deviations. *Quality and Reliability Engineering International*, 17, 397-406.

Chang, Y.S. and Bai, D.S. (2004). A multivariate T^2 control chart for skewed populations using weighted standard deviations. *Quality and Reliability Engineering International*, 20, 31–46.

Chan, L.Y., Xie, M. and Goh, T.N. (2000). Cumulative quantity control charts for monitoring production processes. *International Journal of Production Research*, 38(2), 397-408.

Chan, L.Y., Lin, D.K.J., Xie, M. and Goh, T.N. (2002). Cumulative probability control charts for geometric and exponential process characteristics. *International Journal of Production Research*, 40(1), 133-150.

Chan, L.Y., Lai, C.D., Xie, M. and Goh, T.N. (2003). A two-stage decision procedure for monitoring processes with low fraction nonconforming. *European Journal of Operational Research*, 150, 420-436.

Chen, Y.K., Chen, C.Y. and Chiou, K.C. (2011). Cumulative conformance count chart with variable sampling intervals and control limits. *Applied Stochastic Models in Business and Industry*, 27(4), 410-420.

Chiu, J. E. and Kuo, T.I. (2008). Attribute Control Chart for Multivariate Poisson Distribution. *Communications in Statistics - Theory and Methods*, 37, 146–158.

Crosier R.B. (1988). Multivariate generalizations of cumulative sum quality-control schemes. *Technometrics*, 30, 291–303.

Csörgö, S. and Welsh, A.H. (1989). Testing for exponential and Marshall-Olkin distributions. *Journal of Statistical Planning and Inference*, 23, 287-300.

Duncan, A.J. (1956). The economic design of X-bar charts used to maintain current control of a process. *Journal of American Statistics*, 51, 228-242.

Ding, Y., Zeng, L., and Zhou, S. (2006). Phase I analysis for monitoring nonlinear profiles in manufacturing processes. *Journal of Quality Technology*, 38, 199–216.

Hernandez, F., and Johnson, R.A. (1980). The large-sample behavior of transformations to Normality. *Journal of the American Statistical Association*, 75(372), 855-861.

Goh, T.N. (1987). A control chart for very high yield processes. *Quality Assurance*, 13, 18-22.

Gan, F.F. (1992). Exact run length distributions for one-sided exponential CUSUM schemes. *Statistica Sinica*, 2, 297-312.

Gan, F.F. (1994). Design of Optimal Exponential CUSUM Control Charts. *Journal of Quality Technology*, 26, 109-124.

Gan, F.F. (1998). Designs of one- and two-sided exponential EWMA charts. *Journal of Quality Technology*, 30(1), 55-69.

Gan, F.F. and Chang, T.C. (2000) Computing average run lengths of exponential EWMA charts. *Journal of Quality Technology*, 32(2), 183-187.

Gumbel, E.J. (1960). Bivariate exponential distributions, *Journal of the American Statistical Association*, 55, 698-707.

Healy, J.D. (1987). A note on multivariate CUSUM procedures. *Technometrics*, 29, 409–412.

Hawkins D.M. (1991). Multivariate quality control based on regression-adjusted variables. *Technometrics*, 33, 61–75.

Hawkins, D.M. and Olwell, D.H. (1998). Cumulative Sum Charts and Charting for Quality Improvement, *New York: Springer.*

Hawkins, D.M. (2007). A general Multivariate exponential weighted moving-average control chart. *Journal of Quality Technology*, 39, 2, 118-125.

Hawkins, D.M. and Maboudou-Tchao, E.M. (2007). Self-starting multivariate exponentially weighted moving average control charting. *Technometrics*, 49, 199-209.

Hougaard, P. (1986). A class of multivariate failure time distributions. *Biometrika*, 73, 671-678.

Hougaard, P. (1989). Fitting a multivariate failure time distribution. *IEEE Transactions on Reliability*, 38(4), 444-448.

Hotelling, H. (1947). Multivariate quality control-illustrated by the air testing of sample bombsights, *Techniques of Statistical Analysis*, eds. C. Eisenhart, M. W. Hastay, and W . A. Wallis, New York: McGraw-Hill, 111-184.

Jae, W.B., Hae, W.K., Chang, W.K., and Song M. (2011). The optimal control limit of a G-EWMAG control chart. *International journal of advanced manufacturing technology*, 56, 161-175.

Jamal, A., Seyed, T., Akhavan, N. and Babak, A. (2007). Artificial neural networks in applying MCUSUM residuals charts for AR(1) processes. *Applied Mathematics and Computation*, 189, 1889–1901.

Jiang W., Han S.W., Tsui K.L. and Woodall W.H. (2011). Spatiotemporal surveillance methods in the presence of spatial correlation. *Statistics in Medicine*, 30(5), 568-583.

Jones, L.A. and Champ, C.W. (2002). Phase I control charts for times between events. *Quality and Reliability Engineering International*, 18, 479-488.

Joner M.D., Woodall W.H. and Reynolds M.R. (2008). A one-sided MEWMA chart for health surveillance. *Quality and Reliability Engineering International*, 24(5), 503-518.

Kaminsky, F.C., Benneyan, J.C., Davis, R.D. and Burke, R.J. (1991). Statistical control charts based on geometric distribution. *Journal of Quality Technology*, 24(2), 69-75.

Kang, L., and Albin, S. (2000). On-line monitoring when the process yields a linear profile. *Journal of Quality Technology*, 32, 418–426.

Kao, S.C., Ho, C.C. and Ho, Y.C. (2006). Transforming the exponential by minimizing the sum of the absolute differences. *Journal of Applied Statistics*, 33(7), 691-702.

Kao, S.C. and Ho, C.C. (2007). Monitoring a process of exponentially distributed characteristics through minimizing the sum of the squared differences. *Quality & Quantity*, 41, 137-149.

Kazemzadeh, R., Noorossana, R., and Amiri, A. (2009). Monitoring polynomial profiles in quality control applications. *The International Journal of Advanced Manufacturing Technology*, 42, 703–712.

Kittlitz, R. G. Jr. (1999). Transforming the Exponential for SPC Applications. *Journal of Quality Technology*, 31(3), 301-308.

Kim, K., Mahmoud, M.A. and Woodall, W.H. (2003). On the monitoring of linear profiles. *Journal of Quality Technology*, 35(3), 317-328.

Kramer, H.G., Schmid W. (1997). EWMA charts for multivariate time series. *Sequential Analysis*, 16, 131–154.

Lai, C.D., Govindaraju, K. and Xie, M. (1998). Effects of correlation on fraction non-conforming statistical process control procedures. *Journal of Applied Statistics*, 25(4), 535-543.

Lai, C.D., Xie, M. and Govindaraju, K. (2000). Study of a Markov model for a high-quality dependent process. *Journal of Applied Statistics*, 27(4), 461-473.

Lee, L. (1979). Multivariate distributions having Weibull properties. *Journal of Multivariate Analysis*, 9, 267-277.

Lee, M.H. and Khoo, B.C. Michael. (2006). Optimal Statistical Design of a Multivariate EWMA Chart Based on ARL and MRL. *Communications in Statistics—Simulation and Computation*, 35, 831–847.

Linderman, K, Love, T.E. (2000). Economic and economic statistical designs for MEWMA control charts. *Journal of Quality Technology*; 32, 410–417.

Liu, J.Y., Xie, M., Goh, T.N., Liu, Q.H. and Yang, Z.H. (2006). Cumulative count of conforming chart with variable sampling intervals. *International Journal of Production Economics*, 101, 286-297.

Liu, J.Y., Xie, M. and Goh, T.N. (2006). CUSUM chart with transformed exponential data. *Communications in Statistics-Theory and Methods*, 35, 1829-1843.

Liu, J.Y., Xie, M., Goh, T.N. and Chan, L.Y. (2007). A study of EWMA chart with transformed exponential data. *International Journal of Production Research*, 45(3), 743-763.

Lorenzen, T.J. and Vance, L.C. (1986). The economic design of control charts: A unified approach. *Technometrics*, 28, 3-10.

Lowry, C.A., Woodall, W.H., Champ, C.W. and Rigdon S.E. (1992). A multivariate EWMA control chart. *Technometrics*; 34, 46 – 53.

Lu, J., and Bhattacharryya, G.K. (1991). Inference procedure for bivariate exponential distributions. *Statistics & Probability Letters*, 12, 37-50.

Lu, X.S., Xie, M., Goh, T.N. and Lai, C.D. (1998). Control charts for multivariate attribute processes. *International Journal of Production Research*; 36, 3477-3489.

Lucas, J. M. (1985). Counted data CUCUM's. *Technometrics*, 27(2), 129-144.

Lucas, J.M. and Saccucci, M.S. (1990). Exponetially Weighted Moving Average Control Schemes: Properties and Enhancements. *Technometrics*, 32(1), 1 – 12.

Maboudou-Tchao, E.M. and Hawkins, D.M. (2011). Self-starting multivariate control charts for location and scale. *Journal of Quality Technology*, 43(3), 113-126.

Mahmoud, M.A., and Woodall, W. (2004). Phase I analysis of linear profiles with calibration applications. *Technometrics*, 46, 380–391.

Mahmoud, M.A., Parker, P.A., Woodall, W. and Hawkins, D.M. (2007). A change-point method for linear profile data. *Quality and Reliability Engineering International*, 23, 247–268.

Mason, R.L. and Young, J.C. (2001). Implementing multivariate process control using Hotelling's T^2 statistic. *Quality Progress*; 34(4), 71-73.

Mason, R.L. and Young, J.C. (2002). *Multivariate Statistical Process Control with Industrial Applications.* ASA/SIAM: Philadelphia, PA.

Molnau, W.E., Runger, G.C., Montgomery, D.C., Skinner, K.R., Loredo, E.N., and Prabhu, S.S. (2001). A program for ARL calculation for multivariate EWMA charts. *Journal of Quality Technology*; 33, 515–521.

Molnau, W.E., Montgomery, D.C., Runger, G.C. (2001). Statistically constrained designs of the multivariate exponentially weighted moving average control chart. *Quality and Reliability Engineering International*; 17, 39–49.

Montgomery, D.C. (2005). *Introduction to Statistical Quality Control*. John Viley & Sons.

Ngai H. M. and Zhang J. (2001). Multivariate cumulative sum control charts based on projection pursuit. *Statistica Sinica*; 11, 747–766.

Nelson, P.R. (1979). Control charts for Weibull processes with Standards Given. *IEEE Transactions on Reliability*, 28, 283-287.

Nelson, L.S. (1994). A control chart for parts per million nonconforming items. *Journal of Quality Technology*, 26, 239-240.

Nichols, M.D., and Padgett, W.J. (2006). A bootstrap control chart for Weibull percentiles. *Quality and Reliability Engineering International*, 22, 141-151.

Pascual, F. and Zhang, H.F. (2011). Monitoring the Weibull shape parameter by control charts for the sample range. *Quality and Reliability Engineering International*, 27, 15-25.

Pavel, M., Josef, T., and David, Š. (2006). Transformation of Data for Statistical Processing, *Electronics Technology*, ISSE apos.

Patel H.I. (1973). Quality control methods for multivariate binomial and Poisson distributions. *Technometrics*, 15, 103-112.

Pignatiello, J.J. and Runger, G.C. (1990). Comparisons of multivariate CUSUM charts. *Journal of Quality Technology*, 22, 173–186.

Prabhu, S.S. and Runger, G.C. (1997). Designing a multivariate EWMA control chart. *Journal of Quality Technology*, 29, 8–15.

Qiu, P.H. and Hawkins, D.M. (2001). A rank-based multivariate CUSUM procedure. *Technometrics*, 43, 120–132.

Qiu, P.H. and Hawkins, D.M. (2003). A nonparametric multivariate cumulative sum procedure for detecting shifts in all directions. *Journal of the Royal Statistical Society Series D—The Statistician*; 52, 151–164.

Qiu, P. and Zou, C. (2010). Control chart for monitoring nonparametric profiles with arbitrary design, *Statistica Sinica*, 20, 1655–1682.

Qiu, P., Zou, C. and Wang, Z. (2010). Nonparametric profile monitoring by mixed effects modeling. *Technometrics*, 52, 265–277.

Quesenberry, C.P. (1997). *SPC methods for quality improvement*. New York. NY: Wiley.

Ramalhoto, M.F. and Morais, M. (1999). Shewhart control charts for the scale parameter of a Weibull control variable with fixed and variable sampling intervals. *Journal of applied statistics*, 26(1), 129-160.

Reynolds, M. and Stoumbos, Z. (2008). Combinations of Multivariate Shewhart and MEWMA Control Charts for Monitoring the Mean Vector and Covariance Matrix. *Journal of Quality Technology*, 40(4), 381-393.

Rigdon, S.E. (1995). A double-integral equation for the average run length of a MEWMA control chart. *Statistics and Probability Letters*; 24, 365–373.

Rigdon, S.E. (1995). An integral equation for the in-control average length of a MEWMA control chart. *Journal of Statistical Computations and Simulation*; 52, 351–365.

Roberts, S.W. (1959). Control chart tests based on geometric moving average. *Technometrics*, 1(3), 239-250.

Rogerson, P. A. and Yamada, I. (2004). Monitoring change in spatial patterns of disease: comparing univariate and multivariate cumulative sum approaches. *Statistics in Medicine*, 23, 2195-2214.

Ross, S.M. (1970). Applied Probability Models with Optimization Applications, (*Holden Day: San Francisco, CA*).

Runger, G.C. and Prabhu, S.S. (1996). A markov chain model for the multivariate exponentially weighted moving averages control chart. *Journal of the American Statistical Association*, 91, 1701–1706.

Runger, G.C. and Testik, M.C. (2004). Multivariate extensions to cumulative sum control charts. *Quality and Reliability Engineering International*, 20, 587–606.

Sagias, N.C. and Karagiannidis, G.K. (2005). Gaussian class multivariate Weibull distributions: Theory and applications in fading channels. *IEEE Transactions on Information Theory*, 51(10), 3608-3619.

Sakia. R.M. (1992). The Box-Cox transformation Technique: A Review. *The Statistician*, 41(2), 169-178.

Schaffer, C.P. (1997). A multivariate application of the Q chart. Presented at the 1998 statistical meetings.

Skinner, K.R., Montgomery, D.C., and Runger, G.C. (2003). Process monitoring for multiple count data using generalized linear model-based control charts. *International Journal of Production Research*, 41, 1167-1180.

Stoumbos, Z.G. and Sullivan, J.H. (2002). Robustness to non-normality of the multivariate EWMA control chart. *Journal of Quality Technology*, 34, 260–276.

Sonesson, C. and Frisén, M. (2005). Multivariate surveillance, Chapter 9 in Spatial & Syndromic Surveillance by A. B. Lawson and K. Kleinman, John Wiley & Sons, Ltd.: New York, NY, 133-152.

Sullivan, J.H. and Jones, L.A. (2002). A self-starting control chart for multivariate individual observations. *Technometrics*, 44, 24-33.

Tang, L.C. and Cheong, W.T. (2004). Cumulative conformance count chart with sequentially updated parameters. *IIE Transactions*, 36, 841-853.

Tang, L.C. and Cheong, W.T. (2006). A control scheme for high-yield correlated production under group inspection. *Journal of Quality Technology*, 38(1), 45-55.

Testik, M.C., Runger, G.C., and Borror, C.M. (2003). Robustness properties of multivariate EWMA control charts. *Quality and Reliability Engineering International*, 19, 31 – 38.

Vardeman, S. and Ray, D. (1985). Average run lengths for CUSUM schemes when observation are exponentially distributed. *Technometrics*, 27(2), 145-150.

Williams, W.,Woodall, W.H., and Birch, J. B. (2007). Statistical monitoring of nonlinear product and process quality profiles. *Quality and Reliability Engineering International*, 23, 925–941.

Woodall, W.H. and Ncube, M.M. (1985). Multivariate CUSUM quality control procedures. *Technometrics*, 27, 285-292.

Wu, Z., Zhang, X.L. and Yeo, S.H. (2001). Design of the sum-of-conforming-run-length control charts. *European Journal of Operational Research*, 132, 187-196.

Xie, M. and Goh, T.N. (1997). The use of probability limits for process control based on geometric distribution. *International Journal of Quality & Reliability Management*, 14(1), 64-73.

Xie, M., Goh, T.N. and Lu, X.S. (1998). A comparative study of CCC and CUSUM charts. *Quality and Reliability Engineering International*, 14, 339-345.

Xie, M., Lu, X.S. and Goh, T.N. (1999). A quality monitoring and decision-making scheme for automated production processes. *International Journal of Quality & Reliability Management*, 16(2), 148-157.

Xie, M., Goh, T.N. and Tang, X.Y. (2000). Data transformation for geometrically distributed quality characteristics. *Quality & Reliability Engineering International*, 16, 9-15.

Xie, M., Tang, X.Y. and Goh, T.N. (2001). On economic design of cumulative count of conforming chart. *International Journal of Production Economics*, 72, 89-97.

Xie, M., Goh, T.N. and Ranjan, P. (2002). Some effective control chart procedures for reliability monitoring. *Reliability Engineering and System Safety*, 77, 143-150.

Yang, Z.L., Xie, M. and Kuralmani, V. (2002). On the performance of geometric charts with estimated control limits. *Journal of Quality Technology*, 34(4), 448-458.

Yang Z.L., Stanley P.S. and Xie, M. (2003). Transformation approaches for the construction of Weibull prediction interval, *Computational Statistics & Data Analysis*, 43, 357-368.

Ye, Z.S., Shen, Y. and Xie, M. (2012a). Degradation-based burn-in with preventive maintenance. *European Journal of Operational Researc*h, 221 (2), 360-367.

Ye, Z.S., Xie, M., Tang, L.C. and Shen, Y. (2012b). Degradation-based burn-in planning under competing risks, Technometrics, 54 (2), 159-168.

Zantek, P.F., Wright, G.P. and Plante, R.D. (2002). Process and product improvement in manufacturing systems with correlated stages. *Management Science*, 48, 591-606.

Zhang, C.W., Xie, M. and Goh, T.N. (2006). Design of exponential control charts using a sequential sampling scheme. *IIE Transactions*, 38, 1105-1116.

Zhang, C.W., Xie, M. and Goh, T.N. (2008). Economic design of cumulative count of conforming charts under inspection by samples. *International Journal of Production Economics*. 111(1), 93-104.

Zhang, L.Y. and Chen, G.M. (2004). EWMA charts for monitoring the mean of censored Weibull lifetimes, *Journal of Quality Technology*, 36(3), 321-328.

Zhang, L.Y., Govindaraju, K., Bebbington, M. and Lai, C.D. (2004). On the statistical design of geometric control charts. *Quality Technology and Quantitative Management*, 1(2), 233-243.

Zou, C., Tsung, F. and Wang, Z. (2007). Monitoring general linear profiles using multivariate exponentially weighted moving average schemes. *Technometrics*, 49, 395–408.

Zou, C.L., and Tsung, F. (2008). Directional MEWMA Schemes for Multistage Process Monitoring and Diagnosis. *Journal of Quality Technology*, 40(4), 407-427.

APPENDIX A: OPTIMAL DESIGN SCHEMES OF EWMA CHART WITH TRANSFORMED WEIBULL DATA

Table A-1 The optimal design schemes of EWMA chart with transformed Weibull data
In control ARL=100, $\beta_0 = 1$

Scale Shift (β_1/β_0)		Shape shift η_1/η_0											
		0.2	0.5	0.8	1	1.5	2	2.5	3	3.5	4	4.5	5
0.1	λ	0.02	0.1	0.2	0.3	0.5	0.8	1	1	1	0.8	0.8	0.5
	L	1.469	2.144	2.343	2.42	2.467	2.458	2.452	2.452	2.452	2.458	2.458	2.467
	$ARL_{\min}$	24.201	8.3741	4.789	3.6895	2.3728	1.7758	1.2409	1.0056	1	1	1	1
0.2	λ	0.02	0.05	0.1	0.2	0.3	0.4	0.5	0.8	1	1	1	1
	L	1.469	1.88	2.144	2.343	2.42	2.454	2.467	2.458	2.452	2.452	2.452	2.452
	$ARL_{\min}$	35.177	12.883	7.3937	5.6084	3.4969	2.5509	2.0767	1.6557	1.3069	1.0408	1.0007	1
0.3	λ	0.02	0.05	0.1	0.1	0.2	0.3	0.4	0.5	0.5	0.8	0.8	1
	L	1.469	1.88	2.144	2.144	2.343	2.42	2.454	2.467	2.467	2.458	2.458	2.452
	$ARL_{\min}$	46.931	17.845	10.321	7.9623	4.8974	3.507	2.7345	2.269	2.0201	1.6619	1.4022	1.1344
0.4	λ	0.02	0.02	0.05	0.1	0.2	0.2	0.3	0.4	0.4	0.5	0.5	0.8
	L	1.469	1.469	1.88	2.144	2.343	2.343	2.42	2.454	2.454	2.467	2.467	2.458
	$ARL_{\min}$	59.523	24.332	14.279	10.965	6.8501	4.817	3.7116	3.0289	2.5603	2.2381	2.0448	1.7898
0.5	λ	0.02	0.02	0.05	0.05	0.1	0.2	0.2	0.3	0.3	0.4	0.4	0.5
	L	1.469	1.469	1.88	1.88	2.144	2.343	2.343	2.42	2.42	2.454	2.454	2.467
	$ARL_{\min}$	72.161	32.586	19.621	15.201	9.422	6.7732	5.136	4.1703	3.478	2.9985	2.6337	2.3644
0.6	λ	0.02	0.02	0.02	0.05	0.05	0.1	0.1	0.2	0.2	0.3	0.3	0.3
	L	1.469	1.469	1.469	1.88	1.88	2.144	2.144	2.343	2.343	2.42	2.42	2.42
	$ARL_{\min}$	83.564	44.362	27.427	21.587	13.595	9.619	7.46	5.9573	4.9539	4.2632	3.6967	3.2895
0.7	λ	0.02	0.02	0.02	0.02	0.05	0.05	0.1	0.1	0.1	0.2	0.2	0.2
	L	1.469	1.469	1.469	1.469	1.88	1.88	2.144	2.144	2.144	2.343	2.343	2.343
	$ARL_{\min}$	92.46	60.799	39.769	31.625	20.454	14.719	11.338	9.1102	7.6485	6.5243	5.6271	4.9683
0.8	λ	0.02	0.02	0.02	0.02	0.02	0.02	0.05	0.05	0.05	0.1	0.1	0.1

	L	1.469	1.469	1.469	1.469	1.469	1.469	1.88	1.88	1.88	2.144	2.144	2.144
	$ARL_{\min}$	98.084	80.623	60.753	50.354	33.785	25.009	19.485	15.81	13.312	11.324	9.8183	8.6799
0.9	λ	0.02	0.02	0.02	0.02	0.02	0.02	0.02	0.02	0.02	0.02	0.02	0.05
	L	1.469	1.469	1.469	1.469	1.469	1.469	1.469	1.469	1.469	1.469	1.469	1.88
	$ARL_{\min}$	100.41	96.678	88.929	82.57	66.386	52.989	43.052	35.842	30.543	26.556	23.477	20.826
1.2	λ	0.02	0.05	0.05	0.05	0.05	0.1	0.1	0.2	0.2	0.3	0.3	0.4
	L	1.469	1.88	1.88	1.88	1.88	2.144	2.144	2.343	2.343	2.42	2.42	2.454
	$ARL_{\min}$	92.35	77.724	61.31	52.072	35.619	25.72	19.37	15.152	12.095	9.9019	8.2404	6.9501
1.5	λ	0.05	0.05	0.05	0.1	0.2	0.3	0.5	0.5	0.8	0.8	0.8	0.8
	L	1.88	1.88	1.88	2.144	2.343	2.42	2.467	2.467	2.458	2.458	2.458	2.458
	$ARL_{\min}$	80.883	47.61	29.582	22.515	12.977	8.3911	5.8366	4.3297	3.3815	2.7216	2.2793	1.9706
1.8	λ	0.05	0.05	0.1	0.2	0.4	0.5	0.8	0.8	0.8	0.8	0.8	1
	L	1.88	1.88	2.144	2.343	2.454	2.467	2.458	2.458	2.458	2.458	2.458	2.452
	$ARL_{\min}$	69.524	32.985	18.6	13.642	7.3375	4.574	3.1905	2.3959	1.9332	1.6443	1.4547	1.3256
2	λ	0.05	0.1	0.2	0.2	0.5	0.8	0.8	0.8	0.8	0.8	1	1
	L	1.88	2.144	2.343	2.343	2.467	2.458	2.458	2.458	2.458	2.458	2.452	2.452
	$ARL_{\min}$	63.33	27.372	14.852	10.715	5.5948	3.518	2.4589	1.9065	1.5885	1.3929	1.2654	1.1811
2.5	λ	0.05	0.1	0.3	0.4	0.8	0.8	0.8	0.8	1	1	1	1
	L	1.88	2.144	2.42	2.454	2.458	2.458	2.458	2.458	2.452	2.452	2.452	2.452
	$ARL_{\min}$	51.856	19.241	9.8229	6.8926	3.5698	2.265	1.6938	1.4036	1.2406	1.1461	1.0901	1.0561
3	λ	0.05	0.2	0.4	0.5	0.8	0.8	0.8	1	1	1	1	1
	L	1.88	2.343	2.454	2.467	2.458	2.458	2.458	2.452	2.452	2.452	2.452	2.452
	$ARL_{\min}$	44.266	15.058	7.3755	5.1077	2.6548	1.7796	1.4047	1.2181	1.1207	1.068	1.0387	1.0222
3.5	λ	0.05	0.2	0.5	0.5	0.8	0.8	1	1	1	1	1	1
	L	1.88	2.343	2.467	2.467	2.458	2.458	2.452	2.452	2.452	2.452	2.452	2.452
	$ARL_{\min}$	38.978	12.429	5.9485	4.1311	2.1855	1.5353	1.2617	1.1323	1.0687	1.0361	1.0192	1.0102
4	λ	0.05	0.2	0.5	0.8	0.8	0.8	1	1	1	1	1	1
	L	1.88	2.343	2.467	2.458	2.458	2.458	2.452	2.452	2.452	2.452	2.452	2.452
	$ARL_{\min}$	35.108	10.715	5.0291	3.518	1.9065	1.3929	1.1811	1.0868	1.0425	1.021	1.0105	1.0052
5	λ	0.05	0.3	0.5	0.8	0.8	1	1	1	1	1	1	1
	L	1.88	2.42	2.467	2.458	2.458	2.452	2.452	2.452	2.452	2.452	2.452	2.452
	$ARL_{\min}$	29.838	8.492	3.9562	2.7546	1.5969	1.2375	1.1	1.0435	1.0192	1.0086	1.0038	1.0017
10	λ	0.1	0.5	0.8	0.8	1	1	1	1	1	1	1	1
	L	2.144	2.467	2.458	2.458	2.452	2.452	2.452	2.452	2.452	2.452	2.452	2.452
	$ARL_{\min}$	19.113	4.7313	2.2483	1.6837	1.1835	1.0547	1.017	1.0053	1.0017	1.0005	1.0002	1.0001

Table A-2 The optimal design schemes of EWMA chart with transformed Weibull data
In control ARL=300, $\beta_0 = 1$

Scale Shift (β_1/β_0)		Shape shift η_1/η_0											
		0.2	0.5	0.8	1	1.5	2	2.5	3	3.5	4	4.5	5
0.1	λ	0.02	0.1	0.2	0.3	0.4	0.5	0.8	1	1	1	1	0.8
	L	2.033	2.607	2.75	2.793	2.801	2.792	2.732	2.713	2.713	2.713	2.713	2.732
	$ARL_{\min}$	36.291	11.127	6.1167	4.693	2.8951	2.1479	1.7768	1.2924	1.0092	1	1	1
0.2	λ	0.02	0.05	0.1	0.2	0.3	0.4	0.5	0.5	0.8	0.8	1	1
	L	2.033	2.396	2.607	2.75	2.793	2.801	2.792	2.792	2.732	2.732	2.713	2.713
	$ARL_{\min}$	55.622	17.796	9.6696	7.3457	4.4071	3.1363	2.4442	2.0798	1.8224	1.5552	1.1433	1.0097
0.3	λ	0.02	0.05	0.1	0.1	0.2	0.3	0.4	0.4	0.5	0.5	0.8	0.8
	L	2.033	2.396	2.607	2.607	2.75	2.793	2.801	2.801	2.792	2.792	2.732	2.732
	$ARL_{\min}$	79.114	25.792	14.147	10.51	6.2762	4.4219	3.4073	2.7607	2.3279	2.083	1.9141	1.6893
0.4	λ	0.02	0.02	0.05	0.1	0.1	0.2	0.2	0.3	0.4	0.4	0.5	0.5
	L	2.033	2.033	2.396	2.607	2.607	2.75	2.75	2.793	2.801	2.801	2.792	2.792
	$ARL_{\min}$	108.98	36.51	19.979	15.184	8.9407	6.1577	4.7195	3.7628	3.1501	2.7194	2.3807	2.1566
0.5	λ	0.02	0.02	0.05	0.05	0.1	0.1	0.2	0.2	0.3	0.3	0.4	0.4
	L	2.033	2.033	2.396	2.396	2.607	2.607	2.75	2.75	2.793	2.793	2.801	2.801
	$ARL_{\min}$	146.46	50.863	28.81	21.45	12.732	8.8507	6.6307	5.267	4.3792	3.7264	3.2579	2.8843
0.6	λ	0.02	0.02	0.02	0.02	0.05	0.1	0.1	0.2	0.2	0.2	0.2	0.3
	L	2.033	2.033	2.033	2.033	2.396	2.607	2.607	2.75	2.75	2.75	2.75	2.793
	$ARL_{\min}$	190.63	73.677	41.758	32.201	18.902	13.039	9.7668	7.8852	6.3598	5.3776	4.7017	4.1043
0.7	λ	0.02	0.02	0.02	0.02	0.05	0.05	0.05	0.1	0.1	0.1	0.2	0.2
	L	2.033	2.033	2.033	2.033	2.396	2.396	2.396	2.607	2.607	2.607	2.75	2.75
	$ARL_{\min}$	236.58	112.37	64.399	49.132	30.255	20.678	15.733	12.25	10.044	8.5591	7.3744	6.381
0.8	λ	0.02	0.02	0.02	0.02	0.02	0.02	0.05	0.05	0.05	0.05	0.1	0.1
	L	2.033	2.033	2.033	2.033	2.033	2.033	2.396	2.396	2.396	2.396	2.607	2.607
	$ARL_{\min}$	275.22	177.98	112.24	86.668	53.049	37.645	28.576	22.433	18.461	15.715	13.352	11.59
0.9	λ	0.02	0.02	0.02	0.02	0.02	0.02	0.02	0.02	0.02	0.02	0.02	0.05
	L	2.033	2.033	2.033	2.033	2.033	2.033	2.033	2.033	2.033	2.033	2.033	2.396
	$ARL_{\min}$	297.39	264.44	216.7	186.24	128.17	92.75	70.977	56.864	47.202	40.265	35.085	30.904
1.2	λ	0.02	0.02	0.02	0.02	0.02	0.05	0.05	0.1	0.1	0.2	0.2	0.3
	L	2.033	2.033	2.033	2.033	2.033	2.396	2.396	2.607	2.607	2.75	2.75	2.793
	$ARL_{\min}$	265.14	181.88	121.13	95.154	58.568	39.577	28.809	21.68	17.043	13.638	11.141	9.2668
1.5	λ	0.02	0.02	0.05	0.05	0.1	0.2	0.4	0.5	0.5	0.8	0.8	0.8
	L	2.033	2.033	2.396	2.396	2.607	2.75	2.801	2.792	2.792	2.732	2.732	2.732

	ARL_{min}	196.33	84.174	46.756	34.018	18.359	11.364	7.6659	5.455	4.1296	3.2257	2.6223	2.2133
1.8	λ	0.02	0.02	0.05	0.1	0.3	0.5	0.8	0.8	0.8	0.8	0.8	0.8
	L	2.033	2.033	2.396	2.607	2.793	2.792	2.732	2.732	2.732	2.732	2.732	2.732
	ARL_{min}	148.8	53.563	27.568	19.362	9.8452	5.8158	3.8862	2.7794	2.1645	1.7928	1.5543	1.3947
2	λ	0.02	0.05	0.1	0.2	0.4	0.5	0.8	0.8	0.8	0.8	1	1
	L	2.033	2.396	2.607	2.75	2.801	2.792	2.732	2.732	2.732	2.732	2.713	2.713
	ARL_{min}	127.49	42.552	21.216	14.906	7.3109	4.3028	2.865	2.1298	1.7221	1.4774	1.3204	1.2172
2.5	λ	0.02	0.05	0.2	0.3	0.5	0.8	0.8	0.8	1	1	1	1
	L	2.033	2.396	2.75	2.793	2.792	2.732	2.732	2.732	2.713	2.713	2.713	2.713
	ARL_{min}	94.602	28.601	13.517	9.1815	4.3687	2.6031	1.8558	1.4907	1.2899	1.1747	1.1072	1.0665
3	λ	0.02	0.1	0.3	0.4	0.8	0.8	0.8	1	1	1	1	1
	L	2.033	2.607	2.793	2.801	2.732	2.732	2.732	2.713	2.713	2.713	2.713	2.713
	ARL_{min}	76.507	21.534	9.9022	6.6047	3.1334	1.9657	1.4921	1.2623	1.1439	1.0807	1.0458	1.0262
3.5	λ	0.02	0.1	0.3	0.5	0.8	0.8	1	1	1	1	1	1
	L	2.033	2.607	2.793	2.792	2.732	2.732	2.713	2.713	2.713	2.713	2.713	2.713
	ARL_{min}	65.242	17.539	7.8285	5.1652	2.4969	1.6551	1.3157	1.158	1.0816	1.0428	1.0227	1.012
4	λ	0.02	0.2	0.4	0.5	0.8	0.8	1	1	1	1	1	1
	L	2.033	2.75	2.801	2.792	2.732	2.732	2.713	2.713	2.713	2.713	2.713	2.713
	ARL_{min}	57.582	14.906	6.4919	4.3028	2.1298	1.4774	1.2172	1.1033	1.0504	1.0249	1.0124	1.0062
5	λ	0.05	0.2	0.5	0.8	0.8	1	1	1	1	1	1	1
	L	2.396	2.75	2.792	2.732	2.732	2.713	2.713	2.713	2.713	2.713	2.713	2.713
	ARL_{min}	47.269	11.513	4.9125	3.2716	1.7328	1.286	1.1191	1.0516	1.0228	1.0101	1.0045	1.002
10	λ	0.05	0.5	0.8	0.8	1	1	1	1	1	1	1	1
	L	2.396	2.792	2.732	2.732	2.713	2.713	2.713	2.713	2.713	2.713	2.713	2.713
	ARL_{min}	28.393	6.0504	2.5807	1.843	1.22	1.0649	1.0201	1.0063	1.002	1.0006	1.0002	1.0001

Table A-3 The optimal design schemes of EWMA chart with transformed Weibull data
In control ARL=370.4, $\beta_0 = 1$

Scale Shift (β_1/β_0)		Shape shift η_1/η_0											
		0.2	0.5	0.8	1	1.5	2	2.5	3	3.5	4	4.5	5
0.1	λ	0.02	0.1	0.2	0.2	0.4	0.5	0.8	1	1	1	1	0.8
	L	2.136	2.688	2.82	2.82	2.861	2.848	2.779	2.758	2.758	2.758	2.758	2.779
	$ARL_{\min}$	38.814	11.688	6.3839	4.867	3.0006	2.2008	1.865	1.4696	1.0279	1	1	1
0.2	λ	0.02	0.05	0.1	0.2	0.3	0.4	0.5	0.5	0.8	0.8	1	1
	L	2.136	2.487	2.688	2.82	2.857	2.861	2.848	2.848	2.779	2.779	2.758	2.758
	$ARL_{\min}$	60.16	18.789	10.124	7.7071	4.5923	3.258	2.5295	2.1183	1.9137	1.6541	1.2548	1.0291
0.3	λ	0.02	0.05	0.1	0.1	0.2	0.3	0.3	0.4	0.5	0.5	0.5	0.8
	L	2.136	2.487	2.688	2.688	2.82	2.857	2.857	2.861	2.848	2.848	2.848	2.779
	$ARL_{\min}$	86.651	27.498	14.96	11.024	6.555	4.6082	3.5288	2.8583	2.4029	2.1222	2.013	1.7766
0.4	λ	0.02	0.02	0.05	0.05	0.1	0.2	0.2	0.3	0.4	0.4	0.5	0.5
	L	2.136	2.136	2.487	2.487	2.688	2.82	2.82	2.857	2.861	2.861	2.848	2.848
	$ARL_{\min}$	121.16	39.053	21.151	16.037	9.3449	6.4279	4.895	3.9031	3.2727	2.8148	2.4606	2.2109
0.5	λ	0.02	0.02	0.05	0.05	0.1	0.1	0.2	0.2	0.3	0.3	0.4	0.4
	L	2.136	2.136	2.487	2.487	2.688	2.688	2.82	2.82	2.857	2.857	2.861	2.861
	$ARL_{\min}$	165.84	54.865	30.821	22.749	13.422	9.2489	6.9358	5.4764	4.5624	3.8643	3.3882	2.9892
0.6	λ	0.02	0.02	0.02	0.02	0.05	0.1	0.1	0.1	0.2	0.2	0.2	0.3
	L	2.136	2.136	2.136	2.136	2.487	2.688	2.688	2.688	2.82	2.82	2.82	2.857
	$ARL_{\min}$	220.67	80.469	44.807	34.354	19.985	13.755	10.228	8.2278	6.6446	5.5942	4.8761	4.2678
0.7	λ	0.02	0.02	0.02	0.02	0.05	0.05	0.05	0.1	0.1	0.1	0.2	0.2
	L	2.136	2.136	2.136	2.136	2.487	2.487	2.487	2.688	2.688	2.688	2.82	2.82
	$ARL_{\min}$	280.57	125.13	69.99	52.945	32.419	21.91	16.568	12.899	10.525	8.9382	7.7381	6.6675
0.8	λ	0.02	0.02	0.02	0.02	0.02	0.02	0.05	0.05	0.05	0.05	0.1	0.1
	L	2.136	2.136	2.136	2.136	2.136	2.136	2.487	2.487	2.487	2.487	2.688	2.688
	$ARL_{\min}$	333.65	204.71	124.99	95.292	57.294	40.294	30.563	23.821	19.508	16.548	14.094	12.187
0.9	λ	0.02	0.02	0.02	0.02	0.02	0.02	0.02	0.02	0.02	0.02	0.02	0.05
	L	2.136	2.136	2.136	2.136	2.136	2.136	2.136	2.136	2.136	2.136	2.136	2.487
	$ARL_{\min}$	365.72	318.55	254.26	215.1	143.84	102.29	77.41	61.546	50.809	43.166	37.496	33.139
1.2	λ	0.02	0.02	0.02	0.02	0.02	0.05	0.05	0.1	0.1	0.2	0.2	0.3
	L	2.136	2.136	2.136	2.136	2.136	2.487	2.487	2.688	2.688	2.82	2.82	2.857
	$ARL_{\min}$	322.02	211.18	135.93	105.2	63.387	42.625	30.7	23.08	18.01	14.429	11.715	9.7414
1.5	λ	0.02	0.02	0.05	0.05	0.1	0.2	0.3	0.5	0.5	0.8	0.8	0.8

	L	2.136	2.136	2.487	2.487	2.688	2.82	2.857	2.848	2.848	2.779	2.779	2.779
	ARL_{min}	229.79	92.473	50.686	36.442	19.442	11.956	8.0243	5.6862	4.2743	3.3266	2.6897	2.2604
1.8	λ	0.02	0.02	0.05	0.1	0.2	0.5	0.5	0.8	0.8	0.8	0.8	0.8
	L	2.136	2.136	2.487	2.688	2.82	2.848	2.848	2.779	2.779	2.779	2.779	2.779
	ARL_{min}	169.61	57.798	29.34	20.538	10.348	6.0728	4.0182	2.8552	2.2092	1.8211	1.5731	1.4076
2	λ	0.02	0.05	0.1	0.1	0.4	0.5	0.8	0.8	0.8	0.8	1	1
	L	2.136	2.487	2.688	2.688	2.861	2.848	2.779	2.779	2.779	2.779	2.758	2.758
	ARL_{min}	143.58	45.956	22.57	15.814	7.6641	4.458	2.9454	2.1729	1.7475	1.4933	1.3308	1.2239
2.5	λ	0.02	0.05	0.2	0.3	0.5	0.8	0.8	0.8	1	1	1	1
	L	2.136	2.487	2.82	2.857	2.848	2.779	2.779	2.779	2.758	2.758	2.758	2.758
	ARL_{min}	104.56	30.472	14.297	9.6492	4.5279	2.6695	1.8868	1.5071	1.2992	1.18	1.1104	1.0685
3	λ	0.02	0.1	0.2	0.4	0.8	0.8	0.8	1	1	1	1	1
	L	2.136	2.688	2.82	2.861	2.779	2.779	2.779	2.758	2.758	2.758	2.758	2.758
	ARL_{min}	83.676	22.92	10.405	6.9041	3.2289	2.0015	1.5085	1.2706	1.1483	1.0831	1.0472	1.027
3.5	λ	0.02	0.1	0.3	0.5	0.8	0.8	1	1	1	1	1	1
	L	2.136	2.688	2.857	2.848	2.779	2.779	2.758	2.758	2.758	2.758	2.758	2.758
	ARL_{min}	70.887	18.549	8.19	5.3763	2.5579	1.6778	1.326	1.1628	1.084	1.044	1.0233	1.0124
4	λ	0.02	0.1	0.4	0.5	0.8	0.8	1	1	1	1	1	1
	L	2.136	2.688	2.861	2.848	2.779	2.779	2.758	2.758	2.758	2.758	2.758	2.758
	ARL_{min}	62.283	15.814	6.783	4.458	2.1729	1.4933	1.2239	1.1063	1.0518	1.0256	1.0127	1.0063
5	λ	0.05	0.2	0.5	0.8	0.8	1	1	1	1	1	1	1
	L	2.487	2.82	2.848	2.779	2.779	2.758	2.758	2.758	2.758	2.758	2.758	2.758
	ARL_{min}	51.266	12.118	5.1066	3.3752	1.7586	1.2952	1.1226	1.0531	1.0234	1.0104	1.0046	1.0021
10	λ	0.05	0.5	0.8	0.8	1	1	1	1	1	1	1	1
	L	2.487	2.848	2.779	2.779	2.758	2.758	2.758	2.758	2.758	2.758	2.758	2.758
	ARL_{min}	30.244	6.3247	2.646	1.8734	1.2269	1.0668	1.0207	1.0065	1.002	1.0006	1.0002	1.0001

Table A-4 The optimal design schemes of EWMA chart with transformed Weibull data
In control ARL=500, $\beta_0 = 1$

Scale Shift (β_1/β_0)		Shape shift η_1/η_0											
		0.2	0.5	0.8	1	1.5	2	2.5	3	3.5	4	4.5	5
0.1	λ	0.02	0.1	0.2	0.2	0.4	0.5	0.8	0.8	1	1	1	1
	L	2.278	2.798	2.917	2.917	2.944	2.926	2.844	2.844	2.818	2.818	2.818	2.818
	$ARL_{\min}$	42.49	12.50	6.78	5.12	3.16	2.29	1.99	1.66	1.09	1.00	1.00	1.00
0.2	λ	0.02	0.05	0.1	0.1	0.2	0.4	0.5	0.5	0.5	0.8	1	1
	L	2.278	2.610	2.798	2.798	2.917	2.944	2.926	2.926	2.926	2.844	2.818	2.818
	$ARL_{\min}$	66.97	20.21	10.77	8.23	4.85	3.44	2.66	2.19	2.01	1.78	1.51	1.10
0.3	λ	0.02	0.05	0.1	0.1	0.2	0.2	0.3	0.4	0.5	0.5	0.5	0.5
	L	2.278	2.610	2.798	2.798	2.917	2.917	2.946	2.944	2.926	2.926	2.926	2.926
	$ARL_{\min}$	98.27	29.99	16.15	11.76	6.97	4.87	3.70	3.00	2.52	2.19	2.03	2.00
0.4	λ	0.02	0.02	0.05	0.05	0.1	0.2	0.2	0.3	0.4	0.4	0.5	0.5
	L	2.278	2.278	2.610	2.610	2.798	2.917	2.917	2.946	2.944	2.944	2.926	2.926
	$ARL_{\min}$	140.43	42.76	22.83	17.17	9.92	6.83	5.15	4.11	3.45	2.95	2.58	2.30
0.5	λ	0.02	0.02	0.05	0.05	0.1	0.1	0.2	0.2	0.2	0.3	0.3	0.4
	L	2.278	2.278	2.610	2.610	2.798	2.798	2.917	2.917	2.917	2.946	2.946	2.944
	$ARL_{\min}$	197.25	60.82	33.79	24.63	14.43	9.82	7.39	5.78	4.83	4.07	3.56	3.14
0.6	λ	0.02	0.02	0.02	0.02	0.05	0.2	0.1	0.1	0.2	0.2	0.2	0.3
	L	2.278	2.278	2.278	2.278	2.610	2.798	2.798	2.798	2.917	2.917	2.917	2.946
	$ARL_{\min}$	270.67	90.88	49.28	37.47	21.53	14.80	10.88	8.70	7.07	5.91	5.13	4.51
0.7	λ	0.02	0.02	0.02	0.02	0.02	0.05	0.05	0.1	0.1	0.1	0.1	0.2
	L	2.278	2.278	2.278	2.278	2.278	2.610	2.610	2.798	2.798	2.798	2.798	2.917
	$ARL_{\min}$	356.24	145.38	78.47	58.61	35.46	23.68	17.75	13.84	11.21	9.48	8.25	7.09
0.8	λ	0.02	0.02	0.02	0.02	0.02	0.02	0.05	0.05	0.05	0.05	0.1	0.1
	L	2.278	2.278	2.278	2.278	2.278	2.278	2.610	2.610	2.610	2.610	2.798	2.798
	$ARL_{\min}$	437.69	248.85	145.19	108.69	63.64	44.16	33.49	25.83	21.00	17.73	15.18	13.05
0.9	λ	0.02	0.02	0.02	0.02	0.02	0.02	0.02	0.02	0.02	0.02	0.02	0.02
	L	2.278	2.278	2.278	2.278	2.278	2.278	2.278	2.278	2.278	2.278	2.278	2.278
	$ARL_{\min}$	490.51	413.89	317.92	263.02	168.94	117.19	87.24	68.58	56.15	17.42	41.00	36.11
1.2	λ	0.02	0.02	0.02	0.02	0.02	0.05	0.05	0.1	0.1	0.2	0.2	0.2
	L	2.278	2.278	2.278	2.278	2.278	2.610	2.610	2.798	2.798	2.917	2.917	2.917
	$ARL_{\min}$	423.70	259.80	159.28	120.71	70.57	47.16	33.45	25.15	19.42	15.62	12.57	10.42
1.5	λ	0.02	0.02	0.02	0.05	0.1	0.2	0.3	0.5	0.5	0.8	0.8	0.8

	L	2.278	2.278	2.278	2.261	2.798	2.917	2.946	2.926	2.926	2.844	2.844	2.844
	ARL_{min}	286.01	105.16	56.15	40.01	21.03	12.84	8.55	6.03	4.49	3.47	2.79	2.33
1.8	λ	0.02	0.02	0.05	0.1	0.2	0.4	0.5	0.8	0.8	0.8	0.8	0.8
	L	2.278	2.278	2.610	2.798	2.917	2.944	2.93	2.844	2.844	2.844	2.844	2.844
	ARL_{min}	203.21	64.07	31.91	22.27	11.05	6.45	4.21	2.97	2.27	1.86	1.60	1.43
2	λ	0.02	0.05	0.1	0.1	0.3	0.5	0.8	0.8	0.8	0.8	1	1
	L	2.278	2.610	2.798	2.798	2.946	2.926	2.844	2.844	2.844	2.844	2.818	2.818
	ARL_{min}	169.11	51.05	24.57	16.97	8.15	4.69	3.06	2.24	1.78	1.52	1.35	1.23
2.5	λ	0.02	0.05	0.2	0.2	0.5	0.8	0.8	0.8	1	1	1	1
	L	2.278	2.610	2.917	2.917	2.926	2.844	2.844	2.844	2.818	2.818	2.818	2.818
	ARL_{min}	119.92	33.20	15.47	10.33	4.76	2.77	1.93	1.53	1.31	1.19	1.11	1.07
3	λ	0.02	0.1	0.2	0.4	0.8	0.8	0.8	1	1	1	1	1
	L	2.278	2.798	2.917	2.944	2.844	2.844	2.844	2.818	2.818	2.818	2.818	2.818
	ARL_{min}	94.56	24.97	11.11	7.35	3.37	2.05	1.53	1.28	1.15	1.09	1.05	1.03
3.5	λ	0.02	0.1	0.3	0.5	0.8	0.8	1	1	1	1	1	1
	L	2.278	2.798	2.946	2.926	2.844	2.844	2.818	2.818	2.818	2.818	2.818	2.818
	ARL_{min}	79.26	20.03	8.73	5.69	2.65	1.71	1.34	1.17	1.09	1.05	1.02	1.01
4	λ	0.02	0.1	0.4	0.5	0.8	0.8	1	1	1	1	1	1
	L	2.278	2.798	2.944	2.926	2.844	2.844	2.818	2.818	2.818	2.818	2.818	2.818
	ARL_{min}	69.28	16.97	7.21	4.69	2.24	1.52	1.23	1.11	1.05	1.03	1.01	1.01
5	λ	0.02	0.2	0.5	0.8	0.8	1	1	1	1	1	1	1
	L	2.278	2.917	2.926	2.844	2.844	2.818	2.818	2.818	2.818	2.818	2.818	2.818
	ARL_{min}	56.73	13.02	5.39	3.53	1.80	1.31	1.13	1.06	1.02	1.01	1.00	1.00
10	λ	0.05	0.4	0.8	0.8	1	1	1	1	1	1	1	1
	L	2.610	2.944	2.844	2.844	2.818	2.818	2.818	2.818	2.818	2.818	2.818	2.818
	ARL_{min}	32.94	6.71	2.74	1.92	1.24	1.07	1.02	1.01	1.00	1.00	1.00	1.00

Table A-5 The optimal design schemes of EWMA chart with transformed Weibull data
In control ARL=800, $\beta_0 = 1$

Scale Shift (β_1/β_0)		Shape shift η_1/η_0											
		0.2	0.5	0.8	1	1.5	2	2.5	3	3.5	4	4.5	5
0.1	λ	0.02	0.1	0.2	0.2	0.4	0.5	0.5	0.8	1	1	1	1
	L	2.49	2.961	3.062	3.062	3.067	3.042	3.042	2.94	2.906	2.906	2.906	2.906
	$ARL_{\min}$	48.448	13.811	7.4264	5.5225	3.4049	2.4542	2.0287	1.8439	1.3807	1.0173	1	1
0.2	λ	0.02	0.05	0.1	0.1	0.2	0.3	0.4	0.5	0.5	0.8	0.8	1
	L	2.49	2.793	2.961	2.961	3.062	3.079	3.067	3.042	3.042	2.94	2.94	2.906
	$ARL_{\min}$	78.536	22.49	11.812	8.9163	5.224	3.6903	2.8781	2.331	2.0466	1.9361	1.7835	1.3888
0.3	λ	0.02	0.05	0.05	0.1	0.2	0.2	0.3	0.4	0.5	0.5	0.5	0.5
	L	2.49	2.793	2.793	2.961	3.062	3.062	3.079	3.067	3.042	3.042	3.042	3.042
	$ARL_{\min}$	118.97	34.182	17.807	12.957	7.6465	5.2395	3.9767	3.2276	2.72	2.3374	2.0941	2.008
0.4	λ	0.02	0.02	0.05	0.05	0.1	0.2	0.2	0.3	0.3	0.4	0.5	0.5
	L	2.49	2.49	2.793	2.793	2.961	3.062	3.062	3.079	3.079	3.067	3.042	3.042
	$ARL_{\min}$	176.25	48.772	25.583	18.964	10.834	7.4828	5.5568	4.4447	3.7049	3.1742	2.794	2.4683
0.5	λ	0.02	0.02	0.02	0.05	0.1	0.1	0.2	0.2	0.2	0.3	0.3	0.4
	L	2.49	2.49	2.49	2.793	2.961	2.961	3.062	3.062	3.062	3.079	3.079	3.067
	$ARL_{\min}$	257.97	70.853	38.37	27.71	16.082	10.715	8.1405	6.2768	5.1948	4.3958	3.8189	3.3905
0.6	λ	0.02	0.02	0.02	0.02	0.05	0.1	0.1	0.1	0.2	0.2	0.2	0.2
	L	2.49	2.49	2.49	2.49	2.793	2.961	2.961	2.961	3.062	3.062	3.062	3.062
	$ARL_{\min}$	371.26	109.25	56.653	42.47	24.049	16.525	11.943	9.453	7.7623	6.4243	5.5336	4.9046
0.7	λ	0.02	0.02	0.02	0.02	0.02	0.05	0.05	0.1	0.1	0.1	0.1	0.2
	L	2.49	2.49	2.49	2.49	2.49	2.793	2.793	2.961	2.961	2.961	2.961	3.062
	$ARL_{\min}$	515.51	183.16	93.162	68.102	40.096	26.59	19.638	15.392	12.32	10.328	8.9451	7.7919
0.8	λ	0.02	0.02	0.02	0.02	0.02	0.02	0.02	0.05	0.05	0.05	0.05	0.1
	L	2.49	2.49	2.49	2.49	2.49	2.49	2.49	2.793	2.793	2.793	2.793	2.961
	$ARL_{\min}$	667.88	336.64	182.91	132.84	74.361	50.457	38.089	29.151	23.425	19.612	16.914	14.459
0.9	λ	0.02	0.02	0.02	0.02	0.02	0.02	0.02	0.02	0.02	0.02	0.02	0.02
	L	2.49	2.49	2.49	2.49	2.49	2.49	2.49	2.49	2.49	2.49	2.49	2.49
	$ARL_{\min}$	777.62	621.59	449.13	359.03	216.62	144.31	104.5	80.571	65.064	54.388	46.671	40.871
1.2	λ	0.02	0.02	0.02	0.02	0.02	0.02	0.05	0.05	0.1	0.1	0.2	0.2
	L	2.49	2.49	2.49	2.49	2.49	2.49	2.793	2.793	2.961	2.961	3.062	3.062
	$ARL_{\min}$	649.93	356.68	202.52	148.47	82.682	54.971	38.046	28.505	21.749	17.296	14.005	11.476
1.5	λ	0.02	0.02	0.02	0.05	0.1	0.2	0.3	0.4	0.5	0.8	0.8	0.8
	L	2.49	2.49	2.49	2.793	2.961	3.062	3.079	3.067	3.042	2.94	2.94	2.94

	ARL_{min}	400.04	127.51	64.791	46.074	23.673	14.324	9.407	6.5777	4.8301	3.7117	2.9433	2.4354
1.8	λ	0.02	0.02	0.05	0.1	0.2	0.4	0.5	0.8	0.8	0.8	0.8	1
	L	2.49	2.49	2.793	2.961	3.062	3.067	3.042	2.94	2.94	2.94	2.94	2.906
	ARL_{min}	267.53	74.563	36.183	25.161	12.213	7.0388	4.5168	3.1413	2.3755	1.9252	1.6416	1.4541
2	λ	0.02	0.02	0.05	0.1	0.3	0.5	0.8	0.8	0.8	0.8	1	1
	L	2.49	2.49	2.793	2.961	3.079	3.042	2.94	2.94	2.94	2.94	2.906	2.906
	ARL_{min}	216.75	59.019	27.906	18.85	8.9495	5.0562	3.2498	2.3331	1.8407	1.5512	1.3671	1.2474
2.5	λ	0.02	0.05	0.1	0.2	0.5	0.8	0.8	0.8	1	1	1	1
	L	2.49	2.793	2.961	3.062	3.042	2.94	2.94	2.94	2.906	2.906	2.906	2.906
	ARL_{min}	147.39	37.732	17.147	11.368	5.1425	2.9193	2.0008	1.5669	1.3316	1.1986	1.1214	1.0751
3	λ	0.02	0.05	0.2	0.3	0.8	0.8	0.8	1	1	1	1	1
	L	2.49	2.793	3.062	3.079	2.94	2.94	2.94	2.906	2.906	2.906	2.906	2.906
	ARL_{min}	113.5	28.317	12.286	8.0471	3.5928	2.1335	1.5684	1.2996	1.1633	1.0913	1.0517	1.0295
3.5	λ	0.02	0.1	0.3	0.5	0.8	0.8	1	1	1	1	1	1
	L	2.49	2.961	3.079	3.042	2.94	2.94	2.906	2.906	2.906	2.906	2.906	2.906
	ARL_{min}	93.831	22.471	9.621	6.2033	2.7865	1.761	1.3617	1.1794	1.0922	1.0483	1.0255	1.0136
4	λ	0.02	0.1	0.3	0.5	0.8	0.8	1	1	1	1	1	1
	L	2.49	2.961	3.079	3.042	2.94	2.94	2.906	2.906	2.906	2.906	2.906	2.906
	ARL_{min}	81.066	18.85	7.9039	5.0562	2.3331	1.5512	1.2474	1.1169	1.0568	1.028	1.0139	1.0069
5	λ	0.02	0.2	0.5	0.8	0.8	1	1	1	1	1	1	1
	L	2.49	3.062	3.042	2.94	2.94	2.906	2.906	2.906	2.906	2.906	2.906	2.906
	ARL_{min}	65.5	14.54	5.8636	3.771	1.8535	1.3271	1.1349	1.0582	1.0256	1.0114	1.0051	1.0023
10	λ	0.05	0.4	0.8	0.8	1	1	1	1	1	1	1	1
	L	2.793	3.067	2.94	2.94	2.906	2.906	2.906	2.906	2.906	2.906	2.906	2.906
	ARL_{min}	37.419	7.3405	2.8912	1.9854	1.2507	1.0733	1.0226	1.0071	1.0022	1.0007	1.0002	1.0001

Table A-6 The optimal design schemes of EWMA chart with transformed Weibull data
In control ARL=1000, $\beta_0 = 1$

Scale Shift (β_1/β_0)		Shape shift η_1/η_0											
		0.2	0.5	0.8	1	1.5	2	2.5	3	3.5	4	4.5	5
0.1	λ	0.02	0.1	0.2	0.2	0.4	0.5	0.5	0.8	1	1	1	1
	L	2.585	3.035	3.128	3.128	3.124	3.094	3.094	2.983	2.947	2.947	2.947	2.947
	$ARL_{\min}$	51.331	14.46	7.7487	5.7178	3.5303	2.5379	2.0511	1.9068	1.6692	1.0588	1.0001	1
0.2	λ	0.02	0.05	0.1	0.1	0.2	0.3	0.4	0.5	0.5	0.5	0.8	1
	L	2.585	2.876	3.035	3.035	3.128	3.14	3.124	3.094	3.094	3.094	2.983	2.947
	$ARL_{\min}$	84.384	23.606	12.318	9.245	5.4022	3.8083	2.9698	2.4075	2.0771	2.0014	1.8594	1.6814
0.3	λ	0.02	0.05	0.05	0.1	0.2	0.2	0.3	0.4	0.5	0.5	0.5	0.5
	L	2.585	2.876	2.876	3.035	3.128	3.128	3.14	3.124	3.094	3.094	3.094	3.094
	$ARL_{\min}$	129.89	36.306	18.598	13.542	7.9853	5.4186	4.1125	3.3405	2.8192	2.4144	2.1398	2.0172
0.4	λ	0.02	0.02	0.05	0.05	0.1	0.2	0.2	0.3	0.3	0.4	0.5	0.5
	L	2.585	2.585	2.876	2.876	3.035	3.128	3.128	3.14	3.14	3.124	3.094	3.094
	$ARL_{\min}$	195.92	51.682	26.94	19.83	11.276	7.8093	5.7543	4.6114	3.8238	3.2835	2.8983	2.5528
0.5	λ	0.02	0.02	0.02	0.05	0.05	0.1	0.1	0.2	0.2	0.3	0.3	0.4
	L	2.585	2.585	2.585	2.876	2.876	3.035	3.035	3.128	3.128	3.14	3.14	3.124
	$ARL_{\min}$	292.52	75.87	40.451	29.243	16.905	11.149	8.4809	6.519	5.3713	4.5592	3.9448	3.5149
0.6	λ	0.02	0.02	0.02	0.02	0.05	0.05	0.1	0.1	0.2	0.2	0.2	0.2
	L	2.585	2.585	2.585	2.585	2.876	2.876	3.035	3.035	3.128	3.128	3.128	3.128
	$ARL_{\min}$	430.45	118.86	60.264	44.865	25.283	17.274	12.458	9.8119	8.11	6.6762	5.7297	5.0652
0.7	λ	0.02	0.02	0.02	0.02	0.02	0.05	0.05	0.1	0.1	0.1	0.1	0.2
	L	2.585	2.585	2.585	2.585	2.585	2.876	2.876	3.035	3.035	3.035	3.035	3.128
	$ARL_{\min}$	612.67	203.99	100.72	72.832	42.307	28.029	20.55	16.164	12.861	10.739	9.2754	8.1418
0.8	λ	0.02	0.02	0.02	0.02	0.02	0.02	0.02	0.05	0.05	0.05	0.05	0.1
	L	2.585	2.585	2.585	2.585	2.585	2.585	2.585	2.876	2.876	2.876	2.876	3.035
	$ARL_{\min}$	813.93	387.83	203.69	145.73	79.751	53.511	40.149	30.809	24.612	20.523	17.648	15.157
0.9	λ	0.02	0.02	0.02	0.02	0.02	0.02	0.02	0.02	0.02	0.02	0.02	0.02
	L	2.585	2.585	2.585	2.585	2.585	2.585	2.585	2.585	2.585	2.585	2.585	2.585
	$ARL_{\min}$	965.81	751.75	527.87	415.34	243.33	158.9	113.49	86.648	69.486	57.791	49.405	43.141
1.2	λ	0.02	0.02	0.02	0.02	0.02	0.02	0.05	0.05	0.1	0.1	0.2	0.2
	L	2.585	2.585	2.585	2.585	2.585	2.585	2.876	2.876	3.035	3.035	3.128	3.128
	$ARL_{\min}$	794.08	413.07	226.18	163.21	88.765	58.32	40.355	29.995	22.916	18.111	14.727	12.001
1.5	λ	0.02	0.02	0.02	0.05	0.1	0.2	0.3	0.4	0.5	0.8	0.8	0.8

	L	2.585	2.585	2.585	2.876	3.035	3.128	3.14	3.124	3.094	2.983	2.983	2.983
	ARL_{min}	467.38	139.2	69.037	49.173	25.005	15.073	9.8404	6.8428	4.9952	3.8261	3.0176	2.4862
1.8	λ	0.02	0.02	0.05	0.1	0.2	0.4	0.5	0.8	0.8	0.8	0.8	0.8
	L	2.585	2.585	2.876	3.035	3.128	3.124	3.094	2.983	2.983	2.983	2.983	2.983
	ARL_{min}	303.76	79.78	38.322	26.626	12.793	7.3351	4.6642	3.2255	2.4236	1.9549	1.6611	1.4676
2	λ	0.02	0.02	0.05	0.1	0.3	0.5	0.8	0.8	0.8	0.8	1	1
	L	2.585	2.585	2.876	3.035	3.14	3.094	2.983	2.983	2.983	2.983	2.947	2.947
	ARL_{min}	243	62.728	29.349	19.783	9.3492	5.2346	3.3395	2.3794	1.8674	1.5676	1.3777	1.2543
2.5	λ	0.02	0.05	0.1	0.2	0.5	0.8	0.8	0.8	1	1	1	1
	L	2.585	2.876	3.035	3.128	3.094	2.983	2.983	2.983	2.947	2.947	2.947	2.947
	ARL_{min}	161.96	40.013	17.952	11.885	5.326	2.9924	2.0335	1.5838	1.3411	1.204	1.1246	1.0771
3	λ	0.02	0.05	0.2	0.3	0.8	0.8	0.8	1	1	1	1	1
	L	2.585	2.876	3.128	3.14	2.983	2.983	2.983	2.947	2.947	2.947	2.947	2.947
	ARL_{min}	123.29	29.792	12.871	8.3831	3.7006	2.1715	1.5854	1.308	1.1677	1.0936	1.053	1.0303
3.5	λ	0.02	0.1	0.2	0.4	0.8	0.8	1	1	1	1	1	1
	L	2.585	3.035	3.128	3.124	2.983	2.983	2.947	2.947	2.947	2.947	2.947	2.947
	ARL_{min}	101.18	23.698	10.06	6.4507	2.8533	1.7847	1.3721	1.1842	1.0946	1.0495	1.0262	1.0139
4	λ	0.02	0.1	0.3	0.5	0.8	0.8	1	1	1	1	1	1
	L	2.585	3.035	3.14	3.094	2.983	2.983	2.947	2.947	2.947	2.947	2.947	2.947
	ARL_{min}	86.972	19.783	8.2302	5.2346	2.3794	1.5676	1.2543	1.12	1.0583	1.0287	1.0143	1.0071
5	λ	0.02	0.2	0.5	0.8	0.8	1	1	1	1	1	1	1
	L	2.585	3.128	3.094	2.983	2.983	2.947	2.947	2.947	2.947	2.947	2.947	2.947
	ARL_{min}	69.814	15.306	6.0919	3.8886	1.8806	1.3365	1.1385	1.0597	1.0263	1.0117	1.0052	1.0023
10	λ	0.05	0.3	0.8	0.8	1	1	1	1	1	1	1	1
	L	2.876	3.14	2.983	2.983	2.947	2.947	2.947	2.947	2.947	2.947	2.947	2.947
	ARL_{min}	39.67	7.6578	2.963	2.0175	1.2577	1.0752	1.0232	1.0073	1.0023	1.0007	1.0002	1.0001

Table A-7 The optimal design schemes of EWMA chart with transformed Weibull data
In control ARL=2000, $\beta_0 = 1$

Scale Shift (β_1/β_0)		Shape shift η_1/η_0											
		0.2	0.5	0.8	1	1.5	2	2.5	3	3.5	4	4.5	5
0.1	λ	0.02	0.1	0.1	0.2	0.3	0.5	0.5	0.5	0.8	1	1	1
	L	2.862	3.253	3.253	3.321	3.318	3.249	3.249	3.249	3.114	3.067	3.067	3.067
	ARL_{min}	60.629	16.598	8.7378	6.3382	3.8619	2.8159	2.1927	2.0015	1.9515	1.7569	1.075	1.0002
0.2	λ	0.02	0.05	0.1	0.1	0.2	0.3	0.4	0.5	0.5	0.5	0.5	0.8
	L	2.862	3.117	3.253	3.253	3.321	3.318	3.289	3.249	3.249	3.249	3.249	3.114
	ARL_{min}	104.47	27.18	13.956	10.28	5.9646	4.1839	3.2519	2.6673	2.2447	2.023	2.0001	1.9521
0.3	λ	0.02	0.02	0.05	0.1	0.1	0.2	0.3	0.3	0.4	0.5	0.5	0.5
	L	2.862	2.862	3.117	3.253	3.253	3.321	3.318	3.318	3.289	3.249	3.249	3.249
	ARL_{min}	169.81	42.245	21.071	15.459	8.94	5.9839	4.5482	3.6843	3.1004	2.675	2.3457	2.1019
0.4	λ	0.02	0.02	0.05	0.05	0.1	0.1	0.2	0.2	0.3	0.3	0.4	0.5
	L	2.862	2.862	3.117	3.117	3.253	3.253	3.321	3.321	3.318	3.318	3.289	3.249
	ARL_{min}	272.13	61.076	31.35	22.557	12.695	8.7898	6.3815	5.1211	4.2024	3.6302	3.1689	2.8331
0.5	λ	0.02	0.02	0.02	0.05	0.05	0.1	0.1	0.2	0.2	0.2	0.3	0.3
	L	2.862	2.862	2.862	3.117	3.117	3.253	3.253	3.321	3.321	3.321	3.318	3.318
	ARL_{min}	433.57	92.848	47.008	34.279	19.051	12.542	9.3869	7.2996	5.9282	5.0732	4.347	3.8476
0.6	λ	0.02	0.02	0.02	0.02	0.05	0.05	0.1	0.1	0.1	0.2	0.2	0.2
	L	2.862	2.862	2.862	2.862	3.117	3.117	3.253	3.253	3.253	3.321	3.321	3.321
	ARL_{min}	683.62	153.51	72.127	52.482	29.268	19.489	14.127	10.948	9.0456	7.4903	6.3523	5.5688
0.7	λ	0.02	0.02	0.02	0.02	0.02	0.05	0.05	0.05	0.1	0.1	0.1	0.1
	L	2.862	2.862	2.862	2.862	2.862	3.117	3.117	3.117	3.253	3.253	3.253	3.253
	ARL_{min}	1048.2	285.13	127.34	88.755	49.301	32.731	23.43	18.362	14.62	12.05	10.315	9.0725
0.8	λ	0.02	0.02	0.02	0.02	0.02	0.02	0.02	0.05	0.05	0.05	0.05	0.05
	L	2.862	2.862	2.862	2.862	2.862	2.862	2.862	3.117	3.117	3.117	3.117	3.117
	ARL_{min}	1503.1	604.02	284.65	193.63	98.12	63.411	46.637	36.29	28.429	23.397	19.935	17.421
0.9	λ	0.02	0.02	0.02	0.02	0.02	0.02	0.02	0.02	0.02	0.02	0.02	0.02
	L	2.862	2.862	2.862	2.862	2.862	2.862	2.862	2.862	2.862	2.862	2.862	2.862
	ARL_{min}	1895.3	1355.9	873.5	655.17	349.82	213.82	145.68	107.6	84.278	68.916	58.187	50.336
1.2	λ	0.02	0.02	0.02	0.02	0.02	0.02	0.05	0.05	0.1	0.1	0.1	0.2
	L	2.862	2.862	2.862	2.862	2.862	2.862	3.117	3.117	3.253	3.253	3.253	3.321
	ARL_{min}	1477.7	649.77	317.43	217.56	109.46	69.169	48.056	34.806	26.832	20.786	16.793	13.722
1.5	λ	0.02	0.02	0.02	0.02	0.05	0.1	0.2	0.3	0.5	0.8	0.8	0.8
	L	2.862	2.862	2.862	2.862	3.117	3.253	3.321	3.318	3.249	3.114	3.114	3.114
	ARL_{min}	755.55	181.39	83.048	58.877	29.121	17.144	11.095	7.6907	5.535	4.2092	3.2633	2.6523

1.8	λ	0.02	0.02	0.05	0.05	0.2	0.3	0.5	0.8	0.8	0.8	0.8	1
	L	2.862	2.862	3.117	3.117	3.321	3.318	3.249	3.114	3.114	3.114	3.114	3.067
	$ARL_{\min}$	449.25	97.298	45.412	30.818	14.706	8.2367	5.1437	3.5047	2.581	2.0514	1.7238	1.5097
2	λ	0.02	0.02	0.05	0.1	0.2	0.5	0.8	0.8	0.8	0.8	1	1
	L	2.862	2.862	3.117	3.253	3.321	3.249	3.114	3.114	3.114	3.114	3.067	3.067
	$ARL_{\min}$	345.23	74.836	34	22.868	10.563	5.8194	3.6377	2.5307	1.9534	1.6203	1.4105	1.2753
2.5	λ	0.02	0.05	0.1	0.2	0.5	0.8	0.8	0.8	1	1	1	1
	L	2.862	3.117	3.253	3.321	3.249	3.114	3.114	3.114	3.067	3.067	3.067	3.067
	$ARL_{\min}$	215.66	47.609	20.589	13.578	5.9285	3.2341	2.1396	1.6382	1.3703	1.2205	1.1343	1.083
3	λ	0.02	0.05	0.2	0.3	0.8	0.8	0.8	1	1	1	1	1
	L	2.862	3.117	3.321	3.318	3.114	3.114	3.114	3.067	3.067	3.067	3.067	3.067
	$ARL_{\min}$	158.08	34.552	14.804	9.4746	4.0612	2.295	1.64	1.3341	1.1811	1.1009	1.057	1.0325
3.5	λ	0.02	0.05	0.2	0.4	0.8	0.8	1	1	1	1	1	1
	L	2.862	3.117	3.321	3.289	3.114	3.114	3.067	3.067	3.067	3.067	3.067	3.067
	$ARL_{\min}$	126.61	27.748	11.344	7.222	3.0734	1.8611	1.4044	1.199	1.1019	1.0532	1.0281	1.0149
4	λ	0.02	0.1	0.3	0.5	0.8	0.8	1	1	1	1	1	1
	L	2.862	3.253	3.318	3.249	3.114	3.114	3.067	3.067	3.067	3.067	3.067	3.067
	$ARL_{\min}$	107.02	22.868	9.2884	5.8194	2.5307	1.6203	1.2753	1.1293	1.0627	1.0309	1.0153	1.0076
5	λ	0.02	0.1	0.4	0.5	0.8	1	1	1	1	1	1	1
	L	2.862	3.253	3.289	3.249	3.114	3.067	3.067	3.067	3.067	3.067	3.067	3.067
	$ARL_{\min}$	84.068	17.379	6.8149	4.2794	1.9681	1.3652	1.1494	1.0642	1.0282	1.0125	1.0056	1.0025
10	λ	0.05	0.3	0.8	0.8	1	1	1	1	1	1	1	1
	L	3.117	3.318	3.114	3.114	3.067	3.067	3.067	3.067	3.067	3.067	3.067	3.067
	$ARL_{\min}$	47.164	8.5951	3.2001	2.1216	1.279	1.0809	1.0249	1.0078	1.0025	1.0008	1.0002	1.0001

APPENDIX B: OPTIMAL DESIGN SCHEMES OF THE MEWMA CHART WITH RAW GBE DATA

TableB-1 The optimal design scheme when δ=0.1

$\left(\frac{\theta_1'}{\theta_1},\frac{\theta_2'}{\theta_2}\right)$	ARL_0	100	200	370	500	$\left(\frac{\theta_1'}{\theta_1},\frac{\theta_2'}{\theta_2}\right)$	ARL_0	100	200	370	500
(0.1,1)	r	0.1	0.1	0.1	0.1	(1.2,1)	r	0.05	0.05	0.05	0.05
	ARL_{opt}	0.95	1.33	1.66	1.84		ARL_{opt}	10.34	13.27	16.76	18.68
(0.2,1)	r	0.1	0.1	0.1	0.1	(1.5,1)	r	0.1	0.1	0.1	0.1
	ARL_{opt}	1.18	1.62	2.04	2.28		ARL_{opt}	2.82	3.64	4.52	4.97
(0.3,1)	r	0.1	0.1	0.1	0.1	(1.8,1)	r	0.1	0.1	0.1	0.1
	ARL_{opt}	1.48	2.00	2.51	2.76		ARL_{opt}	1.30	1.74	2.18	2.40
(0.4,1)	r	0.1	0.1	0.1	0.1	(2,1)	r	0.1	0.1	0.1	0.1
	ARL_{opt}	1.87	2.54	3.23	3.57		ARL_{opt}	0.90	1.23	1.51	1.71
(0.5,1)	r	0.1	0.1	0.1	0.1	(2.5,1)	r	0.3	0.3	0.3	0.3
	ARL_{opt}	2.54	3.42	4.33	4.76		ARL_{opt}	0.44	0.60	0.78	0.86
(0.6, 1)	r	0.1	0.1	0.05	0.05	(3, 1)	r	0.3	0.3	0.3	0.3
	ARL_{opt}	3.65	4.93	6.10	6.71		ARL_{opt}	0.24	0.35	0.44	0.50
(0.7,1)	r	0.05	0.05	0.05	0.05	(4,1)	r	0.3	0.3	0.3	0.3
	ARL_{opt}	5.78	7.43	9.18	10.17		ARL_{opt}	0.11	0.16	0.21	0.23
(0.8,1)	r	0.05	0.5	0.05	0.05	(5,1)	r	0.3	0.3	0.3	0.3
	ARL_{opt}	10.06	13.16	16.65	18.71		ARL_{opt}	0.07	0.10	0.12	0.14
(0.9,1)	r	0.02	0.02	0.02	0.02	(10,1)	r	0.3	0.3	0.5	0.3
	ARL_{opt}	25.22	33.41	41.64	46.44		ARL_{opt}	0.01	0.02	0.02	0.03
(0.1,0.1)	r	0.05	0.05	0.05	0.02	(1.5,1.5)	r	0.1	0.05	0.05	0.05
	ARL_{opt}	8.95	11.66	14.83	16.54		ARL_{opt}	15.16	20.67	26.85	30.40
(0.2,0.2)	r	0.05	0.05	0.02	0.02	(2,2)	r	0.1	0.1	0.1	0.05
	ARL_{opt}	10.73	14.14	18.19	19.75		ARL_{opt}	6.55	8.59	10.86	11.98
(0.5,0.5)	r	0.02	0.02	0.02	0.02	(5,5)	r	0.3	0.3	0.3	0.1
	ARL_{opt}	21.55	28.02	34.50	37.91		ARL_{opt}	0.86	1.10	1.45	1.62
(0.8,0.8)	r	0.01	0.01	0.01	0.01	(10,10)	r	0.3	0.3	0.3	0.3

	ARL_{opt}	56.99	83.30	114.73	131.30		ARL_{opt}	0.21	0.29	0.36	0.40
(0.8,1.5)	r	0.1	0.1	0.1	0.1	(0.2,5)	r	0.3	0.3	0.3	0.3
	ARL_{opt}	1.61	2.10	2.69	2.96		ARL_{opt}	0.04	0.07	0.08	0.10
(0.5,2)	r	0.1	0.3	0.3	0.1	(0.1,10)	r	0.3	0.3	0.3	0.3
	ARL_{opt}	0.41	0.57	0.75	0.85		ARL_{opt}	0.01	0.01	0.02	0.02

Table B-2 The optimal design scheme when δ=0.3

$\left(\frac{\theta_1'}{\theta_1},\frac{\theta_2'}{\theta_2}\right)$	ARL_0	100	200	370	500	$\left(\frac{\theta_1'}{\theta_1},\frac{\theta_2'}{\theta_2}\right)$	ARL_0	100	200	370	500
(0.1,1)	r	0.1	0.1	0.05	0.05	(1.2,1)	r	0.05	0.02	0.02	0.02
	ARL_{opt}	3.95	5.49	6.64	7.36		ARL_{opt}	31.11	42.82	53.98	60.45
(0.2,1)	r	0.1	0.05	0.05	0.05	(1.5,1)	r	0.1	0.05	0.05	0.05
	ARL_{opt}	4.82	6.46	7.85	8.66		ARL_{opt}	10.30	13.28	16.40	17.80
(0.3,1)	r	0.1	0.05	0.05	0.05	(1.8,1)	r	0.1	0.05	0.1	0.05
	ARL_{opt}	6.04	7.85	9.59	10.48		ARL_{opt}	5.46	7.14	8.56	9.27
(0.4,1)	r	0.05	0.05	0.05	0.05	(2,1)	r	0.1	0.1	0.1	0.1
	ARL_{opt}	7.63	9.81	12.09	13.41		ARL_{opt}	3.92	5.18	6.24	6.82
(0.5,1)	r	0.05	0.05	0.05	0.05	(2.5,1)	r	0.1	0.1	0.1	0.1
	ARL_{opt}	9.92	12.89	16.06	17.86		ARL_{opt}	2.17	2.84	3.38	3.68
(0.6, 1)	r	0.05	0.05	0.02	0.02	(3, 1)	r	0.1	0.1	0.1	0.1
	ARL_{opt}	13.60	18.00	22.64	24.50		ARL_{opt}	1.41	1.79	2.21	2.40
(0.7,1)	r	0.05	0.02	0.02	0.02	(4,1)	r	0.3	0.3	0.3	0.3
	ARL_{opt}	20.48	26.80	32.58	35.76		ARL_{opt}	0.71	0.93	1.16	1.24
(0.8,1)	r	0.02	0.02	0.02	0.01	(5,1)	r	0.3	0.3	0.3	0.3
	ARL_{opt}	32.69	44.72	57.34	63.80		ARL_{opt}	0.43	0.55	0.67	0.73
(0.9,1)	r	0.01	0.01	0.01	0.01	(10,1)	r	0.3	0.3	0.3	0.3
	ARL_{opt}	60.79	94.41	129.08	151.28		ARL_{opt}	0.09	0.11	0.14	0.16
(0.1,0.1)	r	0.05	0.05	0.05	0.05	(1.5,1.5)	r	0.1	0.05	0.05	0.05
	ARL_{opt}	8.37	10.76	13.34	14.78		ARL_{opt}	13.64	19.35	24.33	27.27
(0.2,0.2)	r	0.05	0.05	0.05	0.05	(2,2)	r	0.1	0.1	0.1	0.1
	ARL_{opt}	10.09	13.03	16.34	18.24		ARL_{opt}	5.83	7.76	9.44	10.61
(0.5,0.5)	r	0.02	0.02	0.02	0.02	(5,5)	r	0.3	0.3	0.3	0.3
	ARL_{opt}	20.48	26.44	32.11	35.18		ARL_{opt}	0.70	0.90	1.12	1.23
(0.8,0.8)	r	0.01	0.01	0.01	0.01	(10,10)	r	0.3	0.3	0.3	0.3
	ARL_{opt}	54.82	80.30	107.61	123.11		ARL_{opt}	0.17	0.22	0.27	0.29
(0.8,1.5)	r	0.1	0.05	0.05	0.05	(0.2,5)	r	0.3	0.3	0.3	0.3
	ARL_{opt}	6.98	8.98	10.74	11.79		ARL_{opt}	0.27	0.37	0.49	0.51
(0.5,2)	r	0.1	0.1	0.1	0.1	(0.1,10)	r	0.3	0.3	0.5	0.3
	ARL_{opt}	2.19	2.87	3.45	3.73		ARL_{opt}	0.07	0.09	0.12	0.13

Table B-3 The optimal design scheme when δ=0.5

$\left(\frac{\theta_1'}{\theta_1},\frac{\theta_2'}{\theta_2}\right)$	ARL_0	100	200	370	500	$\left(\frac{\theta_1'}{\theta_1},\frac{\theta_2'}{\theta_2}\right)$	ARL_0	100	200	370	500
(0.1,1)	r	0.1	0.05	0.05	0.05	(1.2,1)	r	0.05	0.05	0.02	0.02
	ARL_{opt}	6.38	8.27	10.09	11.10		ARL_{opt}	40.53	57.68	78.12	87.93
(0.2,1)	r	0.05	0.05	0.05	0.05	(1.5,1)	r	0.1	0.05	0.05	0.05
	ARL_{opt}	7.69	9.79	12.10	13.34		ARL_{opt}	14.84	19.19	23.86	26.34
(0.3,1)	r	0.05	0.05	0.05	0.05	(1.8,1)	r	0.1	0.1	0.05	0.05
	ARL_{opt}	9.40	12.03	14.94	16.76		ARL_{opt}	8.08	10.58	12.75	13.78
(0.4,1)	r	0.05	0.05	0.05	0.02	(2,1)	r	0.1	0.1	0.1	0.1
	ARL_{opt}	11.73	15.31	19.36	21.57		ARL_{opt}	5.97	7.62	9.37	10.17
(0.5,1)	r	0.05	0.05	0.02	0.02	(2.5,1)	r	0.1	0.1	0.1	0.1
	ARL_{opt}	15.22	20.55	25.41	27.54		ARL_{opt}	3.49	4.32	5.24	5.67
(0.6, 1)	r	0.02	0.02	0.02	0.02	(3, 1)	r	0.1	0.1	0.1	0.1
	ARL_{opt}	21.05	27.92	34.09	37.35		ARL_{opt}	2.31	2.94	3.44	3.76
(0.7,1)	r	0.02	0.02	0.02	0.02	(4,1)	r	0.3	0.3	0.3	0.3
	ARL_{opt}	29.48	39.80	50.78	56.63		ARL_{opt}	1.24	1.51	1.85	2.01
(0.8,1)	r	0.01	0.01	0.01	0.01	(5,1)	r	0.3	0.3	0.3	0.3
	ARL_{opt}	45.07	64.86	83.91	94.95		ARL_{opt}	0.72	0.97	1.13	1.21
(0.9,1)	r	0.01	0.01	0.01	0.01	(10,1)	r	0.3	0.5	0.3	0.3
	ARL_{opt}	75.02	124.59	184.34	216.75		ARL_{opt}	0.18	0.23	0.26	0.29
(0.1,0.1)	r	0.5	0.05	0.05	0.05	(1.5,1.5)	r	0.1	0.1	0.05	0.05
	ARL_{opt}	7.52	9.54	11.63	12.85		ARL_{opt}	12.40	17.12	22.02	24.92
(0.2,0.2)	r	0.05	0.05	0.05	0.05	(2,2)	r	0.1	0.1	0.1	0.1
	ARL_{opt}	9.06	11.51	14.12	15.70		ARL_{opt}	5.17	6.81	8.36	9.02
(0.5,0.5)	r	0.02	0.02	0.02	0.02	(5,5)	r	0.5	0.3	0.3	0.3
	ARL_{opt}	18.85	24.21	29.39	31.91		ARL_{opt}	0.53	0.71	0.85	0.96
(0.8,0.8)	r	0.01	0.01	0.01	0.01	(10,10)	r	0.5	0.3	0.3	0.3
	ARL_{opt}	52.08	74.69	98.08	111.23		ARL_{opt}	0.11	0.16	0.18	0.21
(0.8,1.5)	r	0.05	0.05	0.05	0.05	(0.2,5)	r	0.3	0.3	0.3	0.3
	ARL_{opt}	11.43	14.56	17.55	19.79		ARL_{opt}	0.55	0.69	0.90	0.96
(0.5,2)	r	0.1	0.1	0.1	0.1	(0.1,10)	r	0.3	0.3	0.3	0.3
	ARL_{opt}	3.90	5.02	6.05	6.62		ARL_{opt}	0.13	0.18	0.23	0.25

Table B-4 The optimal design scheme when δ=0.8

$\left(\frac{\theta_1'}{\theta_1},\frac{\theta_2'}{\theta_2}\right)$	ARL_0	100	200	370	500	$\left(\frac{\theta_1'}{\theta_1},\frac{\theta_2'}{\theta_2}\right)$	ARL_0	100	200	370	500
(0.1,1)	r	0.05	0.05	0.05	0.05	(1.2,1)	r	0.1	0.05	0.02	0.02
	ARL_{opt}	8.13	10.38	12.67	13.99		ARL_{opt}	42.94	67.02	91.16	106.37
(0.2,1)	r	0.05	0.05	0.05	0.05	(1.5,1)	r	0.1	0.05	0.05	0.05
	ARL_{opt}	9.63	12.44	15.42	17.11		ARL_{opt}	17.13	23.19	28.76	32.00
(0.3,1)	r	0.05	0.05	0.05	0.05	(1.8,1)	r	0.1	0.1	0.1	0.05
	ARL_{opt}	11.87	15.47	19.33	21.78		ARL_{opt}	9.62	12.61	15.47	16.83
(0.4,1)	r	0.05	0.05	0.02	0.02	(2,1)	r	0.1	0.1	0.1	0.1
	ARL_{opt}	14.89	19.94	24.72	26.98		ARL_{opt}	7.32	9.25	11.43	12.50
(0.5,1)	r	0.05	0.02	0.02	0.02	(2.5,1)	r	0.1	0.1	0.1	0.1
	ARL_{opt}	19.62	25.87	31.43	34.58		ARL_{opt}	4.21	5.26	6.27	6.81
(0.6, 1)	r	0.02	0.02	0.02	0.02	(3, 1)	r	0.3	0.1	0.1	0.1
	ARL_{opt}	25.64	34.41	42.46	47.33		ARL_{opt}	2.73	3.58	4.40	4.62
(0.7,1)	r	0.01	0.02	0.01	0.01	(4,1)	r	0.3	0.3	0.3	0.3
	ARL_{opt}	35.98	49.65	63.26	70.69		ARL_{opt}	1.48	1.89	2.30	2.54
(0.8,1)	r	0.01	0.01	0.01	0.01	(5,1)	r	0.3	0.3	0.3	0.3
	ARL_{opt}	52.97	77.80	103.91	118.18		ARL_{opt}	0.95	1.22	1.41	1.55
(0.9,1)	r	0.01	0.01	0.01	0.01	(10,1)	r	0.3	0.3	0.3	0.3
	ARL_{opt}	82.50	139.21	218.83	262.67		ARL_{opt}	0.24	0.30	0.35	0.39
(0.1,0.1)	r	0.1	0.05	0.05	0.05	(1.5,1.5)	r	0.1	0.1	0.05	0.05
	ARL_{opt}	5.80	7.84	9.34	10.23		ARL_{opt}	10.71	14.41	18.71	20.78
(0.2,0.2)	r	0.1	0.05	0.05	0.05	(2,2)	r	0.3	0.1	0.1	0.1
	ARL_{opt}	7.27	9.36	11.29	12.36		ARL_{opt}	4.14	5.49	6.81	7.50
(0.5,0.5)	r	0.05	0.05	0.02	0.02	(5,5)	r	0.3	0.5	0.5	0.3
	ARL_{opt}	15.28	19.99	24.34	26.53		ARL_{opt}	0.33	0.45	0.55	0.61
(0.8,0.8)	r	0.01	0.01	0.01	0.01	(10,10)	r	0.5	0.5	0.5	0.3
	ARL_{opt}	45.48	64.70	84.19	92.56		ARL_{opt}	0.05	0.07	0.09	0.10
(0.8,1.5)	r	0.1	0.05	0.05	0.05	(0.2,5)	r	0.3	0.3	0.3	0.3
	ARL_{opt}	15.98	20.47	25.12	27.76		ARL_{opt}	0.83	1.04	1.28	1.37
(0.5,2)	r	0.1	0.1	0.1	0.1	(0.1,10)	r	0.5	0.3	0.3	0.3
	ARL_{opt}	5.72	7.44	9.10	9.89		ARL_{opt}	0.21	0.25	0.32	0.35

Table B-5 The optimal design scheme when δ =1

$\left(\frac{\theta_1'}{\theta_1},\frac{\theta_2'}{\theta_2}\right)$	ARL_0	100	200	370	500	$\left(\frac{\theta_1'}{\theta_1},\frac{\theta_2'}{\theta_2}\right)$	ARL_0	100	200	370	500
(0.1,1)	r	0.05	0.05	0.05	0.05	(1.2,1)	r	0.1	0.05	0.02	0.02
	ARL_{opt}	8.36	10.62	13.09	14.33		ARL_{opt}	43.40	67.00	93.40	107.21
(0.2,1)	r	0.05	0.05	0.05	0.05	(1.5,1)	r	0.1	0.05	0.05	0.05
	ARL_{opt}	9.94	12.76	15.91	17.53		ARL_{opt}	17.69	23.55	29.75	32.49
(0.3,1)	r	0.05	0.05	0.05	0.05	(1.8,1)	r	0.1	0.1	0.1	0.05
	ARL_{opt}	12.08	15.82	20.05	22.42		ARL_{opt}	9.73	12.66	15.76	17.16
(0.4,1)	r	0.05	0.05	0.02	0.02	(2,1)	r	0.1	0.1	0.1	0.1
	ARL_{opt}	15.28	20.25	25.34	27.58		ARL_{opt}	7.48	9.29	11.55	12.45
(0.5,1)	r	0.05	0.02	0.02	0.02	(2.5,1)	r	0.1	0.1	0.1	0.1
	ARL_{opt}	20.15	26.61	32.27	35.48		ARL_{opt}	4.37	5.46	6.46	7.13
(0.6, 1)	r	0.02	0.02	0.02	0.02	(3, 1)	r	0.3	0.3	0.1	0.1
	ARL_{opt}	25.94	35.16	43.97	48.28		ARL_{opt}	2.82	3.58	4.32	4.65
(0.7,1)	r	0.02	0.01	0.01	0.01	(4,1)	r	0.3	0.3	0.3	0.3
	ARL_{opt}	36.03	50.74	65.37	72.03		ARL_{opt}	1.51	1.92	2.26	2.48
(0.8,1)	r	0.01	0.01	0.01	0.01	(5,1)	r	0.3	0.3	0.3	0.3
	ARL_{opt}	53.23	78.66	106.57	120.93		ARL_{opt}	0.97	1.21	1.43	1.57
(0.9,1)	r	0.01	0.01	0.01	0.01	(10,1)	r	0.3	0.3	0.3	0.3
	ARL_{opt}	81.41	142.16	220.42	274.48		ARL_{opt}	0.24	0.30	0.34	0.40
(0.1,0.1)	r	0.1	0.1	0.05	0.05	(1.5,1.5)	r	0.1	0.1	0.1	0.05
	ARL_{opt}	4.93	6.35	8.08	8.77		ARL_{opt}	9.67	12.82	16.40	18.42
(0.2,0.2)	r	0.1	0.05	0.05	0.05	(2,2)	r	0.3	0.1	0.1	0.1
	ARL_{opt}	6.05	8.01	9.69	10.49		ARL_{opt}	3.57	4.73	5.91	6.45
(0.5,0.5)	r	0.05	0.05	0.05	0.02	(5,5)	r	0.3	0.3	0.3	0.3
	ARL_{opt}	13.05	16.72	21.11	23.09		ARL_{opt}	0.22	0.31	0.40	0.42
(0.8,0.8)	r	0.01	0.01	0.01	0.01	(10,10)	r	0.3	0.5	0.5	0.5
	ARL_{opt}	41.27	56.78	73.05	81.43		ARL_{opt}	0.03	0.04	0.04	0.05
(0.8,1.5)	r	0.1	0.05	0.05	0.05	(0.2,5)	r	0.3	0.3	0.3	0.3
	ARL_{opt}	17.74	22.74	28.14	31.34		ARL_{opt}	0.90	1.17	1.45	1.50
(0.5,2)	r	0.1	0.1	0.1	0.05	(0.1,10)	r	0.5	0.5	0.5	0.3
	ARL_{opt}	6.66	8.45	10.36	11.25		ARL_{opt}	0.24	0.30	0.36	0.37

APPENDIX C: OPTIMAL DESIGN SCHEMES OF THE MEWMA CHART WITH TRANSFORMED GBE DATA

Table C-1 The optimal design scheme when δ =0.1

$\left(\frac{\theta_1'}{\theta_1},\frac{\theta_2'}{\theta_2}\right)$	ARL_0	100	200	370	500	$\left(\frac{\theta_1'}{\theta_1},\frac{\theta_2'}{\theta_2}\right)$	ARL_0	100	200	370	500
(0.1,1)	r	0.1	0.1	0.3	0.3	(1.2,1)	r	0.1	0.1	0.1	0.1
	ARL_{opt}	0.00	0.00	0.00	0.00		ARL_{opt}	6.73	8.31	9.68	10.53
(0.2,1)	r	0.1	0.3	0.3	0.5	(1.5,1)	r	0.3	0.3	0.3	0.3
	ARL_{opt}	0.00	0.00	0.00	0.00		ARL_{opt}	0.93	1.29	1.64	1.83
(0.3,1)	r	0.5	0.5	0.3	0.3	(1.8,1)	r	0.5	0.3	0.3	0.3
	ARL_{opt}	0.00	0.00	0.00	0.00		ARL_{opt}	0.14	0.27	0.39	0.45
(0.4,1)	r	0.5	0.5	0.5	0.3	(2,1)	r	0.5	0.3	0.3	0.3
	ARL_{opt}	0.00	0.01	0.04	0.06		ARL_{opt}	0.04	0.08	0.15	0.18
(0.5,1)	r	0.5	0.5	0.3	0.3	(2.5,1)	r	0.5	0.3	0.5	0.3
	ARL_{opt}	0.09	0.19	0.32	0.38		ARL_{opt}	0.00	0.00	0.01	0.02
(0.6, 1)	r	0.3	0.3	0.3	0.3	(3, 1)	r	0.3	0.5	0.5	0.5
	ARL_{opt}	0.53	0.79	1.08	1.22		ARL_{opt}	0.00	0.00	0.00	0.00
(0.7,1)	r	0.3	0.3	0.3	0.3	(4,1)	r	0.3	0.3	0.3	0.3
	ARL_{opt}	1.76	2.38	3.10	3.41		ARL_{opt}	0.00	0.00	0.00	0.00
(0.8,1)	r	0.1	0.1	0.1	0.1	(5,1)	r	0.1	0.1	0.3	0.3
	ARL_{opt}	5.25	6.43	7.53	8.01		ARL_{opt}	0.00	0.00	0.00	0.00
(0.9,1)	r	0.02	0.05	0.05	0.05	(10,1)	r	0.02	0.05	0.1	0.1
	ARL_{opt}	14.50	21.05	25.59	27.93		ARL_{opt}	0.00	0.00	0.00	0.00
(0.1,0.1)	r	0.3	0.1	0.1	0.1	(1.5,1.5)	r	0.1	0.05	0.05	0.05
	ARL_{opt}	3.18	3.98	4.61	4.95		ARL_{opt}	23.57	32.29	41.12	45.86
(0.2,0.2)	r	0.1	0.1	0.1	0.1	(2,2)	r	0.1	0.1	0.1	0.1
	ARL_{opt}	5.36	6.57	7.70	8.32		ARL_{opt}	10.74	13.88	16.96	18.04
(0.5,0.5)	r	0.05	0.05	0.05	0.05	(5,5)	r	0.5	0.3	0.3	0.3

	ARL_{opt}	17.48	22.11	27.06	29.29		ARL_{opt}	1.58	2.15	2.65	2.97
(0.8,0.8)	r	0.01	0.01	0.01	0.01	(10,10)	r	0.5	0.5	0.5	0.3
	ARL_{opt}	55.89	82.33	110.63	126.50		ARL_{opt}	0.42	0.59	0.80	0.90
(0.8,1.5)	r	0.5	0.3	0.3	0.3	(0.2,5)	r	all	0.05+	0.05+	0.05+
	ARL_{opt}	0.13	0.23	0.35	0.41		ARL_{opt}	0.00	0.00	0.00	0.00
(0.5,2)	r	0.3	0.3	0.3	0.3	(0.1,10)	r	all	0.02+	0.02+	0.05+
	ARL_{opt}	0.00	0.00	0.00	0.00		ARL_{opt}	0.00	0.00	0.00	0.00

Table C-2 The optimal design scheme when δ=0.3

$\left(\frac{\theta_1'}{\theta_1},\frac{\theta_2'}{\theta_2}\right)$	ARL_0	100	200	370	500	$\left(\frac{\theta_1'}{\theta_1},\frac{\theta_2'}{\theta_2}\right)$	ARL_0	100	200	370	500
(0.1,1)	r	0.5	0.5	0.5	0.5	(1.2,1)	r	0.05	0.02	0.02	0.02
	ARL_{opt}	0.04	0.09	0.18	0.24		ARL_{opt}	28.72	39.09	48.51	53.77
(0.2,1)	r	0.5	0.3	0.3	0.3	(1.5,1)	r	0.1	0.1	0.1	0.1
	ARL_{opt}	0.45	0.72	0.94	1.07		ARL_{opt}	9.22	11.38	13.54	14.64
(0.3,1)	r	0.3	0.3	0.3	0.3	(1.8,1)	r	0.3	0.1	0.1	0.1
	ARL_{opt}	1.26	1.71	2.14	2.45		ARL_{opt}	4.61	5.96	6.95	7.47
(0.4,1)	r	0.3	0.3	0.3	0.1	(2,1)	r	0.3	0.3	0.3	0.3
	ARL_{opt}	2.58	3.42	4.38	4.67		ARL_{opt}	3.17	3.97	4.90	5.37
(0.5,1)	r	0.1	0.1	0.1	0.1	(2.5,1)	r	0.3	0.3	0.3	0.3
	ARL_{opt}	4.85	5.87	6.83	7.29		ARL_{opt}	1.45	1.87	2.28	2.52
(0.6, 1)	r	0.1	0.1	0.1	0.1	(3, 1)	r	0.5	0.3	0.3	0.3
	ARL_{opt}	7.68	9.60	11.44	12.18		ARL_{opt}	0.76	1.04	1.30	1.43
(0.7,1)	r	0.1	0.05	0.05	0.05	(4,1)	r	0.5	0.5	0.5	0.5
	ARL_{opt}	13.34	17.01	20.17	21.80		ARL_{opt}	0.25	0.37	0.51	0.59
(0.8,1)	r	0.05	0.05	0.02	0.02	(5,1)	r	0.5	0.5	0.5	0.5
	ARL_{opt}	24.72	32.92	40.99	44.42		ARL_{opt}	0.09	0.15	0.22	0.25
(0.9,1)	r	0.02	0.01	0.01	0.01	(10,1)	r	0.5	0.5	0.5	0.5
	ARL_{opt}	52.69	76.70	103.68	117.38		ARL_{opt}	0.00	0.01	0.01	0.01
(0.1,0.1)	r	0.3	0.1	0.1	0.1	(1.5,1.5)	r	0.1	0.1	0.05	0.05
	ARL_{opt}	2.73	3.72	4.35	4.63		ARL_{opt}	23.07	31.23	39.24	43.57
(0.2,0.2)	r	0.1	0.1	0.1	0.1	(2,2)	r	0.3	0.1	0.1	0.1
	ARL_{opt}	5.13	6.24	7.27	7.79		ARL_{opt}	9.95	12.96	15.69	17.31
(0.5,0.5)	r	0.05	0.05	0.05	0.05	(5,5)	r	0.5	0.5	0.3	0.3
	ARL_{opt}	16.82	21.06	25.60	27.74		ARL_{opt}	1.30	1.76	2.21	2.44
(0.8,0.8)	r	0.01	0.01	0.01	0.01	(10,10)	r	0.5	0.5	0.5	0.5
	ARL_{opt}	54.62	80.70	106.53	120.56		ARL_{opt}	0.31	0.45	0.57	0.66
(0.8,1.5)	r	0.3	0.1	0.1	0.1	(0.2,5)	r	0.5	0.5	0.5	0.5
	ARL_{opt}	4.87	6.03	7.13	7.48		ARL_{opt}	0.00	0.00	0.00	0.00
(0.5,2)	r	0.5	0.3	0.3	0.3	(0.1,10)	r	0.1+	0.3+	0.3+	0.3+
	ARL_{opt}	0.55	0.76	0.99	1.09		ARL_{opt}	0.00	0.00	0.00	0.00

Table C-3 The optimal design scheme when δ=0.5

$\left(\frac{\theta_1'}{\theta_1},\frac{\theta_2'}{\theta_2}\right)$	ARL_0	100	200	370	500	$\left(\frac{\theta_1'}{\theta_1},\frac{\theta_2'}{\theta_2}\right)$	ARL_0	100	200	370	500
(0.1,1)	r	0.3	0.3	0.3	0.3	(1.2,1)	r	0.1	0.02	0.02	0.02
	ARL_{opt}	0.79	1.12	1.43	1.58		ARL_{opt}	43.23	63.82	83.82	94.56
(0.2,1)	r	0.3	0.3	0.3	0.3	(1.5,1)	r	0.1	0.05	0.05	0.05
	ARL_{opt}	2.09	2.77	3.45	3.81		ARL_{opt}	16.04	22.01	26.53	28.87
(0.3,1)	r	0.1	0.1	0.1	0.1	(1.8,1)	r	0.1	0.1	0.1	0.1
	ARL_{opt}	4.12	5.18	6.00	6.44		ARL_{opt}	9.00	11.72	13.73	14.82
(0.4,1)	r	0.1	0.1	0.1	0.1	(2,1)	r	0.1	0.1	0.1	0.1
	ARL_{opt}	6.10	7.90	9.17	9.94		ARL_{opt}	6.95	8.72	10.30	11.00
(0.5,1)	r	0.1	0.1	0.1	0.05	(2.5,1)	r	0.3	0.3	0.3	0.3
	ARL_{opt}	9.29	12.29	14.56	16.08		ARL_{opt}	3.77	4.78	5.74	6.27
(0.6, 1)	r	0.1	0.05	0.05	0.05	(3, 1)	r	0.3	0.3	0.3	0.3
	ARL_{opt}	14.64	19.19	23.02	25.01		ARL_{opt}	2.43	2.93	3.60	3.83
(0.7,1)	r	0.05	0.05	0.02	0.02	(4,1)	r	0.5	0.5	0.5	0.3
	ARL_{opt}	23.51	32.13	39.41	43.13		ARL_{opt}	1.17	1.53	1.87	1.97
(0.8,1)	r	0.02	0.02	0.02	0.02	(5,1)	r	0.5	0.5	0.5	0.5
	ARL_{opt}	39.72	55.89	71.04	80.48		ARL_{opt}	0.66	0.88	1.07	1.22
(0.9,1)	r	0.01	0.01	0.01	0.01	(10,1)	r	0.5	0.5	0.5	0.5
	ARL_{opt}	70.99	114.27	164.18	193.90		ARL_{opt}	0.10	0.14	0.19	0.21
(0.1,0.1)	r	0.3	0.3	0.3	0.3	(1.5,1.5)	r	0.1	0.05	0.05	0.05
	ARL_{opt}	2.28	2.99	3.75	4.17		ARL_{opt}	20.17	29.59	36.80	40.04
(0.2,0.2)	r	0.1	0.1	0.1	0.1	(2,2)	r	0.1	0.1	0.5	0.1
	ARL_{opt}	4.46	5.65	6.54	6.97		ARL_{opt}	9.09	12.05	14.39	15.51
(0.5,0.5)	r	0.05	0.05	0.05	0.05	(5,5)	r	0.5	0.5	0.5	0.5
	ARL_{opt}	15.47	19.75	23.68	25.68		ARL_{opt}	1.03	1.37	1.69	1.87
(0.8,0.8)	r	0.01	0.01	0.01	0.01	(10,10)	r	0.8	0.8	0.1	0.5
	ARL_{opt}	52.88	77.37	101.41	114.67		ARL_{opt}	0.23	0.30	0.40	0.44
(0.8,1.5)	r	0.1	0.1	0.3	0.1	(0.2,5)	r	0.5	0.5	0.5	0.5
	ARL_{opt}	9.88	12.96	15.48	17.06		ARL_{opt}	0.05	0.08	0.12	0.14
(0.5,2)	r	0.3	0.3	0.5	0.3	(0.1,10)	r	0.5	0.5	0.5	0.5
	ARL_{opt}	2.30	3.02	3.62	3.98		ARL_{opt}	0.00	0.00	0.00	0.01

Table C-4 The optimal design scheme when δ=0.8

$\left(\frac{\theta_1'}{\theta_1},\frac{\theta_2'}{\theta_2}\right)$	ARL_0	100	200	370	500	$\left(\frac{\theta_1'}{\theta_1},\frac{\theta_2'}{\theta_2}\right)$	ARL_0	100	200	370	500
(0.1,1)	r	0.3	0.3	0.3	0.3	(1.2,1)	r	0.02	0.02	0.02	0.01
	ARL_{opt}	2.09	2.76	3.42	3.76		ARL_{opt}	55.55	85.73	117.08	133.87
(0.2,1)	r	0.1	0.1	0.1	0.1	(1.5,1)	r	0.1	0.05	0.05	0.05
	ARL_{opt}	4.64	5.63	6.54	6.90		ARL_{opt}	24.56	31.80	40.97	44.76
(0.3,1)	r	0.1	0.1	0.1	0.1	(1.8,1)	r	0.1	0.1	0.1	0.1
	ARL_{opt}	7.03	8.67	10.16	10.80		ARL_{opt}	14.21	17.75	21.76	23.89
(0.4,1)	r	0.1	0.1	0.05	0.05	(2,1)	r	0.1	0.1	0.1	0.1
	ARL_{opt}	10.47	13.26	15.87	16.92		ARL_{opt}	10.88	13.67	16.14	17.40
(0.5,1)	r	0.05	0.05	0.05	0.05	(2.5,1)	r	0.3	0.3	0.1	0.1
	ARL_{opt}	15.49	19.63	23.48	25.44		ARL_{opt}	6.24	8.04	9.77	10.45
(0.6, 1)	r	0.05	0.05	0.02	0.02	(3, 1)	r	0.3	0.3	0.3	0.3
	ARL_{opt}	22.81	29.89	36.69	40.43		ARL_{opt}	4.23	5.17	6.24	6.78
(0.7,1)	r	0.02	0.02	0.02	0.02	(4,1)	r	0.5	0.5	0.3	0.3
	ARL_{opt}	34.22	46.20	57.98	64.58		ARL_{opt}	2.25	2.84	3.41	3.71
(0.8,1)	r	0.02	0.01	0.01	0.01	(5,1)	r	0.5	0.5	0.5	0.5
	ARL_{opt}	52.71	76.27	101.39	114.85		ARL_{opt}	1.41	1.80	2.16	2.37
(0.9,1)	r	0.01	0.01	0.01	0.01	(10,1)	r	0.5	0.5	0.5	0.5
	ARL_{opt}	82.03	139.73	213.48	259.65		ARL_{opt}	0.36	0.44	0.55	0.58
(0.1,0.1)	r	0.3	0.3	0.3	0.3	(1.5,1.5)	r	0.1	0.1	0.05	0.05
	ARL_{opt}	1.41	1.86	2.28	2.50		ARL_{opt}	18.79	24.91	30.55	33.50
(0.2,0.2)	r	0.3	0.1	0.1	0.1	(2,2)	r	0.3	0.3	0.3	0.1
	ARL_{opt}	3.38	4.46	5.15	5.42		ARL_{opt}	7.38	9.82	11.81	12.63
(0.5,0.5)	r	0.05	0.05	0.05	0.05	(5,5)	r	0.8	0.5	0.5	0.5
	ARL_{opt}	12.88	16.06	18.93	20.31		ARL_{opt}	0.63	0.84	1.06	1.15
(0.8,0.8)	r	0.01	0.01	0.01	0.01	(10,10)	r	0.8	0.8	0.8	0.8
	ARL_{opt}	47.20	66.93	86.57	96.66		ARL_{opt}	0.11	0.14	0.18	0.18
(0.8,1.5)	r	0.05	0.1	0.05	0.05	(0.2,5)	r	0.5	0.5	0.5	0.5
	ARL_{opt}	18.68	24.10	29.31	32.22		ARL_{opt}	0.49	0.68	0.84	0.94
(0.5,2)	r	0.3	0.1	0.1	0.1	(0.1,10)	r	0.5	0.5	0.5	0.5
	ARL_{opt}	5.86	7.33	8.41	9.13		ARL_{opt}	0.06	0.10	0.13	0.15

Table C-5 The optimal design scheme when δ =1

$\left(\frac{\theta_1'}{\theta_1},\frac{\theta_2'}{\theta_2}\right)$	ARL_0	100	200	370	500	$\left(\frac{\theta_1'}{\theta_1},\frac{\theta_2'}{\theta_2}\right)$	ARL_0	100	200	370	500
(0.1,1)	r	0.3	0.3	0.3	0.3	(1.2,1)	r	0.05	0.02	0.01	0.01
	ARL_{opt}	2.39	3.11	4.06	4.27		ARL_{opt}	57.50	90.15	123.71	142.89
(0.2,1)	r	0.1	0.1	0.1	0.1	(1.5,1)	r	0.1	0.05	0.05	0.05
	ARL_{opt}	5.11	6.12	7.22	7.64		ARL_{opt}	25.54	34.92	43.57	48.11
(0.3,1)	r	0.1	0.1	0.1	0.1	(1.8,1)	r	0.1	0.1	0.05	0.05
	ARL_{opt}	7.56	9.42	11.30	12.10		ARL_{opt}	15.04	19.32	23.75	25.96
(0.4,1)	r	0.1	0.1	0.05	0.05	(2,1)	r	0.1	0.1	0.1	0.1
	ARL_{opt}	11.25	14.40	17.06	18.46		ARL_{opt}	11.57	14.57	17.58	19.13
(0.5,1)	r	0.05	0.05	0.05	0.05	(2.5,1)	r	0.3	0.3	0.1	0.1
	ARL_{opt}	16.57	21.09	25.16	27.76		ARL_{opt}	6.73	8.32	10.62	11.09
(0.6, 1)	r	0.05	0.05	0.02	0.02	(3, 1)	r	0.5	0.3	0.3	0.3
	ARL_{opt}	23.89	32.28	39.78	43.24		ARL_{opt}	4.45	5.51	6.84	7.11
(0.7,1)	r	0.02	0.02	0.02	0.02	(4,1)	r	0.5	0.5	0.3	0.3
	ARL_{opt}	36.01	49.35	62.41	69.01		ARL_{opt}	2.36	2.97	3.82	3.88
(0.8,1)	r	0.02	0.01	0.01	0.01	(5,1)	r	0.5	0.5	0.5	0.5
	ARL_{opt}	54.65	80.21	108.00	122.06		ARL_{opt}	1.47	1.83	2.38	2.39
(0.9,1)	r	0.01	0.01	0.01	0.01	(10,1)	r	0.8	0.8	0.8	0.8
	ARL_{opt}	82.35	143.41	223.00	274.01		ARL_{opt}	0.38	0.46	0.65	0.61
(0.1,0.1)	r	0.5	0.5	0.5	0.5	(1.5,1.5)	r	0.1	0.1	0.05	0.05
	ARL_{opt}	0.73	1.06	1.41	1.47		ARL_{opt}	15.47	20.18	25.15	27.27
(0.2,0.2)	r	0.3	0.3	0.3	0.3	(2,2)	r	0.3	0.3	0.1	0.3
	ARL_{opt}	2.18	2.78	3.56	3.68		ARL_{opt}	5.84	7.43	9.52	10.11
(0.5,0.5)	r	0.1	0.1	0.1	0.1	(5,5)	r	0.8	0.8	0.5	0.8
	ARL_{opt}	10.08	12.66	15.07	16.34		ARL_{opt}	0.37	0.48	0.69	0.68
(0.8,0.8)	r	0.02	0.02	0.02	0.01	(10,10)	r	0.8	0.8	0.8	0.8
	ARL_{opt}	40.45	57.05	72.60	81.68		ARL_{opt}	0.04	0.05	0.09	0.07
(0.8,1.5)	r	0.05	0.05	0.05	0.05	(0.2,5)	r	0.5	0.5	0.3	0.5
	ARL_{opt}	23.01	30.39	36.84	41.38		ARL_{opt}	0.95	1.17	1.59	1.58
(0.5,2)	r	0.1	0.1	0.1	0.1	(0.1,10)	r	0.5	0.5	0.5	0.5
	ARL_{opt}	8.07	9.92	11.86	12.55		ARL_{opt}	0.19	0.24	0.34	0.32